
Theses and Dissertations

Fall 2012

Polydicyclopentadiene : a novel organic solvent nanofiltration membrane

Abhinaba Gupta
University of Iowa

Copyright 2012 Abhinaba Gupta

This dissertation is available at Iowa Research Online: <http://ir.uiowa.edu/etd/3460>

Recommended Citation

Gupta, Abhinaba. "Polydicyclopentadiene : a novel organic solvent nanofiltration membrane." PhD (Doctor of Philosophy) thesis, University of Iowa, 2012.
<http://ir.uiowa.edu/etd/3460>.

Follow this and additional works at: <http://ir.uiowa.edu/etd>

 Part of the [Chemistry Commons](#)

POLYDICYCLOPENTADIENE: A NOVEL ORGANIC SOLVENT
NANOFILTRATION MEMBRANE

by
Abhinaba Gupta

An Abstract

Of a thesis submitted in partial fulfillment
of the requirements for the Doctor of
Philosophy degree in Chemistry
in the Graduate College of
The University of Iowa

December 2012

Thesis Supervisor: Associate Professor Ned B. Bowden

ABSTRACT

Macroscopic, hollow thimbles were synthesized from dicyclopentadiene with the Grubbs second generation catalyst at a monomer:catalyst loading of 10,000:1. A series of Buchwald-Hartwig and Sonogashira coupling reactions were completed on the interior of the thimbles followed by extraction of the product to the exterior using hexane. In all examples, palladium was retained by the membranes at $\geq 99.9\%$ levels. Both polar and apolar molecules with molecular weights from 101 to 583 g mol⁻¹ permeated these thimbles with values for flux of 10⁻⁵ to 10⁻⁶ mol cm⁻² h⁻¹, but selected molecules did not permeate them and had flux values 10⁴ to 10⁵ times slower. The difference in flux was large between molecules that permeated and those that did not permeate, but no trend was observed that correlated flux with molecular weight or hydrophobicity. Rather, molecules that did not permeate the membranes had large cross-sectional areas that led to low rates of diffusion within the highly cross-linked polydicyclopentadiene membranes.

Membranes were fabricated from the ring opening metathesis polymerization of dicyclopentadiene with the Grubbs first generation catalyst at a monomer:catalyst loading of 5,000:1. Mixtures of fatty acid salts were separated using polydicyclopentadiene membranes. Mixtures of fatty acids could not be separated by the membranes, but when triisobutylamine was added to the fatty acids, cis-fatty acid salts had slower permeation through the membranes than saturated and trans-fatty acid salts. Oleic, petroselinic, vaccenic, linoleic, and linolenic acid salts with triisobutylamine had slower permeation relative to the permeation of stearic and elaidic acid salts.

Organic catalysts were retained from organic molecules using nanoporous polydicyclopentadiene membranes. Acid or base was added to organic catalysts that increased the critical areas of the organic catalysts to the size range (>0.5 nm²) where PDPCD membranes could retain them. The catalysts by themselves were too small to be

retained by the membrane, but the salts were in the range where PDCPD retains molecules.

Abstract Approved: _____
Thesis Supervisor

Title and Department

Date

POLYDICYCLOPENTADIENE : A NOVEL ORGANIC SOLVENT
NANOFILTRATION MEMBRANE

by
Abhinaba Gupta

A thesis submitted in partial fulfillment
of the requirements for the Doctor of
Philosophy degree in Chemistry
in the Graduate College of
The University of Iowa

December 2012

Thesis Supervisor: Associate Professor Ned B. Bowden

Copyright by
ABHINABA GUPTA
2012
All Rights Reserved

Graduate College
The University of Iowa
Iowa City, Iowa

CERTIFICATE OF APPROVAL

PH.D. THESIS

This is to certify that the Ph.D. thesis of

Abhinaba Gupta

has been approved by the Examining Committee
for the thesis requirement for the Doctor of Philosophy
degree in Chemistry at the December 2012 graduation.

Thesis Committee: _____
Ned B. Bowden, Thesis Supervisor

James B. Gloer

F. Christopher Pigge

Jan-Uwe Rohde

David G. Rethwisch

To my parents Shyamali Gupta and Amar Kumar Gupta

ACKNOWLEDGMENTS

Foremost, I would like to express my sincere gratitude to my advisor Prof. Ned B. Bowden for the continuous support of my Ph.D. study and research, for his patience, motivation, enthusiasm, and immense knowledge. His guidance helped me in all the time of research and writing of this thesis. He has not only inspired me as advisor, he has been an excellent mentor in shaping me up as an organic and polymer chemist. He has guided me to perform my best by example.

I would like to thank all my committee members Dr. Chris Pigge, Dr. James Gloer, Dr. Jan-Uwe Rohde and Dr. David Rethwisch for their time and insightful questions and comments. I would also like to thank instructors for my teaching assignments for making my teaching experiences enjoyable rather than time-consuming process. I would like to thank Earlene Erbe and advanced laboratory manager Brian Morrison for their help during my teaching assignments.

I would like to thank Dr. Sarah Larsen for letting me use her group's ICP-OES spectrometer. Without her help, a lot of this research would not have been possible. I would like to extend my gratitude towards our collaborator Dr. David Rethwisch for valuable inputs during various projects.

All the members of Bowden Research Group have helped me immensely during my graduate school. I would like to thank Lee, Brett, Martin, Matt, Jun, Tyler Graf, Tyler Long, and Adam. I would like to extend special gratitude to Lee for helping me during my initial years of research in the group. I would also like to thank the undergraduate researchers in Bowden Research Group for their important contribution to this work.

My time at the University of Iowa was more enjoyable due to many friends. I would like to thank my closest friends Suman, Nisarga, Pradeep, Nirmal, Oishik, Aashay, Sanmitra, and Bishwanath for being a part of family away from home. I would also like to thank Bhakti and Varsha for numerous memorable moments. My time at Iowa was

also enriched by my experience of being a part of University of Iowa Cricket Club and Iowa Hawkeyes Cricket Team with special mention of Sachin, Urvil, Nikhil, Ankush, and Pradeep. I would like to thank all my other friends who made my stay at Iowa a memorable experience. I would like to also thank all my friends and relatives back in India for their love and support for all these years with special mention to Chandan Gupta, Tripti Gupta and their entire family. I would also like to extend my gratitude to Ranjana Dutt and her family for their love and support for me during these years of graduate school.

Last, but not least, I would like to thank my parents Shyamali Gupta and Amar Gupta along with my brother Ananda for their encouragement and support throughout my life and letting me pursue my dream of going to graduate school.

TABLE OF CONTENTS

LIST OF TABLES	ix
LIST OF FIGURES	xi
CHAPTER 1 INTRODUCTION	1
Palladium-catalyzed reactions	1
Fatty acids	5
Organocatalysis.....	8
Methods to site-isolate selected molecules.....	9
Organic Solvent Nanofiltration (OSN).....	11
Membranes for organic solvent nanofiltration	12
Applications of nanofiltration.....	16
Petroleum industry.....	16
Catalyst Systems.....	17
Food Industry.....	19
CHAPTER 2 RETENTION OF PALLADIUM AND PHOSPHINE LIGANDS USING NANOPOROUS POLYDICYCLOPENTADIENE THIMBLES AND PERMEATION OF ORGANIC LIQUIDS AND SOLIDS THROUGH THEM	21
Abstract.....	21
Introduction.....	21
Results and Discussion	22
Summary.....	28
Experimental Section.....	29
Materials	29
Characterization.....	29
Fabrication of PDCPD thimbles	30
A general description of how the experiments were completed using PDCPD thimbles.....	30
Buchwald-Hartwig reaction of bromobenzene with aniline (Entry 1, Table 2.1).....	31
Buchwald-Hartwig reaction of 4-bromotoluene with aniline (Entry 2, Table 2.1).....	32
Buchwald-Hartwig reaction of 4-bromoanisole with aniline (Entry 3, Table 2.1).....	32
Buchwald-Hartwig reaction of 4-bromoanisole with morpholine (Entry 4, Table 2.1)	32
Buchwald-Hartwig reaction of 4-iodotoluene with aniline (Entry 5, Table 2.1).....	32
Sonogashira coupling of 4-bromoanisole with phenylacetylene (Entry 6, Table 2.1)	33
Sonogashira coupling of 4-bromotoluene with phenylacetylene (Entry 7, Table 2.1)	33
Procedure to measure the flux of diphenylamine and phosphine ligands or organic substrates (Table 2.2).....	34

Procedure to recycle Pd and X-Phos in a Buchwald-Hartwig reaction (Table 2.3)	34
Procedure to recycle Pd and X-Phos in a Buchwald-Hartwig reaction (3 h reaction cycles).....	35
ICP-OES sample preparation	37
Procedure to measure flux of diphenylamine	37
Procedure to measure the retention of Pd(OAc) ₂ without X-Phos present.....	41
Procedure to measure retention of Pd(OAc) ₂ with X-Phos present.....	42
Procedure to measure retention of Pd ₂ (dba) ₃ without X-Phos present.....	42
Procedure to measure retention of Pd ₂ (dba) ₃ with X-Phos present.....	43
Measurement of the critical area	43
CHAPTER 3 SEPARATION OF CIS-FATTY ACIDS FROM SATURATED AND TRANS-FATTY ACIDS BY NANOPOROUS POLYDICYCLOPENTADIENE MEMBRANES	54
Abstract.....	54
Introduction.....	55
Experimental Procedures	60
Materials	60
Characterization.....	60
Fabrication of PDCPD membranes	60
Permeation of oleic acid and elaidic acid with different amines (Table 3.1)	61
Permeation of saturated and cis-fatty acid salts with triisobutylamine through PDCPD (Table 3.2).....	61
Permeation of stearic and oleic acid as triisobutylamine salts through PDCPD in different solvents (Table 3.3).	62
Partition coefficients of molecules in PDCPD (Table 3.4)	62
Critical areas of fatty acids (Table 3.5)	63
Separation of a mixture of four fatty acids using multiple extractions.....	63
Use of pressure to increase the flux through PDCPD membranes (Table 3.6)	64
Results and Discussion	64
Choice of fatty acids and how the experiments were completed	64
Separation of oleic acid and elaidic acid	66
Separation of cis, trans, and saturated fatty acids.....	69
Partitioning coefficients for fatty acids and fatty acid salts	72
Measurement and comparison of critical areas	73
Separation and isolation of cis-fatty acids from saturated and trans-fatty acids.....	77
Use of pressure to increase flux.....	79
Use of pressure to purify fatty acids derived from soybean oil.....	82
Conclusions.....	84
CHAPTER 4 SITE-ISOLATION OF ORGANIC CATALYSTS USING NANOPOROUS POLYDICYCLOPENTADIENE MEMBRANES	86
Introduction.....	86
Experimental.....	89
Materials	89

Characterization.....	89
Fabrication of PDCPD membranes	89
Permeation of octylamine, MacMillan catalyst and carboxylic acids through PDCPD (Table 4.1 and Figure 4.5).....	90
Permeation of octylamine and MacMillan catalyst salts with carboxylic acids through PDCPD (Table 4.2 and Figure 4.6).....	90
Permeation of L-proline, <i>O</i> -tert-butylthreonine and <i>p</i> -dinitrobenzene through PDCPD (Figure 4.8).....	91
Synthesis of L-proline and <i>O</i> -tert-butylthreonine salts with tetrabutylammonium hydroxide	91
Permeation of tetrabutylammonium salts of L-proline or <i>O</i> -tert-butylthreonine salts through PDCPD (Figure 4.9b)	92
Critical areas of molecules (Table 3).....	92
Results and Discussion	92
How the experiments were completed	92
Retention of octylamine	94
Retention of MacMillan organocatalyst	97
Retention of amino acids	99
Measurement of critical area and the reason of retention of molecules using PDCPD membranes.....	101
Conclusions.....	104
 CHAPTER 5 CONCLUSIONS AND RECOMMENDATIONS FOR FUTURE WORK.....	 105
Conclusions.....	105
Recommendations for Future Work	107
 APPENDIX SELECTIVE FLUX OF ORGANIC LIQUIDS AND SOLIDS USING NANOPOROUS MEMBRANES OF POLYDICYCLOPENTADIENE	 109
Abstract.....	109
Introduction.....	109
Experimental.....	114
Characterization and measurements	114
Calibration of UV-VIS spectrophotometer	114
Calibration of ICP-OES.....	115
Optical spectroscopy	115
Synthesis of PDCPD membranes at a 5,000:1 dicyclopentadiene:Grubbs catalyst ratio.....	115
Synthesis of PDMS membrane.....	115
Permeation of Co(salen) through PDCPD membranes (Table A.2).....	116
Permeation of Co(salen) through PDCPD membranes treated with ethyl vinyl ether (Table A.2 entries 6-8)	116
Permeation of Co(salen) through a PDMS membrane (Table A.1)	117
Swelling of PDCPD by various solvents (Table A.3)	117
Permeation of organic molecules through PDCPD membranes with different solvents (Tables A.4 and A.5)	118
Rate of flux of hexadecane through a 5000/1 PDCPD membrane	118
Density of cross-links of PDCPD membranes	119
Isolation of cholesterol from tricyclohexylphosphine, triphenylphosphine, and tributylamine (Figure A.6).....	120
Isolation of nitrobenzaldehyde from binol	120
Recycling of a PDCPD membrane	121

Measurement of the critical dimension and critical area	121
Results and Discussion	122
Fabrication of PDCPD membranes and the apparatus to measure permeation	122
Permeation of Co(salen) using membranes composed of PDCPD or polydimethylsiloxane	123
Measurement of density of cross-links in PDCPD.....	127
Flux of organic molecules through PDCPD membranes	129
Reason for the retention of selected molecules by PDCPD membranes.....	135
Extraction of nitrobenzaldehyde from binol.....	138
Extraction of cholesterol from triphenylphosphine, tricyclohexylphosphine, and tributylamine using a PDCPD membrane	139
Recycling of PDCPD membranes	141
Conclusions.....	141
 BIBLIOGRAPHY.....	 143

LIST OF TABLES

Table 1.1 Polymeric materials used for the preparation of nanofiltration membranes for organic media.....	13
Table 2.1 Site-isolation of palladium in Buchwald-Hartwig and Sonogashira reactions.....	24
Table 2.2 Permeation of NHPH ₂ and other molecules through the walls of a PDCPD thimble.....	25
Table 2.3 Recycling experiments for a Buchwald-Hartwig coupling reaction of bromotoluene and aniline.	28
Table 2.4 Recycling experiments of 4-bromotoluene and aniline.	36
Table 2.5 The physical parameters of molecules reported in this article.....	46
Table 3.1 Permeation of oleic acid and elaidic acid with different amines through PDCPD membranes.	67
Table 3.2 Permeation of cis-fatty acid salts with triisobutylamine through PDCPD membranes.....	70
Table 3.3 Permeation of stearic acid and oleic acid as triisobutylamine salts through PDCPD membranes in different solvents.....	72
Table 3.4 Partitioning coefficients of fatty acids and fatty acid salts into PDCPD	73
Table 3.5 Critical areas of fatty acids.	75
Table 3.6 Use of pressure to increase the flux through PDCPD membranes.	80
Table 3.7 Separation of soybean oil through two PDCPD membranes under pressure.....	83
Table 4.1 Permeation of octylamine and carboxylic acids through PDCPD membranes.....	95
Table 4.2 Permeation of octylamine salts with carboxylic acids through PDCPD membranes.....	96
Table 4.3 Critical areas of molecules used in this study.....	103
Table A.1 Permeation of Co(salen) and hexadecane using PDMS membranes and CH ₂ Cl ₂ as the solvent.	124
Table A.2 Permeation of Co(salen) using PDCPD membranes fabricated with different catalyst loadings.	125
Table A.3 How solvents swell PDCPD.	130

Table A.4 Flux of five organic molecules through PDCPD membranes.....	132
Table A.5 Permeation of organic molecules using PDCPD membranes and CH ₂ Cl ₂ as the solvent.	134
Table A.6 The chemical and physical sizes of molecules that did or did not permeate PDCPD membranes	137

LIST OF FIGURES

Figure 1.1 The mechanism of the palladium catalyzed Buchwald-Hartwig amination reaction.....	2
Figure 1.2 The mechanism of the palladium catalyzed Sonogashira coupling reaction.....	3
Figure 1.3 Phosphine ligands used in palladium catalyzed reactions.....	4
Figure 1.4 Saturated, trans and cis-fatty acids commonly seen in human diet.....	5
Figure 1.5 An example of a triglyceride composed of glycerol and saturated, mono unsaturated, and polyunsaturated fatty acids.....	6
Figure 1.6 Proline-catalyzed aldol reaction.....	8
Figure 1.7 Jacobsen epoxidation catalyst attached to a polystyrene resin.....	10
Figure 1.8 SEM of a microcapsule encapsulating polyethylene imine catalyst.....	11
Figure 1.9 Schematic illustration of (a) flat sheet membrane configuration (b) spirally wound membrane configuration.....	14
Figure 1.10 Plot for determining molecular weight cut-off for Starmem mebranes.....	15
Figure 1.11 Matrimid 5218 used for nanofiltration membranes by W. R. Grace and Mobil Oil.....	16
Figure 1.12 Catalysts used for the study of nanofiltration by Scarpello.....	18
Figure 2.1 a) The polymerization of dicyclopentadiene with the Grubbs catalyst resulted in a highly cross-linked matrix. b) The structure of X-Phos. c) and d) The Buchwald-Hartwig and Sonogashira coupling reactions that were completed as a part of this work.....	23
Figure 2.2 The ball and spoke models of a) NHPH ₂ , b) PPh ₃ , and c) cholesterol. The boxes around the images were used to determine the cross-sectional areas as described in the experimental.....	26
Figure 2.3 Reactions were completed on the interior of the thimbles without any solvent on the exterior. When the reaction was complete, solvent was added to the exterior to extract the product.....	31
Figure 2.4 Permeation of diphenylamine in methanol. a) Diphenylamine was added to the interior of a thimble with methanol on the exterior and interior. The concentration of diphenylamine was monitored as a function of time and b) the data was fit to the equation in the text.....	39
Figure 2.5 Permeation of diphenylamine in organic solvents. a) Diphenylamine was added to the interior of a thimble with toluene on the exterior and interior. The concentration of diphenylamine was monitored as a	

function of time and b) the data was fit to the equation in the text. c) and d) An identical experiment was completed using hexanes as the solvent.....	39
Figure 2.6 Flux of diphenylamine in toluene.....	40
Figure 2.7 Flux of diphenylamine in hexanes.....	40
Figure 2.8 Flux of diphenylamine in methanol.....	41
Figure 2.9 Two views of the lowest energy conformation of diphenylamine. The image in a) has the lowest cross-sectional area and the image in b) has a much larger cross-sectional area.	44
Figure 2.10 Two views of the lowest energy conformation of triphenylphosphine. The image in a) has the lowest cross-sectional area and the image in b) has a much larger cross-sectional area.	45
Figure 2.11 Two views of the lowest energy conformation of cholesterol. The image in a) has the lowest cross-sectional area and the image in b) has a much larger cross-sectional area.....	45
Figure 2.12 ^1H NMR spectrum of Entry 1, Table 2.1.....	46
Figure 2.13 ^{13}C NMR spectrum of Entry 1, Table 2.1.....	47
Figure 2.14 ^1H NMR spectrum of Entry 2, Table 2.1.....	47
Figure 2.15 ^{13}C NMR spectrum of Entry 2, Table 2.1.....	48
Figure 2.16 ^1H NMR spectrum of Entry 3, Table 2.1.....	48
Figure 2.17 ^{13}C NMR spectrum of Entry 3, Table 2.1.....	49
Figure 2.18 ^1H NMR spectrum of Entry 4, Table 2.1.....	49
Figure 2.19 ^{13}C NMR spectrum of Entry 4, Table 2.1.....	50
Figure 2.20 ^1H NMR spectrum of Entry 5, Table 2.1.....	50
Figure 2.21 ^{13}C NMR spectrum of Entry 5, Table 2.1.....	51
Figure 2.22 ^1H NMR spectrum of Entry 6, Table 2.1.....	51
Figure 2.23 ^{13}C NMR spectrum of Entry 6, Table 2.1.....	52
Figure 2.24 ^1H NMR spectrum of Entry 7, Table 2.1.....	52
Figure 2.25 ^{13}C NMR spectrum of Entry 7, Table 2.1.....	53
Figure 3.1 The structure of the fatty acids used in this study.	56
Figure 3.2 A retention of 100% indicated that the molecule did not permeate the membrane at any level and a retention of 0% indicated that the molecule readily permeated the membrane and was not retained. a) The plot of	

retention versus molecular weight for 35 samples is shown. b) The plot of retention versus critical area is shown for the molecules in part a).....	59
Figure 3.3 The polymerization of dicyclopentadiene by the Grubbs first generation catalyst yielded a highly cross-linked solid polymeric slab.....	65
Figure 3.4 A schematic of the apparatus that was used in these experiments. Molecules A and B were initially added to the solvent upstream of the membrane and only molecule A permeated to the downstream solvent.	66
Figure 3.5 The addition of triisobutylamine led to formation of a stable salt with the fatty acids.....	68
Figure 3.6 The values for S_d/S_u at 24, 48, and 72 h for stearic, linoleic, vaccenic, petroselinic, and linolenic acid are shown. The lines are meant for ease of viewing the data and do not represent a fit to any equation.	69
Figure 3.7 Energy-minimized space filling models for each fatty acid and fatty acid salt with triisobutylamine. One image shows the fatty acid to emphasize any curvature. The other image shows a view of the critical area of each fatty acid salt. These images for a) elaidic acid, b) stearic acid, c) oleic acid, d) linoleic acid, e) linolenic acid, f) vaccenic acid, and g) petroselinic acid are shown.....	76
Figure 4.1 Proline catalyzed aldol reaction.....	86
Figure 4.2 The polymerization of dicyclopentadiene by the Grubbs first generation catalyst yielded a highly cross-linked polymer.....	93
Figure 4.3 A schematic of the apparatus that was used for the permeation experiments. Organic catalyst was retained by the membranes, whereas molecule A permeated through the membranes.....	94
Figure 4.4 The addition of triphenylpropionic acid led to formation of a stable salt with octylamine.....	96
Figure 4.5 Study of Macmillan catalyst and carboxylic acids. a) Permeation of MacMillan catalyst and carboxylic acids through PDCPD membranes (b) The addition of triphenylpropionic acid to MacMillan catalyst formed a stable salt.	97
Figure 4.6 S_d/S_u of permeation studies of salts of the MacMillan catalyst with carboxylic acids through PDCPD membranes after 72 h.	98
Figure 4.7 Amino acid based organic catalysts used in this study.....	99
Figure 4.8 Permeation of proline and <i>O</i> - <i>tert</i> -butylthreonine through PDCPD membranes.	100
Figure 4.9 Retention of amino acids. a) The addition of tetrabutylammonium hydroxide led to formation of stable salt with proline (b) S_d/S_u of permeation studies of tetrabutylammonium salts of proline and <i>O</i> - <i>tert</i> -butylthreonine through PDCPD membranes.	101

Figure 5.1 Different trisubstituted amines which can be tried to study the permeation of oleic acid and polyunsaturated acids through PDCPD membranes.	107
Figure A.1 a) Polydicyclopentadiene was synthesized by polymerizing dicyclopentadiene with the Grubbs first generation catalyst at monomer to catalyst loadings of 5,000:1. b) Despite the large difference in molecular weight between RuBINAP and the product of the reaction, RuBINAP was only site-isolated at 98% using an OSN membrane.....	111
Figure A.2 A cross-sectional schematic of the apparatus used to measure permeation through PDCPD membranes.....	123
Figure A.3 Cross-linking density in PDCPD. a) The unreacted five membered ring that is responsible for the peak at 704 cm^{-1} . b) The IR spectrum of PDCPD in the region of interest.	128
Figure A.4 The amount of hexadecane in mmol that was downstream of a membrane as a function of time. The solvent was a) CH_2Cl_2 and b) toluene.....	131
Figure A.5 The molecules that were studied for their permeation through PDCPD membranes.	133
Figure A.6 Extraction of cholesterol from a mixture of molecules. a) The ^1H NMR spectra of the initial mixture of cholesterol, OPCy_3 , PCy_3 , PPh_3 , and NBu_3 ; b) the mixture of molecules upstream of the membrane after 48 h; c) the mixture of molecules downstream of the membrane after 48 h; and d) cholesterol. The peaks for cholesterol at 3.52 and 5.35 ppm were observed in all four spectra but were omitted from this figure to emphasize the region from 0.5 to 2.7 ppm.....	140

CHAPTER 1

INTRODUCTION

This thesis focuses on the selective retention of organic and organometallic molecules using a novel organic solvent nanofiltration membrane based on highly cross-linked polydicyclopentadiene. The thesis will concentrate mainly on the use of polydicyclopentadiene membranes to separate palladium catalysts from organic products, the separation of cis-fatty acids from saturated and trans-fatty acids, and the separation of organic catalysts from other organic molecules. In this Chapter, I will discuss palladium catalyzed reactions, fatty acids, and organic catalysts and why each of them must be purified by a membrane. I will also briefly discuss some of the methods of site-isolation reported in the literature. Finally, I will introduce the field of organic solvent nanofiltration and its various applications in different fields.

Palladium-catalyzed reactions

Carbon-carbon bond formation by activation of a C-X bond is one of the most important transformations in synthetic organic chemistry.¹ Amongst the transition metals, palladium is without question most commonly utilized. Named reactions such as Sonogashira, Stille, Heck, Suzuki, and others are not only well-known, but few total syntheses are completed without using at least one of these reactions.² The well known contributions of Buchwald and Hartwig opened a new chapter in the field of transition metal-catalyzed cross-coupling chemistry with a new approach to the syntheses of derivatized anilines and aryl ethers.³

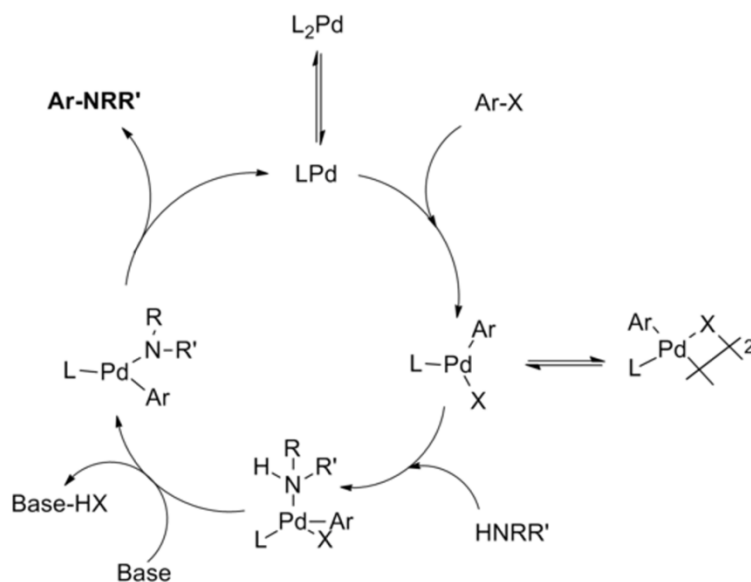


Figure 1.1 The mechanism of the palladium catalyzed Buchwald-Hartwig amination reaction.

The reaction mechanism for the Buchwald-Hartwig reaction has been demonstrated (Figure 1.1) to proceed through steps similar to those known for palladium catalyzed C-C coupling reactions.⁴ Steps include oxidative addition of the aryl halide to a Pd(0) species, addition of the amine to the oxidative addition complex, and deprotonation followed by reductive elimination. The catalytic system contains four components to efficiently generate a C-N bond. A palladium precursor is typically stabilized in solution by a ligand that also raises the electron density at the metal to facilitate oxidative addition and provides sufficient bulkiness to accelerate reductive elimination. A base is required to deprotonate the amine prior to or after coordination to the palladium centre. Owing to the often heterogeneous nature of the reaction due to solubilities of the base or palladium, the solvent plays a more prominent role than in other transition metal-mediated processes.

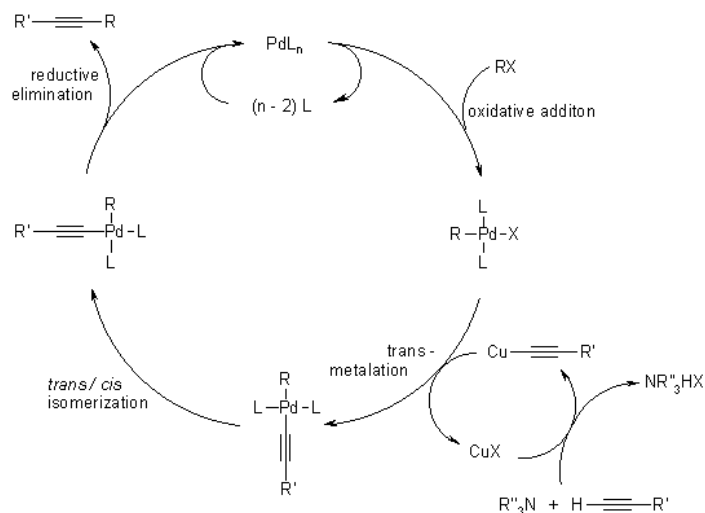


Figure 1.2 The mechanism of the palladium catalyzed Sonogashira coupling reaction.

The reaction mechanism of the Sonogashira coupling revolves around a palladium cycle and a copper cycle (Figure 1.2). In the palladium cycle, the active palladium catalyst is the 14-electron compound Pd^0L_2 , which reacts with the aryl or vinyl halide in an oxidative addition to produce a Pd^{II} intermediate. This step is believed to be the rate-limiting step of the reaction. The Pd^{II} intermediate reacts in a transmetalation reaction with the copper acetylide, which is produced in the copper cycle, to produce a new complex and expelling copper halide at the same time. Both organic ligands are trans oriented and convert to cis in a trans-cis isomerization to produce a final complex, which undergoes reductive elimination to produce the alkyne, with regeneration of the palladium catalyst.

In the copper cycle, copper coordinates to the pi bond which makes the terminal proton on the alkyne more acidic. A base abstracts the proton and leads to the formation of a copper acetylide. The copper acetylide continues to react with the palladium intermediate to regenerate the copper halide.

Although catalyst systems containing no ligand have been reported over the last few years for some organometallic transformations, C-N coupling reactions are usually

carried out with an added ligand.^{5,6} The ratio of ligand to palladium depends mostly on the choice of ligand and can have a distinct influence on the catalytic performance. The quest for suitable ligands showing higher reactivity and selectivity has been a field of enormous activity over the last few years.^{4,7-9} The first ligands to be used were $P(o\text{-Tol})_3$ and $P(t\text{-Bu})_3$.^{3,10,11} The chelating biphosphines such as BINAP used by Buchwald and Hartwig then defined the state of the art until Buchwald reported the synthesis of monodentate phosphine ligands with a biphenyl backbone in 1998.¹² These ligands (Figure 1.3) greatly enhanced the scope of aminations to include aryl chlorides and unactivated aryl halides even under very mild conditions.¹³ The design of the new bulky 2,4,6-triisopropyl substituted ligand X-Phos led to the most active and stable biphenyl based ligand to date.¹⁴ With the advent of carbenes showing outstanding performance in other organometallic transformations as sterically bulky and good electron-donating ligands, highly active phosphine based ligands such as XantPhos and DPEPPhos were synthesized.¹⁵⁻¹⁷

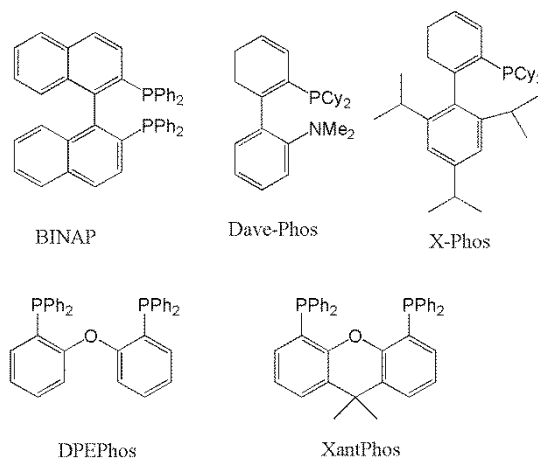


Figure 1.3 Phosphine ligands used in palladium catalyzed reactions.

In spite of the decline in price in the last few years, palladium catalysts and the phosphine ligands are very expensive. One mole of $\text{Pd}(\text{OAc})_2$ costs \$9,000, one mole of $\text{Pd}(\text{PPh}_3)_4$ costs \$26,600, and one mole of X-Phos costs \$19,000. Due to the high cost of palladium catalysts and phosphine ligands, they need to be recovered from organic products and recycled to make an industrial process cost effective. Removal of palladium from final product is also important to reduce the toxicity of the product.

Fatty acids

Most fatty acids (Figure 1.4) have 16, 18, or 20 carbon atoms with a carboxylic acid at one end and a methyl group at the other end. They possess zero, one, or multiple carbon-carbon double bonds in either the cis or trans configurations. The overall composition of different food sources differs, but all sources contain saturated and unsaturated fatty acids.

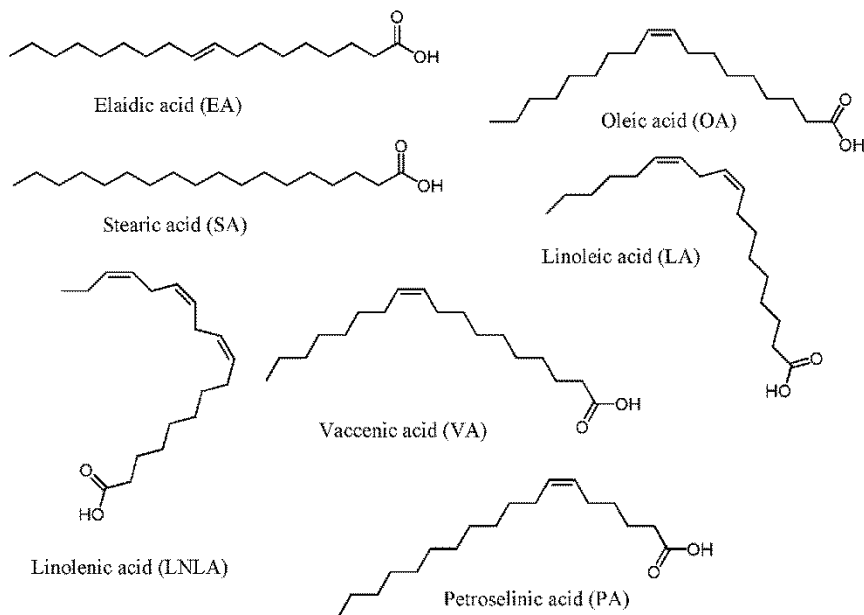


Figure 1.4 Saturated, trans and cis-fatty acids commonly seen in human diet.

Vegetable oils are composed of triglycerides that are composed of a triester of glycerol with three fatty acids as shown in Figure 1.5. The fatty acids can be easily cleaved from glycerol and isolated as a mixture of numerous fatty acids.

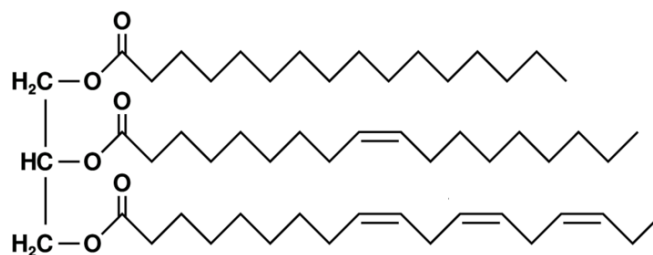


Figure 1.5 An example of a triglyceride composed of glycerol and saturated, mono unsaturated, and polyunsaturated fatty acids.

Fatty acids derived from vegetables are the most important biorenewable feedstock for the chemical industry with over 140 million tons of vegetable oils produced last year.¹⁸ The largest application of vegetable oils is as a food source for humans and animals and over 25 million tons of vegetable oils are partially hydrogenated each year to be used in food for humans and animals.¹⁹⁻²³ Trans-fatty acids are present in variable quantities in a broad range of foods (over 40,000 foods contain trans-fatty acids), including most foods prepared with partially hydrogenated vegetable oils such as baked and fried foods and most margarine products. The consumption of fatty acids has both positive and negative implications for health. The consumption of saturated and trans-fatty acids has a direct correlation with various health problems including thrombogenesis which leads to increased risk for coronary heart and cardiovascular diseases, increased levels of low-density lipoproteins, and decreased levels of high-density lipoproteins.^{24,25} In contrast, the consumption of cis-fatty acids are often associated with positive health benefits.^{26,27} For instance, omega-three fatty acids- which possess a cis olefin at the third carbon from the methyl group – are considered “essential

fatty acids” because the human body does not synthesize them, but they are required from dietary sources for essential biological functions.

The production of vegetable oils with the right chemical and physical properties for human consumption and that contain zero trans-fatty acids would lead to very positive health outcomes. Unfortunately, this has proven to be an elusive goal. Some food is advertised as containing “zero trans-fats” but this label is misleading because it can be applied if food contains less than 0.5 g of trans-fatty acids per serving. The consumption of multiple servings over the course of a day leads to significant consumption of trans-fatty acids even from food labeled as containing “zero trans-fats”. Of the over 140 million metric tons of vegetable oils produced each year, approximately 25% are partially hydrogenated and contain trans-fatty acids.

Vegetable oils are the most important renewable feedstock for the chemical industry and their use has grown by 5% per year since 2000. A critical problem in the field of fatty acids is that no method exists to separate fatty acids into their individual components on an industrial scale of millions of tons per year. Separating a mixture of fatty acids into individual fatty acids is very challenging due to their similarities in size and molecular formula. Furthermore, although fatty acids are a critically important feedstock, their applications in commercial products outside of food and biodiesel have been slow to develop. One major reason is that fatty acids derived from vegetable oils are a mixture of five or more different fatty acids. The development of commercial products nearly always requires starting with a mixture of fatty acids even if only one fatty acid is desired. The development of a method to separate a mixture of fatty acids into a series of pure, individual fatty acids on an industrial size scale will expand the opportunities for fatty acids as starting materials for new applications and allow the preparation of edible oils without trans-fatty acids.

Organocatalysis

In organic chemistry, organocatalysis refers to a form of catalysis, where the rate of a reaction is increased by an organic catalyst which consists of carbon, hydrogen, nitrogen, sulfur and other non-metal elements found in organic compounds.²⁸⁻³⁰ Many enzymes are remarkable asymmetric catalysts, performing reactions effectively and selectively. Aspiring to imitate enzymatic efficiencies, chemists have delved into Nature's toolbox, transforming amino acids into various catalysts.

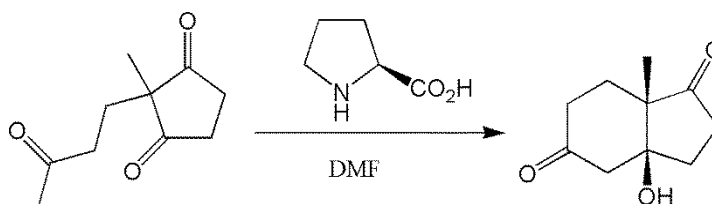


Figure 1.6 Proline-catalyzed aldol reaction.

In the reaction shown in Figure 1.6, naturally occurring chiral proline is the organocatalyst in an aldol reaction.³¹ The starting material is an achiral triketone, and proline is needed to obtain the reaction product in 93% enantiomeric excess. This is the first example of an amino acid catalyzed asymmetric aldol reaction. Organic catalysts can be broadly classified into four major classes. The first one is represented by biomolecules (e.g., proline, threonine, phenylalanine).³² The second class is represented by imidazolidinone based organic catalysts.^{33,34} The third major class is based on hydrogen bonding, and includes derivatives of binol and thiourea. The final class of organic catalyst is based on quarternary ammonium salts.

Several decades after the first use of an amino acid as a catalyst, amino acids and simple peptides have become an important subset of asymmetric catalysts. Organic catalysts have several advantages over inorganic and organometallic catalysts. The most

important one is that an organic catalyst does not have any metal, so there is no need to remove any metal from a final product as compared to inorganic catalysts like palladium catalysts. From that perspective, organic catalysts are much less toxic as compared to the organometallic catalysts and that makes the synthetic process greener. These organic catalysts are not sensitive to moisture and oxygen which makes them much easier to use as compared to organometallic catalysts like $\text{Pd}_2(\text{dba})_3$ and many other catalysts which are very sensitive to oxygen. Organic catalysts are readily available and are not overly expensive. For example, L-proline which is widely used as an organic catalyst costs \$74 per mole, whereas $\text{Pd}(\text{OAc})_2$ costs \$8,980 per mole. Thus organic catalysts are an attractive option for use in organic reactions.

Methods to site-isolate selected molecules

Site-isolation can be defined in organic chemistry as a physical separation of multiple catalysts and or reagents to prevent two species from coming into contact with each other. A lot of research has been done in the last few years to develop site-isolation methods, most of which involve catalyst immobilization to organic or inorganic solid supports.

Zeolites have been utilized for site-isolation for quite some time in catalysis, gas purification, drug delivery systems, hydrogen storage, petrochemicals, and other processes.³⁵⁻³⁸ The microporous structure of zeolites and their well-defined structures make them useful for site-isolation. Recent advances in zeolite technology allow for the modification of both the interior and exterior of these materials to allow for specific uses. Encapsulated catalysts within zeolites have been used as alternatives to traditional homogeneous catalysis. Due to various pore sizes, it is also worth noting that zeolite encapsulated catalysts have been used to give different products or different selectivities compared to homogeneous catalysts. Zeolites are used in chemical reactions because they are cheap, straightforward to synthesize, easy to remove from the reaction mixture, and

The microencapsulation of catalysts in polymeric materials has recently made a significant advancement in site-isolation.^{42,43} Palladium⁴⁴ and nickel⁴⁵ organometallic catalysts as well as organic catalysts such as DMAP⁴⁶ have been encapsulated into polymeric micelles⁴⁷ and microcapsules⁴⁵. These methods allow easy catalyst removal and recycling. The catalysts are homogeneous inside the microcapsule (Figure 1.8) because they are dissolved in solution and has selectivity similar to a free catalyst. A solvent must be used that swells the polymer and allows the product to flux through but retains the catalyst inside the microcapsule.



Figure 1.8 SEM of a microcapsule encapsulating polyethylene imine catalyst.

Organic Solvent Nanofiltration (OSN)

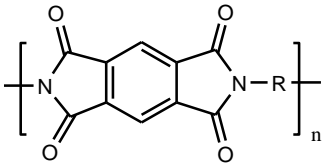
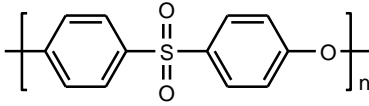
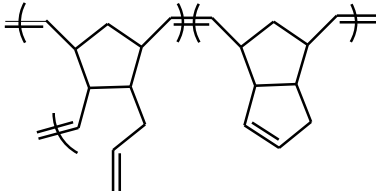
Over the years membrane separation methods became widespread in different fields of industry and medicine. One of them, nanofiltration separates target molecules with molecular weights ranging from hundreds to several thousand g mol^{-1} from multicomponent solutions.⁴⁸ Until recently, nanofiltration has been used primarily for the separation of aqueous media. In the past one and a half decades, significant progress was achieved in the separation of molecules and concentration of organic solutions. Nanofiltration of organic solutions is applied to separate compounds dissolved in solvents

with molecular weight ranging from 200 to 1400 g mol⁻¹ with simultaneous permeation of the organic solvent through the membrane. Sometimes nanofiltration is applied in combination with other separation processes (distillation, extraction, pervaporation and others) as a preliminary stage of a target product purification.⁴⁹⁻⁵¹ In some cases organic solvent nanofiltration is the only possible way of separation of thermally unstable systems. One of the major factors in the success of organic solvent nanofiltration process is the proper choice of membrane used for the process.

Membranes for organic solvent nanofiltration

Membranes used in this process should possess mechanical and chemical resistance in organic solvents, and exhibit high retention with respect to a target product and allow permeation of organic solvent. Modern polymeric materials used to fabricate nanofiltration membranes for organic solvents can be divided into four classes as shown in Table 1.1. The first class contains highly permeable polymers, mostly cross-linked silicon rubbers. These polymers are used to produce composite membranes in which the selective layer is deposited on the porous supporting material.^{52,53} The second class comprises low permeable linear polymeric membranes. These consist of polyamides, polyimides, and polysulfones. These polymers are used to fabricate asymmetric membranes, in which the selective and support layers are made of the same polymeric material.⁵⁴ The third class consists of low permeable highly cross-linked polymers such as polyaniline and polydicyclopentadiene membranes. These polymers are highly cross-linked, and membranes fabricated using these polymers are nanoporous when swelled in organic solvents. The fourth class of polymeric materials used for the production of nanofiltration membranes contains highly permeable polymeric glasses, for example, poly(1-trimethylsilylprop-1-yne) (PTMSP). PTMSP is a hydrophobic glassy polymer with a high free volume fraction (up to 25%) and exhibits nanoporosity in the membranes.^{55,56}

Table 1.1 Polymeric materials used for the preparation of nanofiltration membranes for organic media.

Polymer	Representative	Formula
Highly permeable polymers	Silicon rubbers	$\left[\begin{array}{c} R_1 \\ \\ -Si-O- \\ \\ R_2 \end{array} \right]_n$ <p>$R_1, R_2 = \text{Alkyl}$</p>
Low permeable linear polymers	polyimides	
	polysulfones	
Low permeable highly cross-linked polymers	polydicyclopentadiene	
Highly permeable polymeric glasses	PTMSP	$\left[\begin{array}{c} Me \\ \\ -C=C- \\ \\ SiMe_3 \end{array} \right]_n$

Along with the choice of polymer used in the fabrication of nanofiltration membranes, the configuration of the membranes is an important factor in the success of the process. The three basic configurations of membranes used in a nanofiltration process are flat sheet, spirally wound, and tubular. The flat sheet configuration is used in the plate-and-frame membrane module (Figure 1.9a). The spirally wound configuration has a membrane rolled on top of one another and this configuration is widely used in the industry (Figure 1.9b). The spiral-wound module provides a relatively large membrane area per unit volume. The large scale production is cost-effective and the cost of a module per membrane area is low. The tubular membrane module consists of membrane tubes placed into porous stainless steel or fiber glass reinforced plastic pipes.

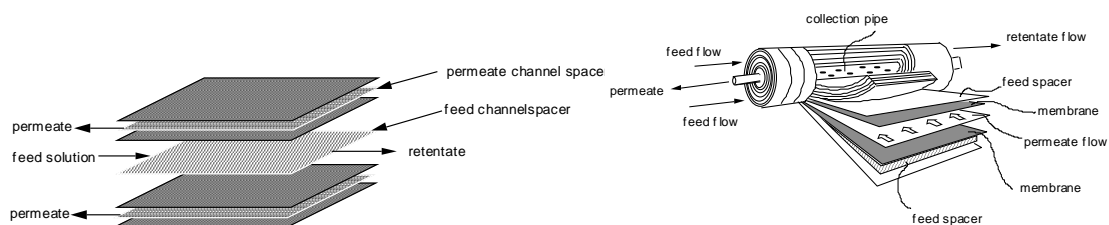


Figure 1.9 Schematic illustration of (a) flat sheet membrane configuration (b) spirally wound membrane configuration

Inorganic nanofiltration membranes are less widespread as compared to relatively cheap membranes based on polymeric materials despite their excellent mechanical characteristics and the absence of swelling upon contact with solvents. Silicozirconium inorganic membranes were prepared using a sol-gel method.^{57,58} The nanoporous structure of the selective layer varied in the range of 0.8-5 nm and the membranes possessed high molecular weight cut-off values in organic solvents. Using such membranes, it became possible to separate higher alcohols and hydrocarbons (C_6 , C_8 and

C_{10}) from their solutions in ethanol at temperatures up to 60 °C and pressures up to 30 atm.

In the field of organic solvent nanofiltration, membrane selection for the separation of a target product is based on the molecular weight cut-off (MWCO) as specified by the manufacturer. MWCO is defined by plotting the rejection of solutes versus their molecular weight (Figure 1.10), to find the molecular weight corresponding to 90% rejection. In Figure 1.10, the Starmem membrane 122 has a MWCO of 220 g mol^{-1} and Starmem 240 has a MWCO of 400 g mol^{-1} . Molecular weight cut-off of a membrane is a starting point to predict the permeability of a molecule through the membrane, but there have been numerous instances where molecules having molecular weights above the MWCO have permeated the membrane.

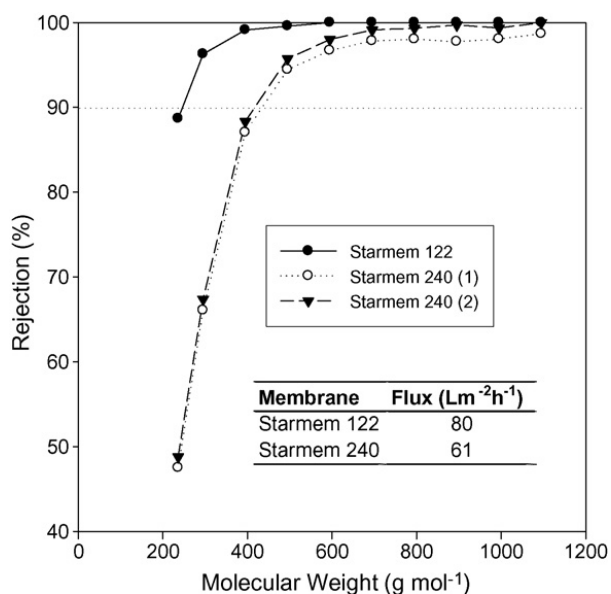


Figure 1.10 Plot for determining molecular weight cut-off for Starmem membranes.

Unfortunately, there are few commercially available OSN membranes and it is not always possible to find the required combination of permeability and selectivity parameters, which essentially limits the scope of application of this promising technique.

Applications of nanofiltration

Petroleum industry

It is well-known that the presence of long-chain saturated hydrocarbons (paraffins) essentially increases the solidification temperature of motor oils. One of the ways to extract the paraffins from motor oil is solvent dewaxing. The approach is based on cooling the solution of motor oil in an organic solvent (down to $-20\text{ }^{\circ}\text{C}$) to crystallize paraffins and subsequently filtering the solution on a drum filter. The presence of an organic solvent favours the decrease in viscosity of the system at such a low temperature. After filtration, the solvent is normally regenerated by distillation. It was suggested to apply nanofiltration at the stage of motor oil concentration before the distillation stage in order to reduce energy consumption.^{49,51} In the framework of a pilot joint project of 'W R Grace' and 'Mobil Oil', a similar process was carried out using asymmetric membranes based on polyimide Matrimid 5218 (Figure 1.11).⁵⁹

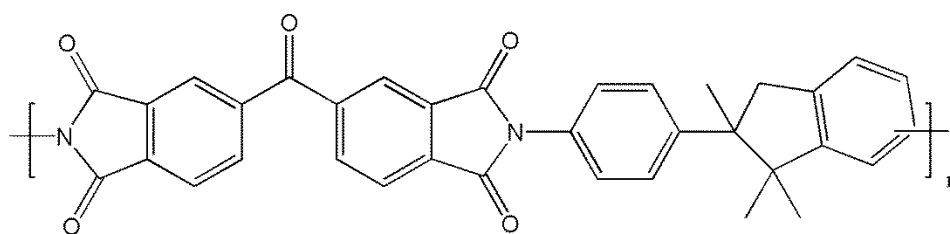


Figure 1.11 Matrimid 5218 used for nanofiltration membranes by W. R. Grace and Mobil Oil.

That pilot unit used spirally wound membrane modules of Matrimid 5218. The oil content in permeate did not exceed 1 wt%. The separation process was carried out at 41 atm and 10 °C, which significantly reduced the consumption of energy. After performing the initial pilot experiments, Mobil Beaumont Refinery (Texas) in 1998 started the industrial production of dewaxed motor oil with the nanofiltration recycling of organic solvent mixture at low temperature.⁵⁰ The daily capacity on the initial mixture was 11,500 m³ and the residual oil content in permeate was equal to 0.2 wt% - 0.8 wt%. Optimization of conditions of industrial dewaxing of motor oil with the application of nanofiltration separation (MAX-DEWAX-process) allowed Exxon Mobil and W R Grace to increase oil productivity by 25% with simultaneous decrease in paraffin content in the final product. The reduction of energy consumption per product unit increased the annual profit of these companies by \$6.1 million and helped them overcome capital costs for the process optimization.

Catalyst Systems

Transition metal complexes (Pt, Pd, Ru, Rh and others) with organic ligands are used as homogeneous catalysts in many catalytic processes in organic synthesis, petrochemical industry, and pharmacy. The technology of such processes requires a stage of product separation from an expensive catalyst, and for continuous modes, a recycling stage, which in many cases is associated with high investments and energy cost. This is often the factor that limits the commercialization of new inventions. Many rhodium-containing catalytic systems that possess high activity and selectivity and ensure mild conditions of a process are partially or completely deactivated at the recycling stage.⁶⁰ Efficient separation of the catalyst from the reaction products along with its reactivation and recycling is the best way to use a homogeneous catalyst and to increase the lifetime of the metal catalyst. An effective way to recycle homogeneous catalysts without their deactivation is the use of a chemical reactor combined with a nanofiltration separation

unit. The separation can be performed in a continuous mode with the reaction in the reactor or a batch mode.

The first reported separation of homogeneous catalysts from reaction mixtures using polymeric membranes was half a century ago. In 1959, American Oil patented a method of membrane isolation of acid catalysts employed in hydrocarbon conversion processes using hydrophobic, continuous membranes based on polyethylene.⁶¹ After a significant amount of research in this field for many years, in 2002 Scarpello used a range of commercial nanofiltration membranes (MPF-50, Desal-5 and STARMEM 120, 122 and 240) for the separation of complexes of ruthenium, manganese, and palladium (Figure 1.12) from a number of solvents used in organic synthesis such as dichloromethane, tetrahydrofuran and ethyl acetate.⁶²

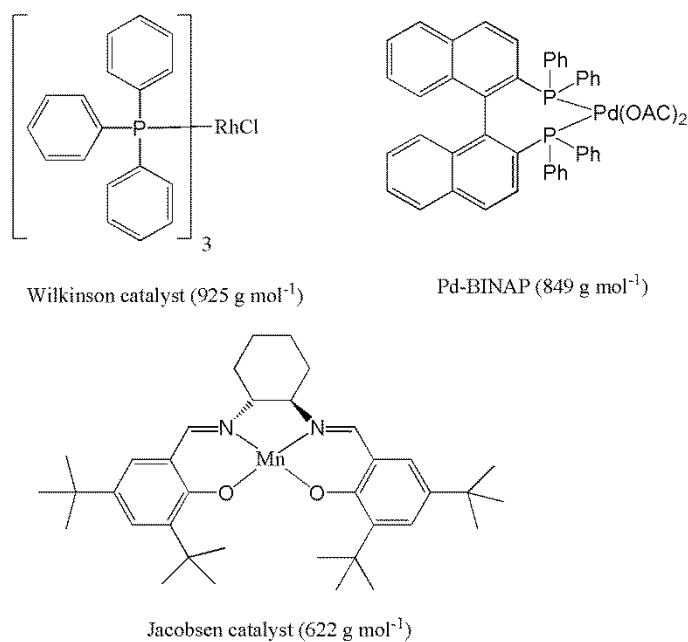


Figure 1.12 Catalysts used for the study of nanofiltration by Scarpello.

It was shown that membranes of the STARMEM series are preferable for the nanofiltration of solutions in ethyl acetate (the highest fluxes and catalyst rejection >95%).⁶³ Unfortunately, in dichloromethane and tetrahydrofuran, the polyimide STARMEM 240 membranes are unstable, while STARMEM 120 and 122 membranes have low permeability. Significantly better transport characteristics in dichloromethane were shown by Desal-5 membrane, while in tetrahydrofuran, the MPF-50 was the superior one. Thus, the solvent used for the process plays an important role in the selection of the membrane.

Food Industry

In the food industry, vegetable oil is usually prepared by either seed pressing or solvent extraction. If the oil in seeds is higher than 25%, the extraction method is economically profitable. One of the most energy consuming stages of the process of vegetable oil preparation is the distillation recycling of an organic solvent. It was suggested to use nanofiltration for partial removal of solvent and concentration of the oil before the final distillation. In 1996, the German company 'GKSS' patented a method of preparation of membranes with a selective layer based on radiation-induced cross-linked PDMS for nanofiltration of 10% solution of corn oil in organic solvents.⁶⁴ The cross-linking of PDMS membranes increased the oil content from 66% to 90% while permeability of molecules was reduced by 20%. Researchers investigated the rejection of many triglycerides dissolved in hexane at different pressure and temperature.⁶⁵ Nanofiltration was performed using commercial composite membranes based on silicon rubber (Membrane D, 'Osmonics'). The rejection of triglycerides was increased with the rise in the molecular weight of triglycerides, and the molecular weight cut-off of Membrane D in hexane was estimated as 900 g mol^{-1} .

Another important and actively investigated problem of nanofiltration purification of vegetable oil is the removal of free fatty acids from triglycerides. There are two major

approaches to the solution of this problem with the help of membrane technology. The first method is the addition of organic solvent such as acetone and methanol into oil.^{66,67} Solvent increases the flux of fatty acids through a membrane, whereas the permeation of triglycerides changes insignificantly. The second method is the nanofiltration separation of triglycerides and free fatty acids without addition of an organic solvent.⁶⁸

In the subsequent chapters, I will describe different methods of retention of organic and inorganic molecules using polydicyclopentadiene membranes. I will also discuss how nanoporous polydicyclopentadiene membranes were used to separate catalysts from products and cis-fatty acids from saturated and trans-fatty acids.

CHAPTER 2
RETENTION OF PALLADIUM AND PHOSPHINE LIGANDS USING
NANOPOROUS POLYDICYCLOPENTADIENE THIMBLES AND
PERMEATION OF ORGANIC LIQUIDS AND SOLIDS THROUGH
THEM

Abstract

Thimbles composed of polydicyclopentadiene retained Pd and phosphines used in Buchwald-Hartwig and Sonogashira coupling reactions but allowed the products to permeate. The products were isolated in high yields on the exteriors of the thimbles with no detectable contamination from phosphine and with Pd loadings as low as <5.5 ppm.

Introduction

The removal of catalysts from products of reactions is critically important in drug discovery, the synthesis of pharmaceuticals, and in the academic laboratory.⁶⁹⁻⁸² One critical reason for this importance is that the upper limit of metals and organic impurities in pharmaceutical drugs is determined by the FDA and these values are often very low.⁸³⁻⁸⁵ For instance, the allowed upper limit for Pd in a pharmaceutical drug is approximately 20 ppm and requires extensive cleaning of the final product. Phosphines are also an impurity in an active pharmaceutical ingredient so their removal is necessary. A second motivation to remove catalysts from products is their high costs that make recycling them very desirable. For instance, Pd coordinated to a new Buchwald phosphine catalyses reactions with substrates that were previously unreactive,⁸⁶⁻⁸⁸ but their cost (one mole of X-Phos costs \$19,000 compared to \$8,700 for a mole of Pd(OAc)₂) makes recycling them very important.⁸⁹

We recently developed membranes based on highly cross-linked polydicyclopentadiene (PDCPD) that separates organic molecules with molecular weights from 100 to 600 g mol⁻¹ based on their cross-sectional areas (Figure 1a).

Molecules with cross-sectional areas above ca. 0.50 nm^2 did not permeate these membranes and molecules with cross-sectional areas below 0.38 nm^2 permeated readily. Molecular weights and the presence of functional groups did not impact whether molecules would permeate these membranes; for instance, nonaethylene glycol monododecyl ether (MW: 583 g mol^{-1}) permeated PDCPD, but tributylamine (MW: 185 g mol^{-1}) did not permeate. These membranes also separated constitutional isomers; triisobutylamine permeated PDCPD with a value for its flux at least 10^4 to 10^5 times greater than the value for tributylamine.

In our prior work, mixtures of two to five molecules were separated with membranes composed of PDCPD, but the separation of metals or phosphines from the products of a reaction were not studied.⁹⁰ In this chapter the separation of both phosphines and Pd from the products of two Pd-coupling reactions is demonstrated. Furthermore, the Pd and phosphines were recycled five times. This work is critically important because it demonstrates how commercially available, unmodified phosphines and Pd can be separated from the products of a reaction through simple filtrations and recycled.

Results and Discussion

We investigated Buchwald-Hartwig and Sonogashira coupling reactions that were catalysed by Pd coordinated to one of the new Buchwald phosphine ligands (Figure 2.1). These reactions were completed on the interior of hollow, macroscopic thimbles composed of PDCPD. The thimbles were 5 cm tall, 1.2 cm in diameter, and possessed walls that were 0.10 cm thick. A schematic of a thimble is found in the experimental. The reactions were run in solvent on the interior of thimbles until they were complete and then the products were extracted to the exterior of the thimbles by the addition of hexane only on the exterior of the thimbles.

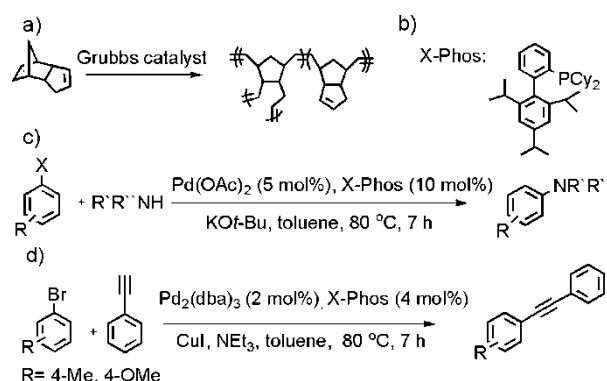
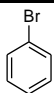
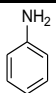
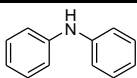
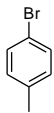
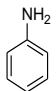
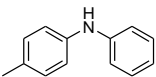
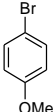
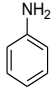
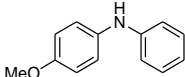
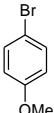
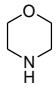
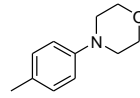
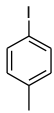
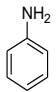
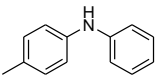
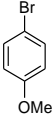
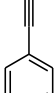
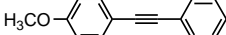
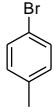
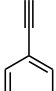
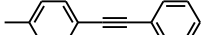


Figure 2.1 a) The polymerization of dicyclopentadiene with the Grubbs catalyst resulted in a highly cross-linked matrix. b) The structure of X-Phos. c) and d) The Buchwald-Hartwig and Sonogashira coupling reactions that were completed as a part of this work.

The hexane extracts were removed from the reaction vessel, volatile organics were evaporated under vacuum, and the crude products were initially characterized by ¹H NMR spectroscopy. No evidence of phosphine ligand was observed despite the presence of two cyclohexyl and three isopropyl groups on the phosphine ligand that would appear in an unobstructed region of the ¹H NMR spectra. The loadings of Pd in the crude product were characterized by inductively coupled plasma-optical emission spectroscopy (ICP-OES) prior to any purification (Table 2.1). In all experiments, between 99.1% and >99.98% of the Pd added to the interior of the thimbles did not permeate to the exterior which lead to loadings of Pd in the crude product as low as <5.5 ppm. Furthermore, the crude product was purified by column chromatography and the isolated yields were between 85% and 98%. The isolated yields demonstrated that the products selectively permeated to the exterior of the thimbles in high yields despite the low permeation of Pd and phosphines

Table 2.1 Site-isolation of palladium in Buchwald-Hartwig and Sonogashira reactions.

Entry	Aryl halide	Amine	Product	Isolated Yield (%)	^a Retention of Pd (%)	^b Concentration of Pd in product (ppm)
1				85	99.69	113.5
2				94	≥99.98	≤6.1
3				91	99.3	228
4				91	99.98	5.9
5				90	99.1	314
6				95	99.25	7.62
7				98	99.79	2.80

^aPercentage of Pd that did not flux to the exterior of the thimbles. ^bMeasured by ICP- OES.

To further study the lower limit for the amount of X-Phos that permeated PDCPD thimbles, the permeation of various molecules through the walls of the thimbles were investigated (Table 2.2). In these experiments, diphenylamine (NHPh₂) and a second substrate were added to the interior of a thimble at a 1:10 molar ratio. Solvent was added to the interiors and exteriors of the thimbles and the molecules were allowed to permeate through the walls of the thimble. The concentration of NHPh₂ and the substrate were found on the exteriors and interiors of the thimbles at 24 and 48 h. The results in Table

2.2 clearly demonstrate that PPh_3 , PCy_3 , NPh_3 , and NBu_3 , X-Phos did not permeate the walls of the thimbles when toluene was used as the solvent. Furthermore, PPh_3 did not permeate the walls of the thimbles when chloroform, toluene, hexane, or methanol was used as the solvent, but NHPPh_2 permeated the thimbles with each of these solvents. The ability of 1-octadecene, hexanoic acid, cholesterol, and nitrobenzaldehyde to permeate the membranes was studied, and each of these molecules permeated at reasonable rates.

Table 2.2 Permeation of NHPPh_2 and other molecules through the walls of a PDCPD thimble

Substrate	^c Se/Si of NHPPh_2		^f Se/Si of substrate	
	24 h	48 h	24 h	48 h
^a PPh_3	0.93	1	≤ 0.0085	≤ 0.010
^b PPh_3	0.86	1	≤ 0.0041	≤ 0.0055
^c PPh_3	0.55	1	≤ 0.0039	≤ 0.0077
^d PPh_3	0.29	1	≤ 0.0043	≤ 0.0071
^b PCy_3	0.86	1	≤ 0.0041	≤ 0.0046
^b NPh_3	0.86	1	≤ 0.0036	≤ 0.044
^b NBu_3	0.86	1	≤ 0.0041	≤ 0.0078
^b X-Phos	0.86	1	≤ 0.0035	≤ 0.0064
^b 0.05 $\text{Pd}(\text{OAc})_2$ + X-Phos	0.85	1	≤ 0.0033	≤ 0.0059
^b 0.05 $\text{Pd}(\text{OAc})_2$ + PPh_3	0.85	1	≤ 0.0032	≤ 0.0054
^b cholesterol	0.85	1	0.43	0.80
^b octadecene	0.85	1	0.61	1.0
^b hexanoic acid	0.86	1	0.7	1.0
^b nitrobenzaldehyde	0.86	1	0.75	1.0

^a The solvent on the interior and exterior of the thimbles was chloroform. ^bThe solvent was toluene. ^cThe solvent was hexane. ^dThe solvent was methanol. ^eThe ratio of the concentration of NHPPh_2 on the exterior (Se) to interior (Si) of the thimble. ^fThe ratio of the concentration of the substrate on the exterior (Se) to the interior (Si) of the thimble. Many of the substrates were not observed in the ^1H NMR spectra of aliquots removed from the exteriors of the thimbles so upper limits are given.

The flux of NHPH_2 through the walls of the PDCPD thimbles were measured as described in the supporting information. The values for the flux were 8.81×10^{-7} mmole $\text{cm}^{-2} \text{s}^{-1}$ in toluene, 4.81×10^{-7} mmole $\text{cm}^{-2} \text{s}^{-1}$ in hexanes, and 3.39×10^{-7} mmole $\text{cm}^{-2} \text{s}^{-1}$ in methanol. In contrast, the upper limit for the flux of PPh_3 , PCy_3 , NPh_3 , NBu_3 , and X-Phos through the walls of the thimbles was at least three orders of magnitude lower than that of NHPH_2 .

The large differences in flux resulted from small differences in cross-sectional areas (Figure 2.2).⁹⁰ Phosphines and trisubstituted amines possess rigid three-dimensional shapes and large cross-sectional areas of at least 0.49 nm^2 . In contrast, molecules that permeated PDCPD had lower cross sectional areas of 0.060 to 0.28 nm^2 (see the supporting information for cross sectional areas of all molecules in this article). It is notable that cholesterol (MW: 387 g mol^{-1}) and octadecene (MW: 252 g mol^{-1}) permeated the thimbles but lower molecular weight trisubstituted phosphines and amines did not permeate.

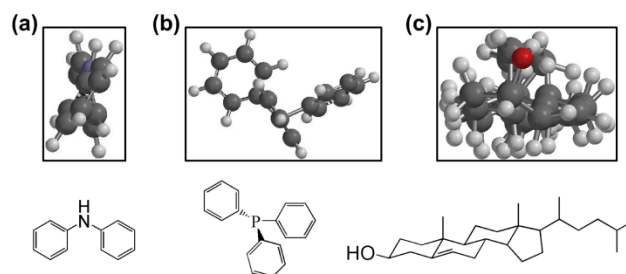


Figure 2.2 The ball and spoke models of a) NHPH_2 , b) PPh_3 , and c) cholesterol. The boxes around the images were used to determine the cross-sectional areas as described in the experimental.

There are several possible reasons for the retention of Pd on the interior of the thimbles that led to little to no detectable amounts of Pd in the products of the reactions in Table 2.1. Four possible reasons included that Pd was coordinated to the phosphine

and did not permeate because phosphines did not permeate the thimbles, Pd(II) may possess a low solubility in the hydrophobic matrix of PDCPD which lead to a low flux, Pd coordinated to the olefins in PDCPD which lead to a low rate of diffusion, or the Pd at the end of the reaction may have been primarily in the form of nano or microparticles which were too large to permeate PDCPD.

To study the effect, if any, that X-Phos had on the retention of Pd, several experiments were conducted. First, X-Phos and either Pd(OAc)₂ or Pd₂(dba)₃ were added to the interior of the thimble with toluene at the same ratio and concentration as was used in the reactions listed in Table 2.1. Next, toluene was added to the exterior of the thimbles and the system was stirred for 24 h. The solvent on the exterior of the thimble was removed from the flask and the amount of Pd in that solvent was analysed by ICP-OES. The percentage of the original amount of Pd(OAc)₂ and Pd₂(dba)₃ added to the thimbles that permeated to the exterior of the thimbles was only 0.34% and 0.13%, respectively. In identical experiments without X-Phos, only 0.37% and 0.32% of Pd(OAc)₂ and Pd₂(dba)₃ permeated to the exterior of the thimbles. Thus, the presence of X-Phos had no measurable effect on the retention of either Pd(0) or Pd(II). Although the exact mechanism for the retention of Pd is not known, it is clear that very little Pd permeated PDCPD with or without the presence of phosphines.

The ability to recycle a Pd/phosphine catalyst was investigated in a series of Buchwald-Hartwig coupling reactions between 4-bromotoluene and aniline using 5 mol% Pd(OAc)₂ and 10 mol% X-Phos (Table 2.3). The reaction was completed on the interior of a thimble and extracted to the exterior upon completion. Fresh KO^t-Bu, 4-bromotoluene, and aniline were added at the start of each cycle, but Pd and X-Phos were only added at the start of the first cycle.

Table 2.3 Recycling experiments for a Buchwald-Hartwig coupling reaction of bromotoluene and aniline.

^a Cycle	^b NMR yield (%)	^c Retention of Pd (%)	^d Concentration of Pd in product (ppm)
1	94	99.997	0.85
2	94	99.993	2.41
3	93	99.979	7.65
4	92	99.71	109
5	93	99.36	241

^aThe coupling reactions were completed at 80 °C for 7 h.

^bThese values were found using tetraethylene glycol as an internal standard. ^cThese values represent the amount of the Pd added to the interior of the thimble that did not extract to the exterior. ^dMeasured by ICP-OES.

The crude products were studied by ¹H NMR spectroscopy and no evidence of X-Phos was observed. The concentration of Pd in the crude product was also investigated by ICP-OES. In five cycles the amount of Pd that permeated to the exterior was between 0.003 and 0.64% of the amount of Pd that was originally added to the interior (Table 2.3). These reactions were run for 7 h at 80 °C and all went to quantitative conversions. To study catalyst stability, the reactions were run for only 3 h at 80 °C and then the product was extracted as before. The conversions for 4 cycles were 84, 76, 74, and 73% with retention of Pd between 99.97% and 99.77%. These experiments demonstrated that the catalyst maintained similar activities throughout these experiments.

Summary

The significance of this work is that the retention of Pd and phosphines was successful in reactions that used commercially available phosphines and Pd sources as homogeneous catalysts in solvent that has been shown by others to facilitate these reactions. No modifications to the catalyst or reaction conditions were necessary to retain Pd and phosphines. Other methods to retain and recycle Pd catalysts typically involve

attaching the Pd to a polymeric ligand, attaching the catalyst to a solid support which renders it heterogeneous, or the use of exotic ligands that allow the catalyst to partition into a second layer.^{81,83,91-96} These other methods require additional reactions to change the structure of a catalyst and affect its reactivity. In contrast, the method described in this article is successful for commercially available phosphines and Pd sources and the retention is implemented at the conclusion of the reaction. This is a new approach to retention that may be generally applicable to any ligands with cross-sectional areas larger than ca 0.50 nm².

Experimental Section

Materials

Dicyclopentadiene, palladium acetate, X-Phos, bromobenzene, bromotoluene, bromoanisole, iodotoluene, aniline, morpholine, phenylacetylene, diphenylamine, nitrobenzaldehyde, cholesterol, 1-octadecene, hexanoic acid, triphenylamine, tricyclohexylphosphine, triphenylamine, tributylamine, 1000 ppm palladium standard, and solvents were purchased at their highest purity from Aldrich and Acros and used as received. Geduran silica gel 60 from Fisher Scientific was used for all column chromatography.

Characterization

¹H NMR and ¹³C NMR spectra were acquired using a Bruker DPX-300 spectrometer at 300 MHz and 75 MHz, respectively, and referenced to TMS. Palladium concentrations were measured on a Varian 720-ES ICP optical emission spectrometer. IR spectra were acquired on a Bruker Tensor 27. The detector used was the standard room temperature DTGS (deuterated tri-glycine sulfate) detector.

Fabrication of PDCPD thimbles

A mold was prepared by placing an aluminum rod (18 mm x 86 mm) in a glass vial (20 mm x 78 mm) with paper spacers between the rod and glass. The rod was centered in the glass vial with the spacers and was 1 mm from the bottom of the glass vial. Commercially available dicyclopentadiene (24 mL, 0.177 mol) was heated at 35 °C for 10 minutes to melt it. The Grubbs second generation catalyst (15 mg, 0.017 mmol) was mixed with dichloromethane (0.5 mL) and added to the dicyclopentadiene and thoroughly mixed. This solution was then added to a mold via a pipette. The mold was heated in a water bath at 50 °C for 1.5 h. Next, the mold was immersed in liquid nitrogen to remove the glass vial from the PDCPD. The PDCPD on the rod was then swelled in dichloromethane mixed with ethyl vinyl ether to remove the PDCPD thimble from the aluminum rod. The thimbles were dried in air and then under vacuum.

A general description of how the experiments were completed using PDCPD thimbles

In the experiments described here, the PDCPD thimbles were initially added to glass reaction vessels. Next, the catalysts, solvent, and a stir bar were added to the interior of the thimbles. The reactions were completed at the indicated times and temperatures. Next, a stir bar was added to the exterior of the thimbles with solvent to extract the product. The extraction was based on diffusion as no external pressure was applied. The solvent on the exterior of the thimble was easily removed from the glass vessel.

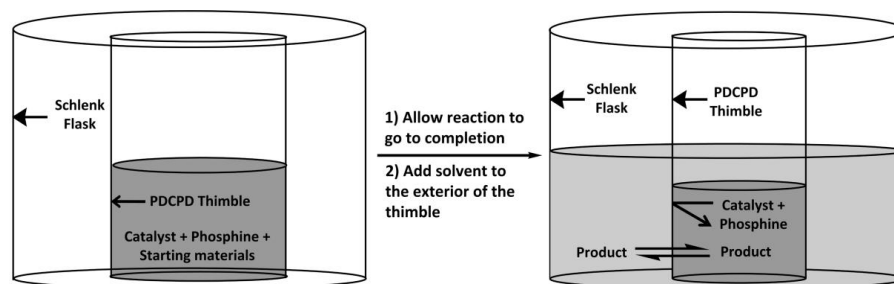


Figure 2.3 Reactions were completed on the interior of the thimbles without any solvent on the exterior. When the reaction was complete, solvent was added to the exterior to extract the product.

Buchwald-Hartwig reaction of bromobenzene with aniline

(Entry 1, Table 2.1)

A PDCPD thimble containing Pd(OAc)₂ (10 mg, 0.045 mmol), X-phos (42 mg, 0.089 mmol), and KO^t-Bu (0.139 g, 1.25 mmol) was placed in a Schlenk flask with a stir bar. The whole set-up was evacuated and backfilled with N₂ three times. Under flowing N₂, bromobenzene (0.093 ml, 0.89 mmol), aniline (0.097 ml, 1.07 mmol), and toluene (5 mL) were added. The Schlenk flask was then heated in an oil bath at 80 °C for 7 h. The reaction was allowed to cool to room temperature. Hexane (15 mL) was added to the exterior of the thimble to extract the product. During the extraction, the solvents on the interior and exterior of the thimble were stirred. After 24 h, the solvent on the exterior was replaced with 15 mL of fresh hexane. After 48 h, the hexane extracts were combined, and the solvent was removed in vacuo. The amine was isolated as a white solid by column chromatography using hexanes/EtOAc (95/5). NMR spectra matched those reported in the literature.⁹⁷ ¹H NMR (300 MHz, CDCl₃, δ): 7.25-7.28 (m, 4H), 7.07 (d, 4H), 6.91 (t, 2H), 5.72 (s, 1H). ¹³C NMR (75 MHz; CDCl₃, δ): 145.91, 132.18, 123.80, 120.61.

Buchwald-Hartwig reaction of 4-bromotoluene with aniline

(Entry 2, Table 2.1)

The same procedure as entry 1 was followed. The amine was isolated as a yellow solid by column chromatography using hexanes/EtOAc (95/5). NMR spectra matched those reported in the literature.⁹⁸ ¹H NMR (300 MHz, CDCl₃, δ): 7.20 (t, 2H), 7.04 (d, 2H), 6.93-6.99 (m, 4H), 6.81 (t, 1H), 5.54 (s, 1H), 2.24 (s, 3H). ¹³C NMR (75 MHz; CDCl₃, δ): 143.07, 139.37, 130.05, 128.98, 128.44, 119.40, 117.99, 115.96, 19.84.

Buchwald-Hartwig reaction of 4-bromoanisole with aniline

(Entry 3, Table 2.1)

The same procedure as entry 1 was followed. The amine was isolated as a brown solid by column chromatography using hexanes/EtOAc (95/5). NMR spectra matched those reported in the literature.^{97,99} ¹H NMR (300 MHz, CDCl₃, δ): 7.21 (t, 2H), 7.09 (d, 2H), 6.83-6.92 (m, 5H), 5.50 (s, 1H), 3.80 (s, 3H). ¹³C NMR (75 MHz; CDCl₃, δ): 155.32, 143.04, 130.08, 128.96, 128.44, 119.40, 117.99, 115.95, 55.6.

Buchwald-Hartwig reaction of 4-bromoanisole with

morpholine (Entry 4, Table 2.1)

The same procedure as entry 1 was followed. The amine was isolated as a white solid by column chromatography using hexanes/EtOAc (95/5). NMR spectra matched those reported in the literature.¹⁰⁰ ¹H NMR (300 MHz, CDCl₃, δ): 6.83-6.91 (m, 4H), 3.84-3.87 (m, 4H), 3.77 (s, 3H), 3.03-3.07 (m, 4H). ¹³C NMR (75 MHz; CDCl₃, δ): 156.63, 148.31, 120.51, 117.17, 69.74, 58.26, 53.50.

Buchwald-Hartwig reaction of 4-iodotoluene with aniline

(Entry 5, Table 2.1)

The same procedure as entry 1 was followed. The amine was isolated as a yellow solid by column chromatography using hexanes/EtOAc (95/5). NMR spectra matched

those reported in the literature.⁹⁸ ¹H NMR (300 MHz, CDCl₃, δ): 7.23-7.27 (t, 2H), 7.09 (d, 2H), 7.01-7.05 (m, 4H), 6.87-6.93 (t, 1H), 5.63 (s, 1H), 2.31 (s, 3H). ¹³C NMR (75 MHz; CDCl₃, δ): 143.04, 139.37, 130.05, 128.96, 128.44, 119.40, 117.99, 115.96, 19.84.

Sonogashira coupling of 4-bromoanisole with
phenylacetylene (Entry 6, Table 2.1)

A PDCPD thimble containing Pd₂(dba)₃ (8 mg, 0.089 mmol), X-phos (84 mg, 0.178 mmol), and CuI (22.4 mg, 0.12 mmol) was placed in a Schlenk flask with a stir bar. The whole set-up was evacuated and backfilled with N₂ three times. Under flowing N₂, 4-bromoanisole (0.55 ml, 4.45 mmol), phenylacetylene (0.65 ml, 5.91 mmol), triethylamine (0.82 mL, 5.91 mmol), and toluene (5 mL) were added. The Schlenk flask was then heated in an oil bath at 80 °C for 7 h. The reaction was allowed to cool to room temperature. Hexane (15 mL) was added to the exterior of the thimble to extract the product. After 24 h, the solvent on the exterior was replaced with 15 mL of fresh hexane. After 48 h, the hexane extracts were combined and the solvent was removed in vacuo. The product was isolated by column chromatography using hexanes/EtOAc (95/5). NMR spectra matched those reported in the literature.¹⁰¹ ¹H NMR (300 MHz, CDCl₃, δ): 7.45-7.52 (m, 4H), 7.31-7.33 (m, 3H), 6.85 (d, 2H), 3.82 (s, 3H). ¹³C NMR (75 MHz; CDCl₃, δ): 159.97, 133.39, 131.79, 128.66, 128.28, 123.95, 115.73, 114.35, 89.74, 88.43, 55.61.

Sonogashira coupling of 4-bromotoluene with
phenylacetylene (Entry 7, Table 2.1)

The same procedure as entry 6 was followed. The product was extracted by column chromatography using hexanes/EtOAc (95/5). NMR spectra matched those reported in the literature.¹⁰¹ ¹H NMR (300 MHz, CDCl₃, δ): 7.49-7.52 (m, 2H), 7.40 (d, 2H), 7.29-7.31 (m, 3H), 7.11 (d, 2H), 2.33 (s, 3H). ¹³C NMR (75 MHz; CDCl₃, δ): 138.73, 131.92, 131.87, 129.49, 128.68, 128.44, 123.87, 120.58, 89.96, 89.13, 21.85.

Procedure to measure the flux of diphenylamine and phosphine ligands or organic substrates (Table 2.2)

Diphenylamine (0.059 mmol) and phosphine ligand or organic substrate (0.59 mmol) were dissolved in 4 mL of toluene and added to the interior of a PDCCPD thimble. On the exterior 10 mL of fresh toluene was added. Aliquots (0.2 mL) were removed from the interior and exterior after 24 h and larger aliquots (1 mL) were removed from the interior and exterior after 48 h. A solution was prepared by adding 0.1 mL tetraethyleneglycol to 49.9 mL CHCl₃. 1 mL of this solution was diluted by adding 49 mL CHCl₃. Known amounts of the above solution were added to the aliquots to provide an internal standard to find the absolute concentration of the reagents. The solvent was removed in vacuo. ¹H NMR spectroscopy of the aliquots provided Se/Si after 24 h and 48 h. For each aliquot of diphenylamine, the integration of the multiplet at 3.6-3.7 ppm corresponding to tetraethylene glycol was compared to the integration of the peak at 6.91 ppm for diphenylamine to calculate the absolute amount of diphenylamine in the aliquot. The amount of other substrates in each aliquot was measured using the same method, where the integration of a peak corresponding to the molecule was compared to the integration of the tetraethylene glycol peak.

Procedure to recycle Pd and X-Phos in a Buchwald-Hartwig reaction (Table 2.3)

A PDCCPD thimble containing Pd(OAc)₂ (10 mg, 0.045 mmol), X-Phos (42 mg, 0.089 mmol), and KO^t-Bu (0.14 g, 1.25 mmol) was placed in a Schlenk flask with a stir bar. The whole set-up was evacuated and backfilled with N₂ three times. Under flowing N₂, 4-bromotoluene (0.11 mL, 0.89 mmol), aniline (0.097 mL, 1.07 mmol), and toluene (5 mL) were added. The Schlenk flask was then heated in an oil bath at 80 °C for 7 h. Hexane (15 mL) was added to the exterior of the thimble to extract the product. During the extraction, the solvent on the interior and exterior of the thimble was stirred. After 24

h, the solvent on the exterior was replaced with 15 mL of fresh hexane. After 48 h, the hexane extracts were combined and the hexane was removed in vacuo. Toluene on the interior of the thimble was removed in vacuo. Fresh toluene (4 mL) was added to the interior of the thimble. The phosphine and palladium were allowed to diffuse to the toluene on the interior of the thimble for 24 h.

KO*t*-Bu (0.139 g, 1.25 mmol), 4-bromotoluene (0.11 mL, 0.89 mmol), and aniline (0.097 mL, 1.07 mmol) were added to the interior of the thimble for cycle 2. The Schlenk flask was heated at 80° C. After the reaction went to completion for 2nd cycle, the same procedure was followed as for cycle 1. Palladium and phosphine ligand could be recycled for 5 cycles by the same procedure. The thimble broke during the reaction of the 6th cycle.

The hexane extracts were analyzed to calculate the yield of product and the retention of palladium for each cycle. The yield of product was calculated based on ¹H NMR spectra of the extracts using internal standards of tetraethylene glycol. No evidence of the phosphine was found in the products in the ¹H NMR spectra of extracts. The same extracts were used to prepare the sample for ICP-OES. The ICP-OES results determined the retention of palladium for each cycle.

Procedure to recycle Pd and X-Phos in a Buchwald-Hartwig reaction (3 h reaction cycles)

A PDCPD thimble containing Pd(OAc)₂ (10 mg, 0.045 mmol), X-Phos (42 mg, 0.089 mmol), and KO*t*-Bu (0.14 g, 1.25 mmol) was placed in a Schlenk flask with a stir bar. The whole set-up was evacuated and backfilled with N₂ three times. Under flowing N₂, 4-bromotoluene (0.11 mL, 0.89 mmol), aniline (0.097 mL, 1.07 mmol), and toluene (5 mL) were added. The Schlenk flask was then heated in an oil bath at 80 °C for 3 h. Hexane (15 mL) was added to the exterior of the thimble to extract the product. During the extraction, the solvent on the interior and exterior of the thimble was stirred. After 24 h, the solvent on the exterior was replaced with 15 mL of fresh hexane. After 48 h, the

hexane extracts were combined and the hexane was removed in vacuo. Toluene on the interior of the thimble was removed in vacuo. Fresh toluene (4 mL) was added to the interior of the thimble. The phosphine and palladium were allowed to diffuse to toluene on the interior of the thimble for 24 h.

KO t -Bu (0.139 g, 1.25 mmol), 4-bromotoluene (0.11 mL, 0.89 mmol), and aniline (0.097 mL, 1.07 mmol) were added to the interior of the thimble for cycle 2. The Schlenk flask was heated at 80° C. After 3 h of reaction for 2nd cycle, the same procedure was followed as for cycle 1. Four cycles were completed and each had only 3 h of heating at 80 °C to complete the reactions. The thimble broke during the extraction of the 5th cycle.

The hexane extracts were analyzed to calculate the yield of product and the retention of palladium for each cycle (Table 2.4). The yield of product was calculated based on ¹H NMR spectra of the extracts using internal standards of tetraethylene glycol. No evidence of the phosphine was found in the products in the ¹H NMR spectra of extracts. The same extracts were used to prepare the sample for ICP-OES. The ICP-OES results determined the retention of palladium for each cycle.

Table 2.4 Recycling experiments of 4-bromotoluene and aniline.

Cycle	Conversion	^a NMR yield (%)	^b Retention of Pd (%)	^c Concentration of Pd in product (ppm)
1	84	77	99.97	10.1
2	76	70	99.97	10.1
3	74	67	99.77	82.1
4	73	65	99.97	10.1

^aThese values were found using tetraethylene glycol as an internal standard. ^bThese values represent the amount of the Pd added to the interior of the thimble that did not extract to the exterior. ^cMeasured by ICP-OES.

The results demonstrated that the catalyst activity was nearly constant over the course of 4 cycles. The product and unreacted starting materials were extracted to the

exterior of PDCPD thimbles leaving behind palladium and X-Phos inside the thimble. The retention of palladium was excellent for 4 cycles.

ICP-OES sample preparation

After each reaction in Table 1 went to completion on the interior of a thimble, hexane (15 mL) was added to the exterior of the thimble. After 24 h, the solvent on the exterior was replaced with 15 mL of fresh hexane. After 48 h, the hexane extracts were combined, and the solvent was removed in vacuo. HCl (0.85 mL), HNO₃ (0.85 mL), and H₂O (4.3 mL) were added to the crude product. A watch glass was placed on top of the jar and it was heated to 95 °C for 30 min. The solution was diluted to 10 mL with HCl to prepare the sample. The 1000 ppm palladium ICP standard was diluted with HCl to prepare standards to calibrate the instrument. The internal standard for the measurement was 1 ppm yttrium solution. After calibration with the standards, the sample gave a concentration in ppm.

Procedure to measure flux of diphenylamine

Diphenylamine (0.59 mmol) was dissolved in 4 mL of solvent and added to the interior of a PDCPD thimble. Solvent (10 mL) was added to the exterior. Aliquots of 0.1 mL were taken from the interior and the exterior of the thimble after 2, 4, 6, 8, 10, 12, 14, 16, 18, 22, 24, 26, 36, and 48 h. A solution was prepared by adding 0.1 mL tetraethyleneglycol to 49.9 mL CHCl₃. This solution was diluted by adding CHCl₃ (49 mL) to 1 mL of the original solution. Known amounts of the above solution were added to the aliquots to provide an internal standard to find absolute concentration of diphenylamine. The solvent was removed in vacuo. ¹H NMR spectroscopy of the aliquots provided Se/Si at different time intervals. The concentrations of diphenylamine as a function of time are shown in Figure 2.4 and Figure 2.5.

The permeability coefficient, P (cm s⁻¹), was measured by fitting the data to the equation (1) shown below.

$$C_1 = \frac{M_0}{V_1} \left(\frac{V_1}{V_1 + V_2} + \frac{V_2}{V_1 + V_2} \exp\left(-\left(1 + \frac{V_1}{V_2}\right) \frac{PA t}{V_1}\right) \right)$$

Where C_1 is the concentration on the upstream side of the membrane, V_1 is the upstream volume, V_2 is the downstream volume, M_0 is the total moles of HNPh₂ in the system, A is the membrane area, and t is the time. The permeability coefficient indicates how rapidly a solute will pass through a membrane and is linearly proportional to diffusion coefficient, D , according to $P = D/\lambda$ where λ is the membrane thickness.

The data measured for the concentration of HNPh₂ through PDCPD in toluene, hexanes, and methanol all fit the equation well (Figures 2.4 and 2.5). The values for the permeation constant were $3.39 \times 10^{-2} \text{ cm s}^{-1}$ in toluene, $2.45 \times 10^{-2} \text{ cm s}^{-1}$ in hexanes, and $2.27 \times 10^{-2} \text{ cm s}^{-1}$ in methanol. The decrease in these values as the solvent was changed from one that swells PDCPD well to one that did not swell it well was expected because PDCPD is a hard, cross-linked polymer that becomes rubbery when swollen. The amount that each solvent swells PDCPD is found in the following reference.¹⁰²

Flux is defined as the amount of a molecule that moves through a unit area per unit time. To find the flux of diphenylamine in toluene, hexanes, and methanol the initial concentrations of diphenylamine on the exterior were used (Figures 3, 4, and 5). At early times the flux of diphenylamine was almost entirely in one direction, so this approximation was used to calculate flux. The flux was found from the slope of a plot of the amount of diphenylamine on the exterior of the thimble versus time.

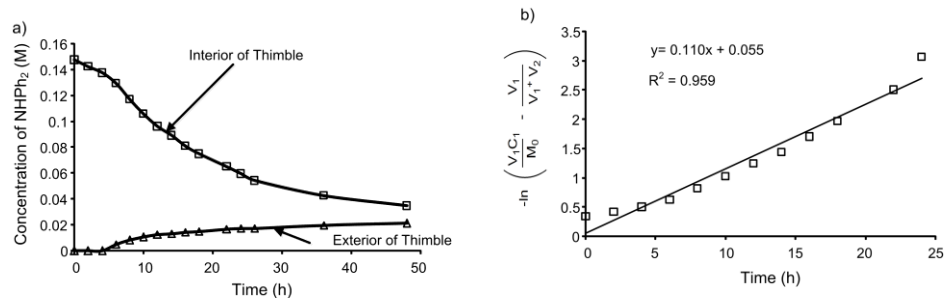


Figure 2.4 Permeation of diphenylamine in methanol. a) Diphenylamine was added to the interior of a thimble with methanol on the exterior and interior. The concentration of diphenylamine was monitored as a function of time and b) the data was fit to the equation in the text.

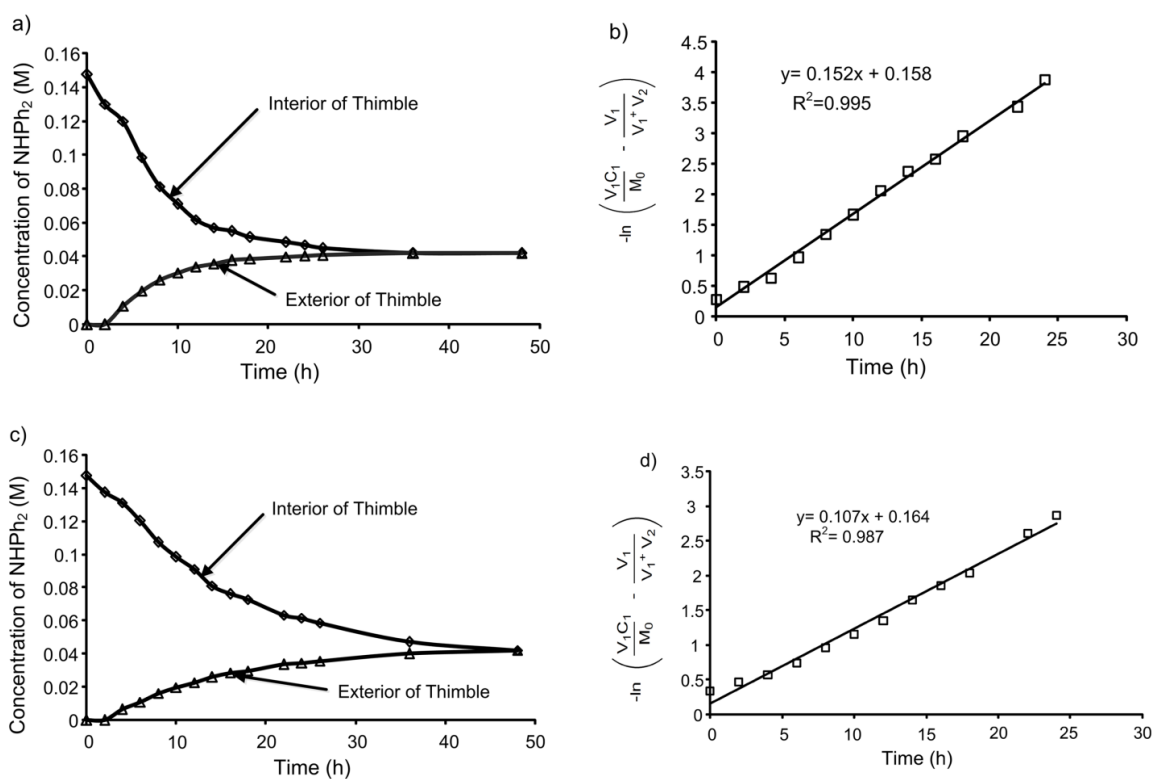


Figure 2.5 Permeation of diphenylamine in organic solvents. a) Diphenylamine was added to the interior of a thimble with toluene on the exterior and interior. The concentration of diphenylamine was monitored as a function of time and b) the data was fit to the equation in the text. c) and d) An identical experiment was completed using hexanes as the solvent.

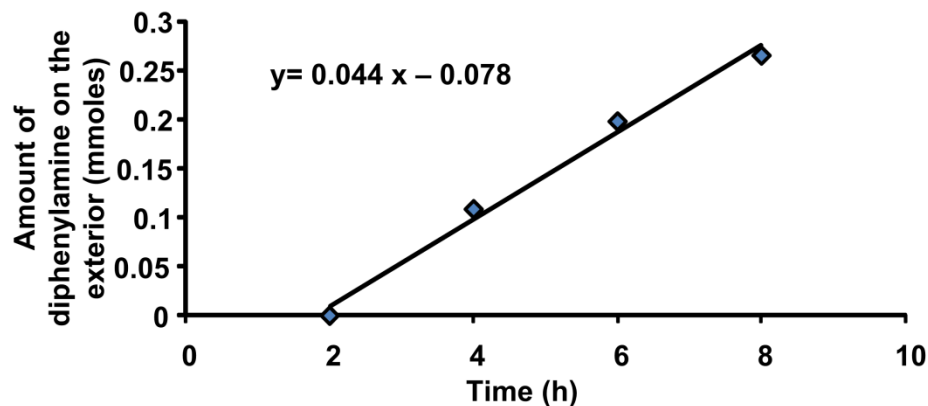


Figure 2.6 Flux of diphenylamine in toluene.

Inner radius of the thimble = 0.9 cm

Height of solvent in the thimble = 2 cm

Area of the thimble = $\pi r^2 + 2\pi rh = 13.85 \text{ cm}^2$

Flux = Slope / Area

Flux of diphenylamine = $3.17 \times 10^{-6} \text{ moles/cm}^2 \text{ h}$ for toluene

$1.73 \times 10^{-6} \text{ moles/cm}^2 \text{ h}$ for hexanes

$1.22 \times 10^{-6} \text{ moles/cm}^2 \text{ h}$ for methanol

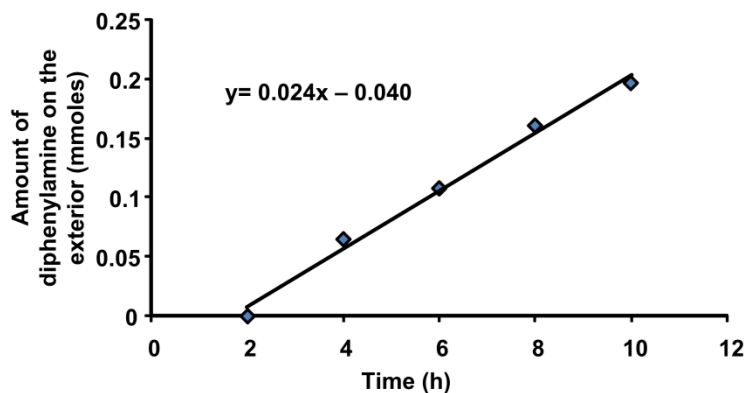


Figure 2.7 Flux of diphenylamine in hexanes.

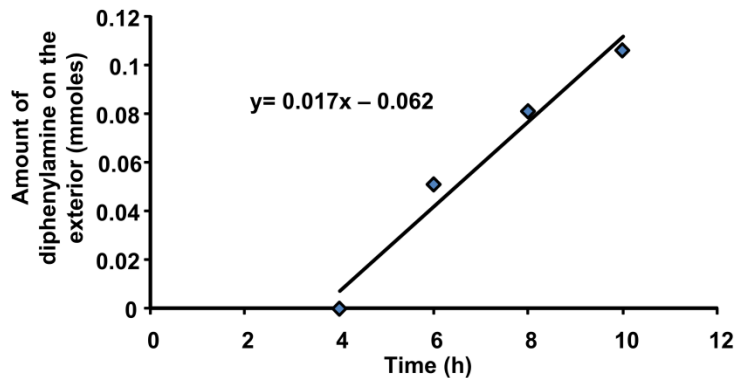


Figure 2.8 Flux of diphenylamine in methanol.

Procedure to measure the retention of Pd(OAc)₂ without X- Phos present

Pd(OAc)₂ (9.9 mg, 0.044 mmol) and octadecene (0.140 g, 0.565 mmol) were dissolved in 4 mL of toluene and added to the interior of a PDCPD thimble. Toluene (10 mL) was added to the exterior of the thimble. Aliquots (0.1 mL) were removed from the interior and exterior after 48 h. A solution was prepared by adding 0.1 mL tetraethyleneglycol to 49.9 mL CHCl₃. 1 mL of this solution was diluted by adding 49 mL CHCl₃. Known amounts of the above solution were added to the aliquots to provide an internal standard to find the absolute concentration of octadecene. The solvent was removed in vacuo. The concentrations of octadecene on the interior and exterior of the thimbles were measured from the ¹H NMR spectra of the aliquots. The remaining solvent from the interior and exterior of the thimbles were removed separately and evaporated in vacuo. HCl (0.85 mL), HNO₃ (0.85 mL), and H₂O (4.3 mL) were added to the interior and exterior samples in a glass vial. A watch glass was placed on top of the vials and they were heated to 95 °C for 30 min. The solution was diluted to 10 mL with HCl to prepare the sample. The 1000 ppm palladium ICP standard was diluted with HCl to prepare standards to calibrate the instrument. The internal standard for the measurement was 1

ppm yttrium solution. After calibration with the standards, the concentration of Pd in the samples from the interior and exterior of the thimbles was measured.

Procedure to measure retention of Pd(OAc)₂ with X-Phos

present

Pd(OAc)₂ (9.9 mg, 0.044 mmol), X-Phos (0.042 g, 0.088 mmol) and octadecene (0.140 g, 0.565 mmol) were dissolved in 4 mL of toluene and added to the interior of a PDCPD thimble. Toluene (10 mL) was added to the exterior of the thimble. Aliquots (0.1 mL) were removed from the interior and exterior after 48 h. A solution was prepared by adding 0.1 mL tetraethyleneglycol to 49.9 mL CHCl₃. 1 mL of this solution was diluted by adding 49 mL CHCl₃. Known amounts of the above solution were added to the aliquots to provide an internal standard to find the absolute concentration of octadecene. The solvent was removed in vacuo. The concentrations of octadecene on the interior and exterior of the thimbles were measured from the ¹H NMR spectra of the aliquots. The remaining solvent from the interior and exterior of the thimbles were removed separately and evaporated in vacuo. The samples removed from the interior and exterior of the thimbles were analyzed by ICP-OES as described above.

Procedure to measure retention of Pd₂(dba)₃ without X-

Phos present

Pd₂(dba)₃ (9.2 mg, 0.01 mmol) and octadecene (0.140 g, 0.565 mmol) were dissolved in 4 mL of toluene and added to the interior of a PDCPD thimble. Toluene (10 mL) was added to the exterior of the thimble. Aliquots (0.1 mL) were removed from the interior and exterior after 48 h. A solution was prepared by adding 0.1 mL tetraethyleneglycol to 49.9 mL CHCl₃. 1 mL of this solution was diluted by adding 49 mL CHCl₃. Known amounts of the above solution were added to the aliquots to provide an internal The concentrations of octadecene on the interior and exterior of the thimbles were measured from the ¹H NMR spectra of the aliquots. The remaining solvent from the

interior and exterior of the thimbles were removed separately and evaporated in vacuo. HCl (0.85 mL), HNO₃ (0.85 mL), and H₂O (4.3 mL) were added to the interior and exterior samples in a glass vial. A watch glass was placed on top of the vials and they were heated to 95 °C for 30 min. The solution was diluted to 10 mL with HCl to prepare the sample. The 1000 ppm palladium ICP standard was diluted with HCl to prepare standards to calibrate the instrument. The internal standard for the measurement was 1 ppm yttrium solution. After calibration with the standards, the concentration of Pd in the samples from the interior and exterior of the thimbles was measured.

Procedure to measure retention of Pd₂(dba)₃ with X-Phos

present

Pd₂(dba)₃ (9.2 mg, 0.01 mmol), X-Phos (4.8 mg, 0.01 mmol) and octadecene (0.140 g, 0.565 mmol) were dissolved in 4 mL of toluene and added to the interior of a PDCPD thimble. Toluene (10 mL) was added to the exterior of the thimble. Aliquots (0.1 mL) were removed from the interior and exterior after 48 h. A solution was prepared by adding 0.1 mL tetraethyleneglycol to 49.9 mL CHCl₃. 1 mL of this solution was diluted by adding 49 mL CHCl₃. Known amounts of the above solution were added to the aliquots to provide an internal standard to find the absolute concentration of octadecene. The solvent was removed in vacuo. The concentrations of octadecene on the interior and exterior of the thimbles were measured from the ¹H NMR spectra of the aliquots. The remaining solvent from the interior and exterior of the thimbles were removed separately and evaporated in vacuo. The samples removed from the interior and exterior of the thimbles were analyzed by ICP-OES as described above.

Measurement of the critical area

Each molecule was drawn in Spartan '08 V1.2.0 and imaged using a ball and spoke representation. The energy was minimized by finding the equilibrium geometry at ground state with a semi-empirical method using AM1 parameters. The surface area and

molecular volume were calculated based on a space filling model. The space filling model was a 3D molecular model with atoms represented by spheres whose radius was assumed to be the Van der Waals radius determined by the electron density cut-off at $0.002 \text{ electrons}/\text{\AA}^3$. Each molecule was analyzed to find the conformation with the lowest rectangular, cross-sectional area (Table 2.5).

In Figure 6 two different images of the lowest energy conformer of diphenylamine are shown using ball and spoke models. Beneath these images are diphenylamine with an arrow to indicate how the molecule was viewed to find the cross-sectional area. To find the minimum cross-sectional area (Figure 2.9a), the molecule was viewed from many different angles. The image in Figure 2.9b is shown to demonstrate one of many ways to view diphenylamine that had a much larger cross-sectional area than in Figure 6a. The lowest cross-sectional area for triphenylphosphine (Figure 2.10) and cholesterol (Figure 2.11) were found using the same method.

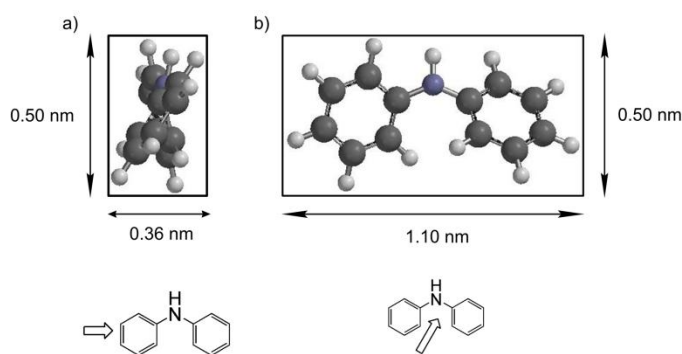


Figure 2.9 Two views of the lowest energy conformer of diphenylamine. The image in a) has the lowest cross-sectional area and the image in b) has a much larger cross-sectional area.

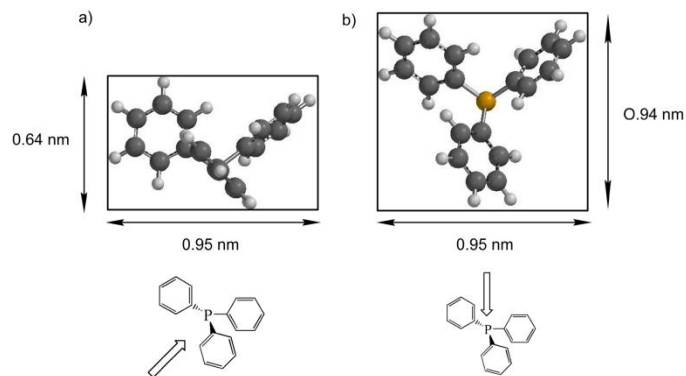


Figure 2.10 Two views of the lowest energy conformation of triphenylphosphine. The image in a) has the lowest cross-sectional area and the image in b) has a much larger cross-sectional area.

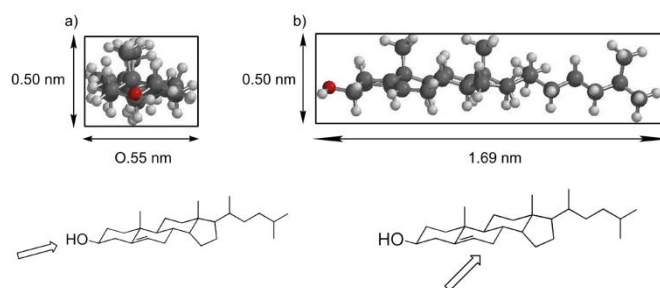
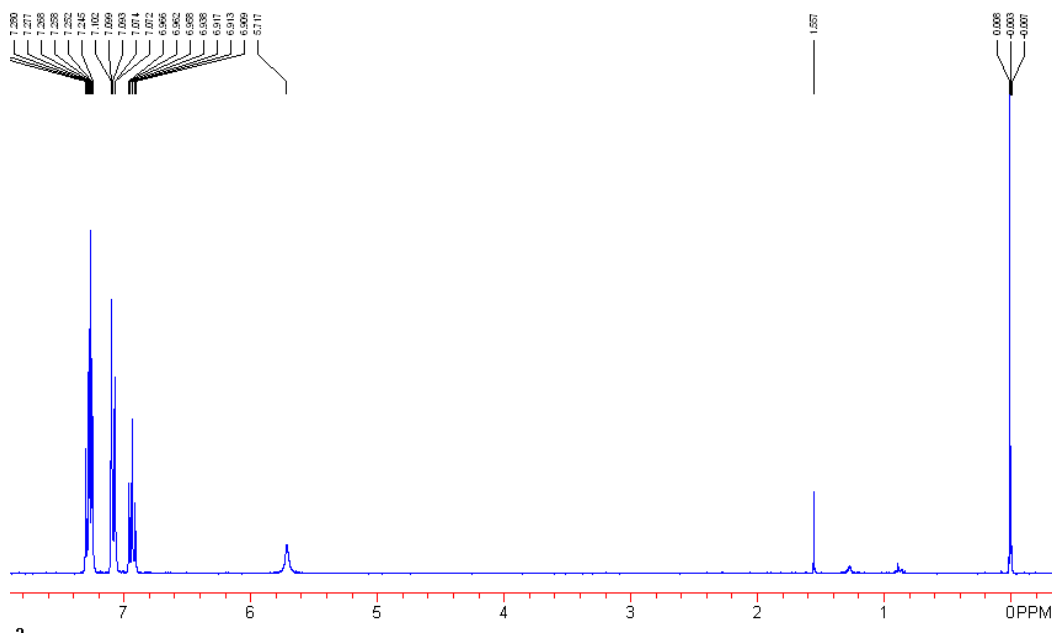
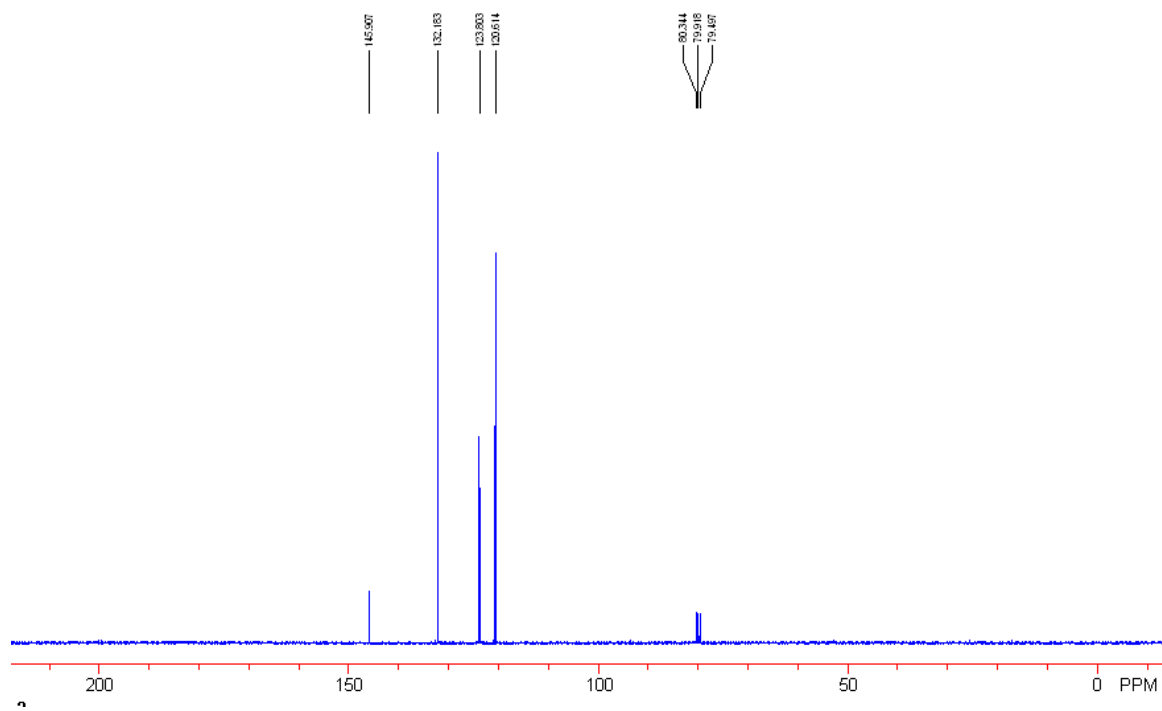
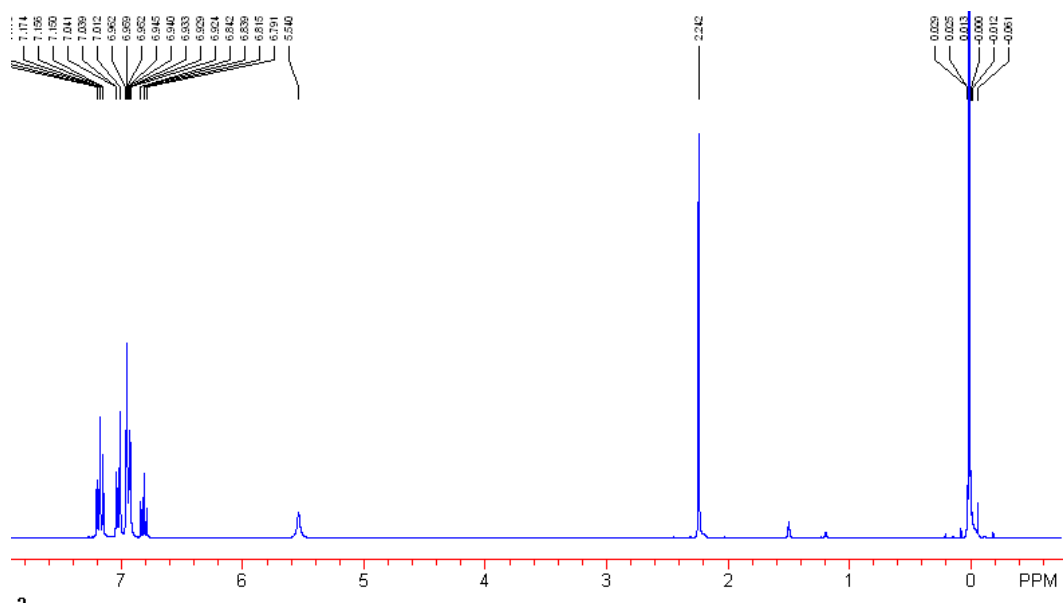


Figure 2.11 Two views of the lowest energy conformation of cholesterol. The image in a) has the lowest cross-sectional area and the image in b) has a much larger cross-sectional area.

Table 2.5 The physical parameters of molecules reported in this article.

Molecule	Permeates PDCPD	Molecular Weight (g mol ⁻¹)	Surface Area (nm ²)	Molecular Volume (nm ³)	Critical Area (nm ²)
hexanoic acid	Yes	116	1.65	0.135	0.067
<i>p</i> -nitrobenzaldehyde	Yes	151	1.64	0.142	0.060
diphenylamine	Yes	169	2.09	0.195	0.18
<i>N</i> -phenyl- <i>p</i> -toluidine	Yes	183	2.30	0.213	0.24
4-(4-methoxyphenyl)morpholine	Yes	191	2.34	0.217	0.20
4-(phenylethynyl)toluene	Yes	192	2.48	0.229	0.10
<i>N</i> -phenyl- <i>p</i> -anisidine	Yes	199	2.40	0.222	0.27
4-(phenylethynyl)anisole	Yes	208	2.58	0.238	0.24
octadecene	Yes	252	3.87	0.341	0.067
cholesterol	Yes	387	4.49	0.454	0.28
NBu ₃	No	185	2.86	0.249	0.50
NPh ₃	No	245	2.86	0.279	0.49
PPh ₃	No	262	2.92	0.286	0.61
PCy ₃	No	280	3.24	0.323	0.57
X-Phos	No	476	5.43	0.554	0.97

Figure 2.12 ¹H NMR spectrum of Entry 1, Table 2.1.

Figure 2.13 ^{13}C NMR spectrum of Entry 1, Table 2.1.Figure 2.14 ^1H NMR spectrum of Entry 2, Table 2.1.

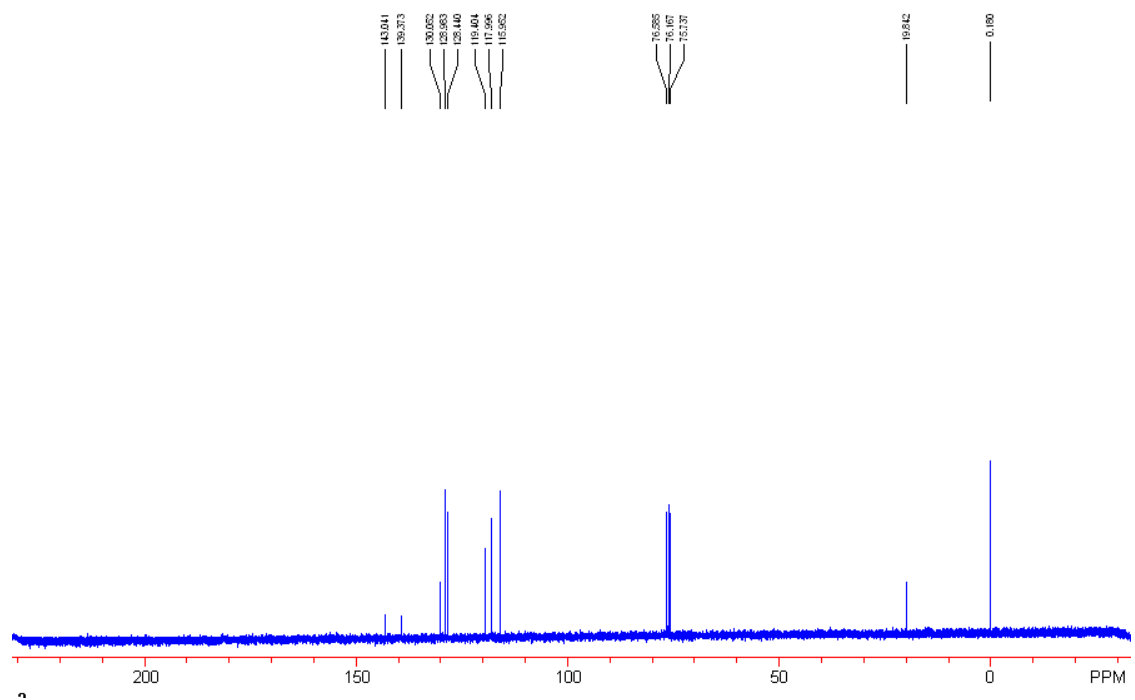


Figure 2.15 ^{13}C NMR spectrum of Entry 2, Table 2.1.

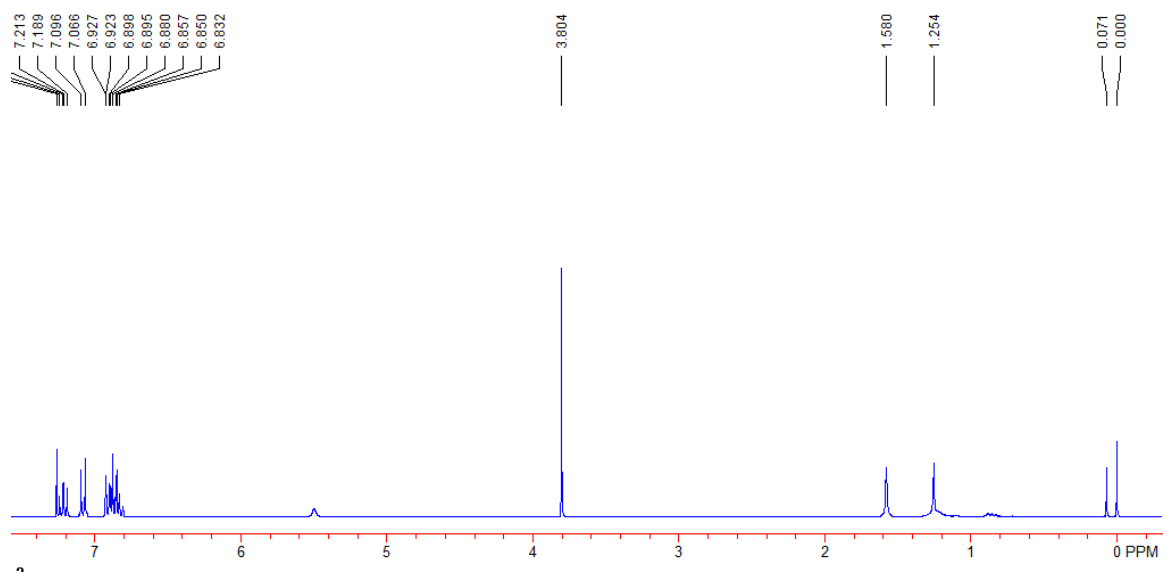


Figure 2.16 ^1H NMR spectrum of Entry 3, Table 2.1.

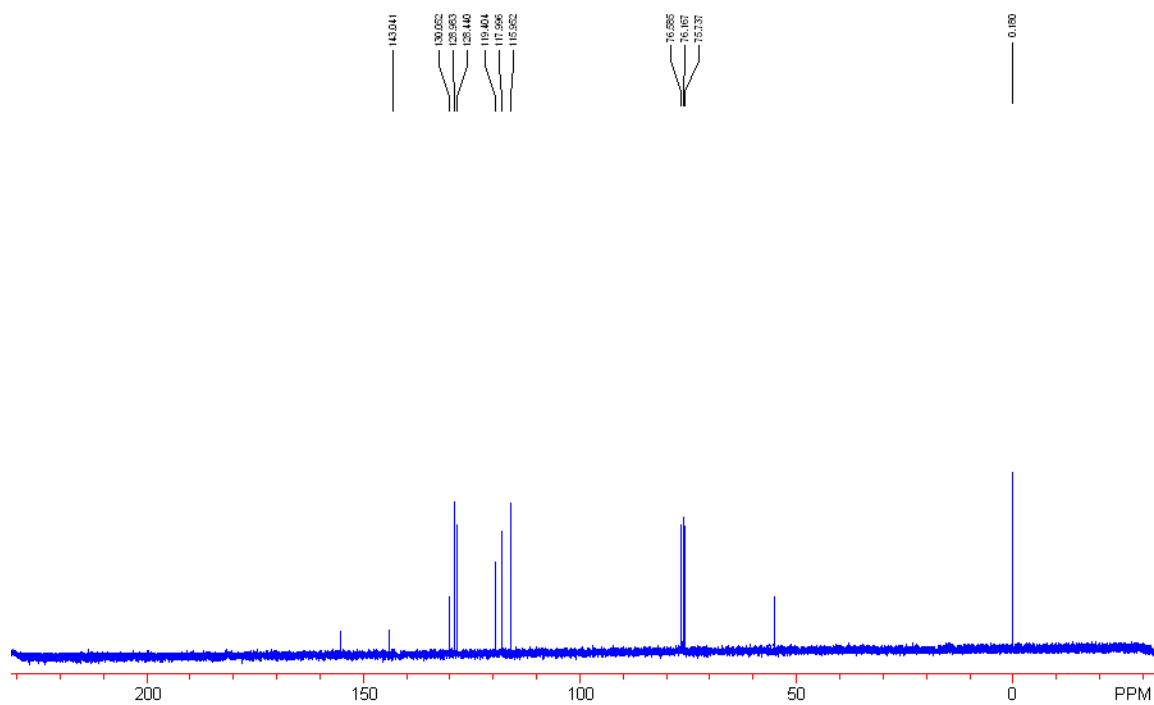


Figure 2.17 ^{13}C NMR spectrum of Entry 3, Table 2.1.

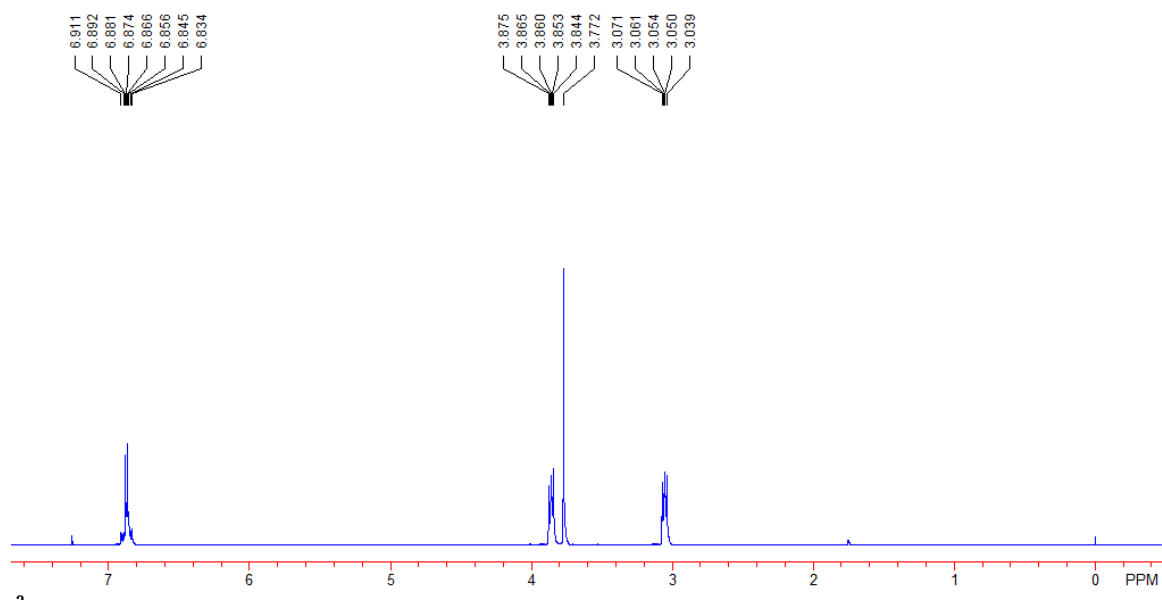


Figure 2.18 ^1H NMR spectrum of Entry 4, Table 2.1.

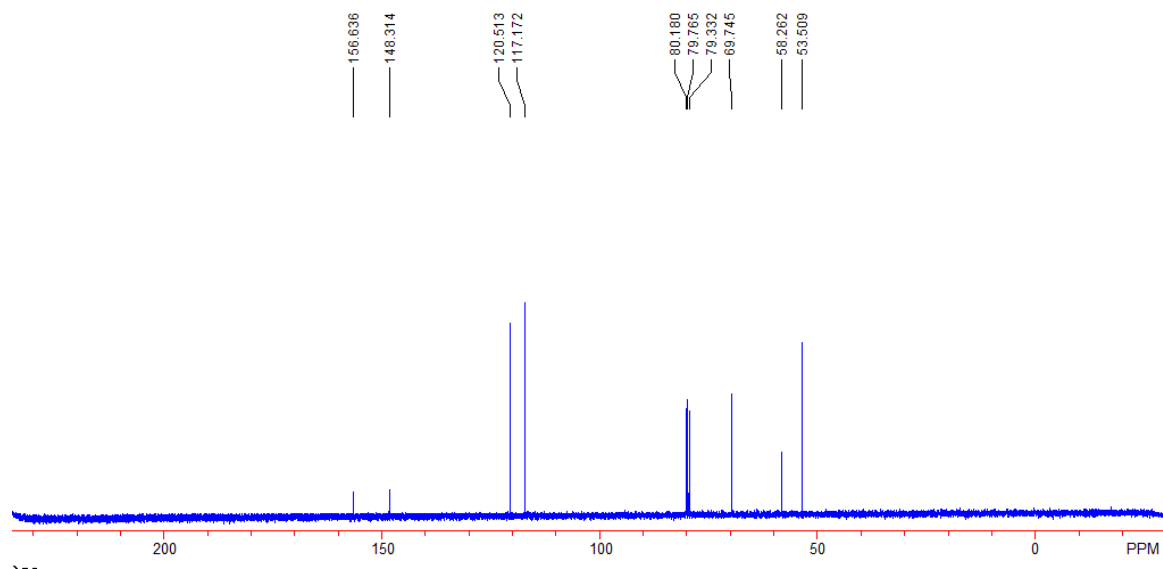


Figure 2.19 ^{13}C NMR spectrum of Entry 4, Table 2.1.

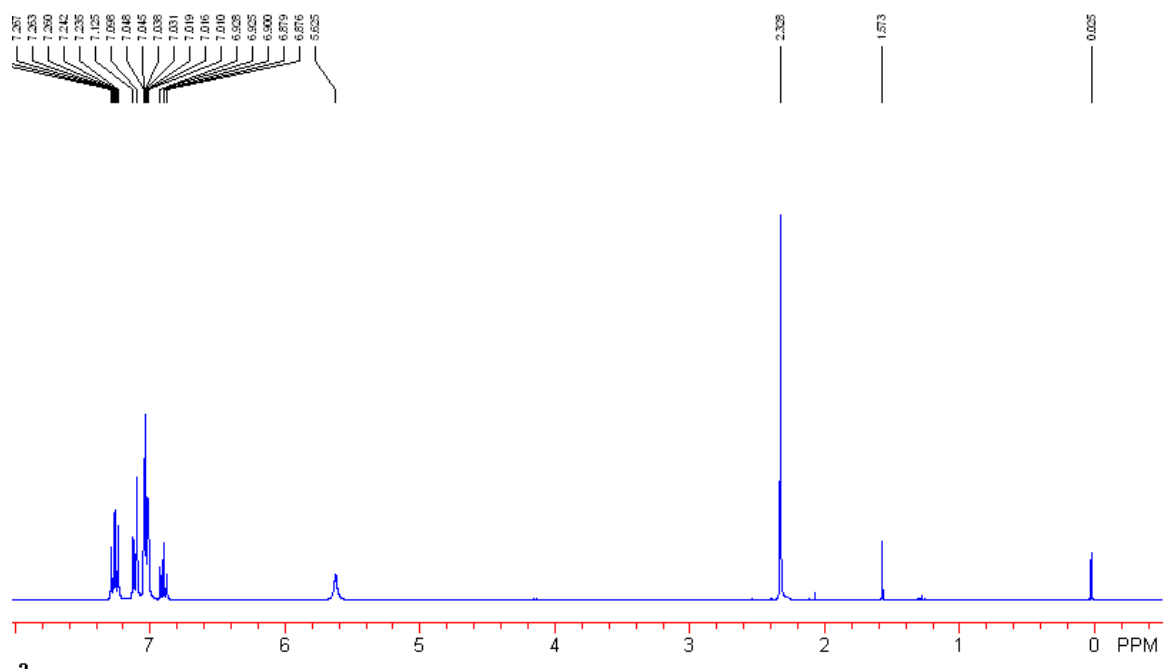


Figure 2.20 ^1H NMR spectrum of Entry 5, Table 2.1.

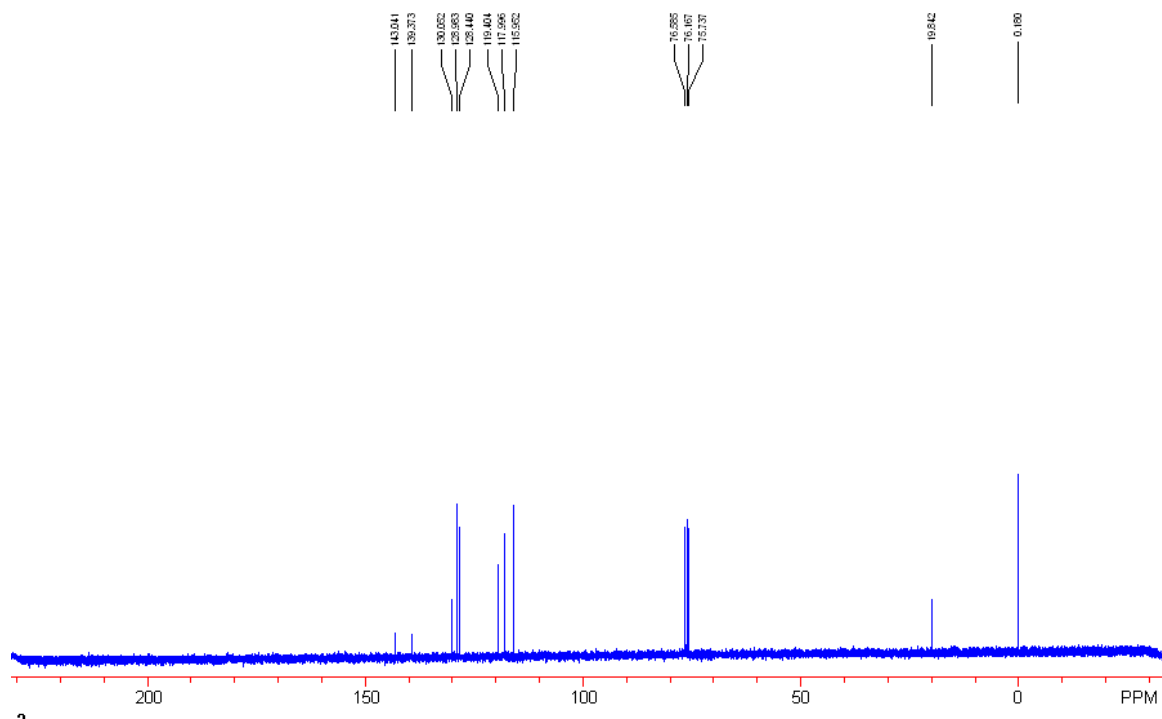


Figure 2.21 ¹³C NMR spectrum of Entry 5, Table 2.1.

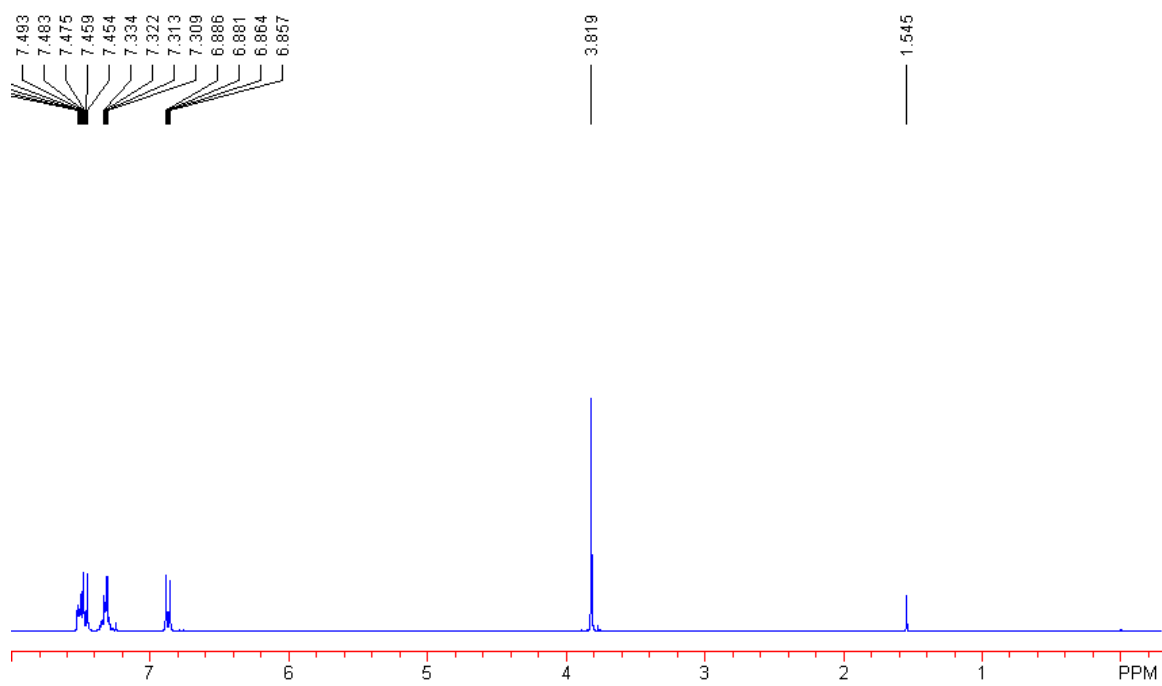


Figure 2.22 ¹H NMR spectrum of Entry 6, Table 2.1.

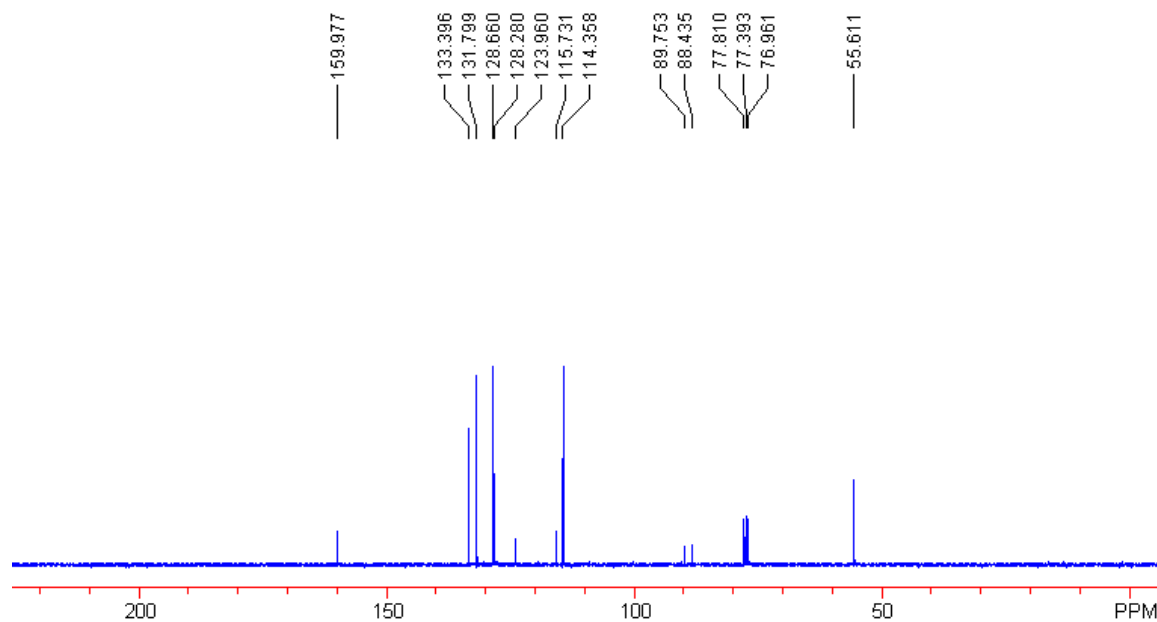


Figure 2.23 ¹³C NMR spectrum of Entry 6, Table 2.1.

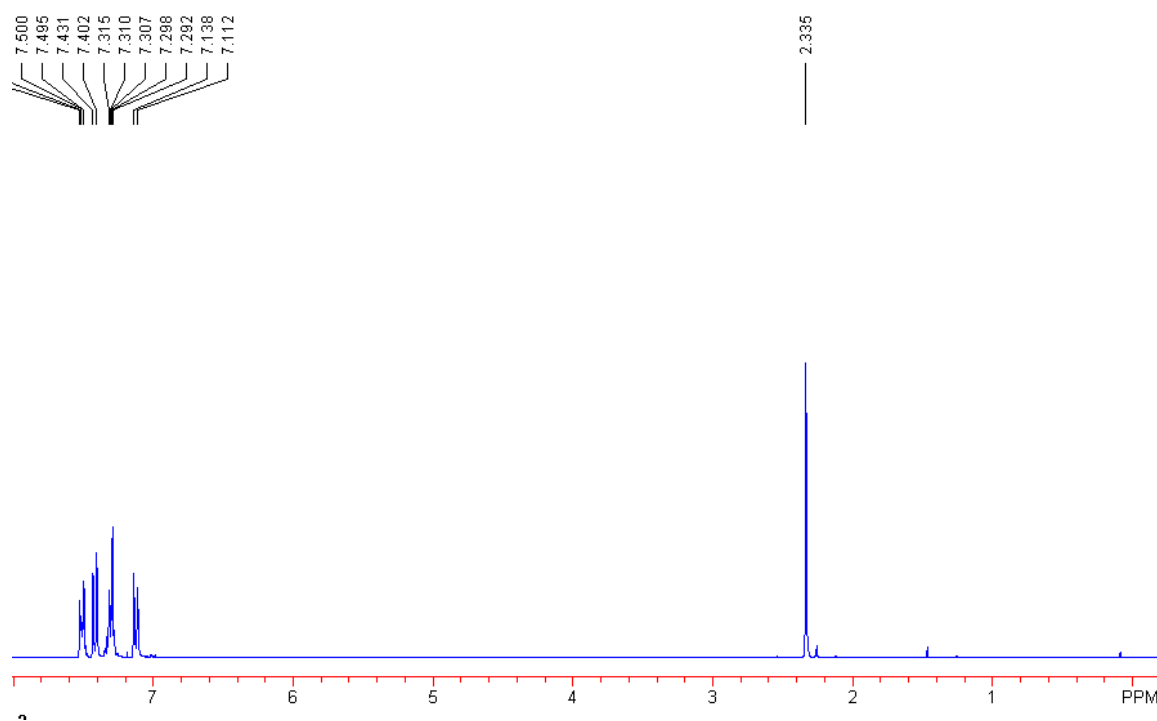


Figure 2.24 ¹H NMR spectrum of Entry 7, Table 2.1.

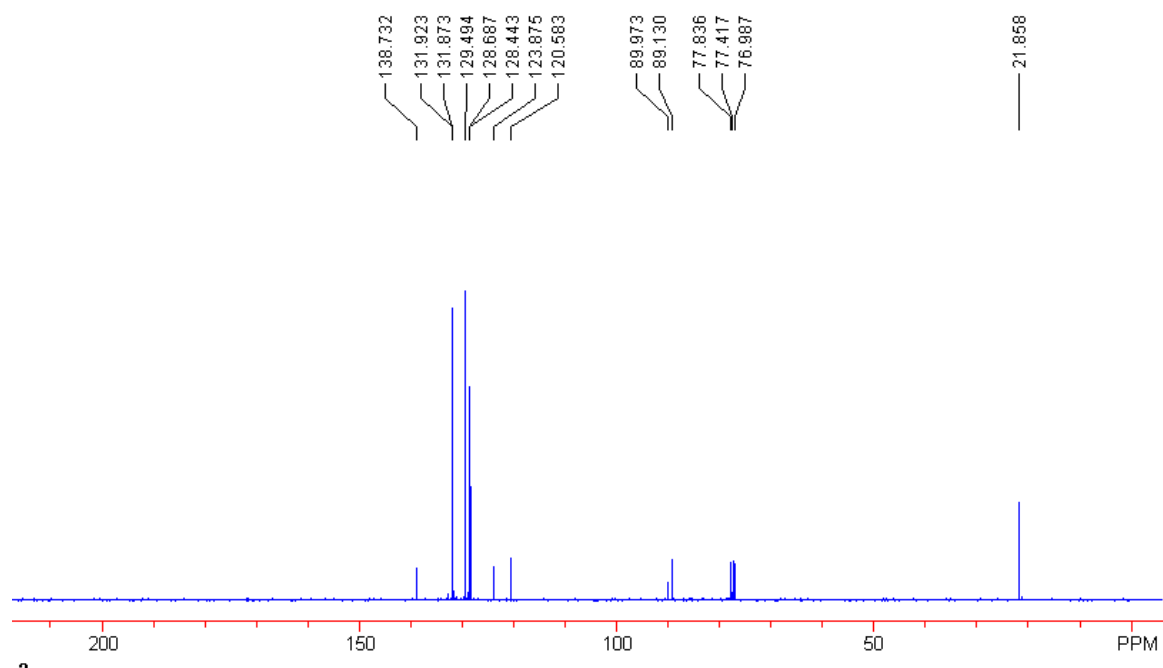


Figure 2.25 ^{13}C NMR spectrum of Entry 7, Table 2.1.

CHAPTER 3
SEPARATION OF CIS-FATTY ACIDS FROM SATURATED AND
TRANS-FATTY ACIDS BY NANOPOROUS
POLYDICYCLOPENTADIENE MEMBRANES

Abstract

This article describes the separation of mixtures of fatty acid salts using a new organic solvent nanofiltration membrane based on polydicyclopentadiene. Mixtures of fatty acids could not be separated by the membranes, but when triisobutylamine was added to the fatty acids, the cis-fatty acid salts had slower permeation through the membranes than the saturated and trans-fatty acid salts. Oleic, petroselinic, vaccenic, linoleic, and linolenic acid salts with triisobutylamine had slowed permeation relative to the permeation of stearic and elaidic acid salts. The addition of triisobutylamine immediately resulted in stable salt pairs with the fatty acids. The salt pairs had larger cross-sectional areas than the fatty acids, and this increase in size led to a decrease in permeation for the cis-fatty acid salts. The fatty acid salts from stearic (a saturated fatty acid) and elaidic (a trans-fatty acid) acid were smaller than the critical area cutoff for the PDCPD membranes so they readily permeated. The partitioning coefficients of fatty acids and fatty acid salts were investigated to demonstrate that solubility differences were not responsible for the difference in permeation. The use of pressure was investigated to greatly accelerate the permeation through the membranes. For a solvent mixture of 35/65 (v/v) toluene/hexanes the permeation of solvent was approximately $39 \text{ L m}^{-2} \text{ h}^{-1}$. This value is similar to values reported for permeation through membranes used in industry. Furthermore, the separation of cis-fatty acid salts from saturated and trans-fatty acid salts was readily achieved when pressure was used in the separations. A mixture of fatty acids based on the composition of soybean oil was investigated using pressure. The saturated fatty acid salts were almost completely removed from the cis-fatty acid salts when $i\text{Bu}_3\text{N}$

was used as the amine to form the salt pairs. The separation of the cis-fatty acids found in soybean oil was investigated with Pr_3N as the amine. The oleic acid salt (oleic acid has one cis-olefin) preferentially permeated the membrane while the linoleic (two cis-olefins) and linolenic (three cis-olefins) salts were partly retained. The separation of fatty acids using membranes may have real applications in industry to purify fatty acids on a large scale.

Introduction

Over 140 million tons of vegetable oils are produced in the United States each year and approximately 96% of the production of these oils are used for food for humans, feed for animals, and biodiesel.^{18,103-108} These oils are triesters of glycerol ($\text{HOCH}_2\text{CHOHCH}_2\text{OH}$) and three fatty acids; each fatty acid contains 16, 18, 20, or 22 carbons and zero, one, or more carbon-carbon double bonds (Figure 3.1). Vegetable oils are found in over 20,000 different foods and they are the source of 95% of the trans-fatty acids within the human diet.^{19,21-23} The consumption of fatty acids from the dietary sources has both positive and negative implications for health. Consumption of trans-fatty acids have a direct correlation with various health problems including thrombogenesis which leads to increased risk for coronary heart and cardiovascular diseases, increased levels of low-density lipoproteins, and decreased levels of high-density lipoproteins.^{24,25,109-113} Significant consumption trans-fatty acids also leads to an increased risk diabetes from a rise in blood insulin levels when these fats are consumed.^{111,114} In 2011 the United States government banned the sale of food with more than 2 grams of trans-fatty acid per 100 grams of oil or fat. In the US, food with trans-fatty acid levels of less than 0.5 grams per serving can be labeled as “Trans Fat Free”, but critics of the this plan have expressed concern that the 0.5 gram per serving threshold is too high to refer to a food as free of trans fat. A person eating many servings of a product – or eating multiple products over the course of the day – may still consume significant amounts of trans-fatty

acids. In contrast to trans-fatty acids, the consumption of cis-fatty acids are often associated with positive health benefits.^{26,27,115-118}

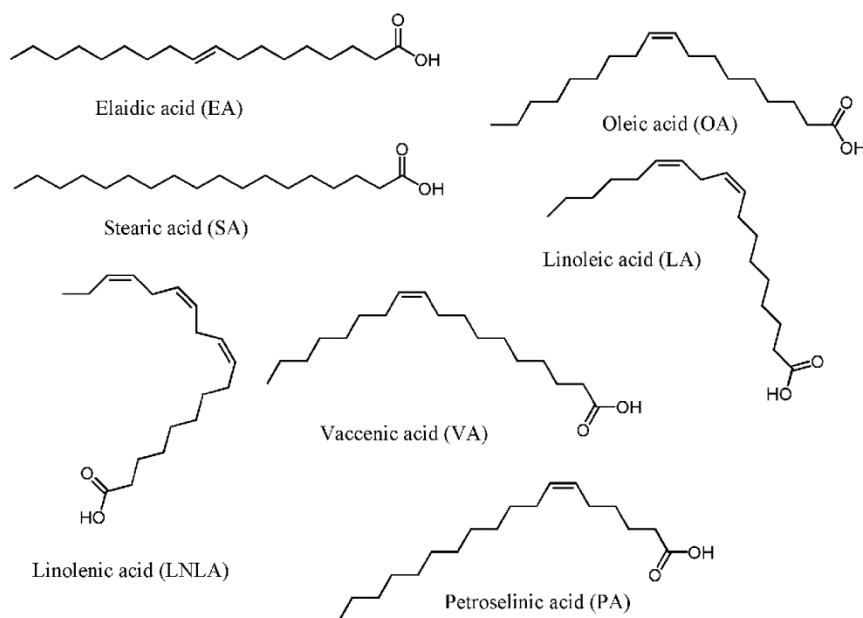


Figure 3.1 The structure of the fatty acids used in this study.

Although partially hydrogenated vegetable oils account for 95% of the trans-fatty acids that are consumed each year, virgin vegetable oils do not possess any trans-fatty acids prior to hydrogenation. For example, over 35 million tons of soybean oil are produced each year, and it has a composition of 10% palmitic acid, 4% stearic acid, 18% oleic acid, 55% linoleic acid, and 13% linolenic acid (palmitic oil is a 16 carbon saturated fatty acid, see Figure 1 for the structures of the other fatty acids).¹⁸ One major limitation with soybean oil as a food source is that it has a significant fraction of polyunsaturated fats that are problematic for applications in food and animal feed. Polyunsaturated fatty acids are prone to oxidation which leads to rancidity and off flavors. Hydrogenation is the most common method to lower the levels of polyunsaturated fatty acids (over 10 million

tons of partially hydrogenated soybean oil is produced each year, primarily for human consumption), but this process leads to the formation of significant amounts of trans-fatty acids.

In addition to their uses in food, vegetable oils are the most important renewable feedstock for the chemical industry and have grown by 5% a year since 2000.¹⁸ Despite the large scale production of vegetable oils and the fact that they are a critical renewable source of starting materials, both the oils and their fatty acids are used only in small quantities in industrial applications. Over 96% of vegetable oils are “burned” by humans or animals after being consumed or in engines when used as biodiesel. A critical reason for the lack of applications of fatty acids as a starting material for industrial applications is that it is not possible to separate a mixture of fatty acids into individual components on a scale of millions of tons per year. Fatty acids isolated from vegetable oils are a mixture of five or more different fatty acids with different reactivities and that will yield different products after a reaction. Simply, when a mixture of five fatty acids derived from soybean oil are used as starting materials in an industrial process, many different products are obtained. The challenge of utilizing a mixture of fatty acids as starting materials limits their broader transformations into more valuable commercial products.

In this article we describe a method to purify fatty acids using an organic solvent nanofiltration membrane based on polydicyclopentadiene (PDCPD). This is the first report of the use of a membrane to separate fatty acids from one another and represents an important advance in this field. The purification of fatty acids would allow the synthesis of oils with desired ratios of saturated and cis-fatty acids with no trans-fatty acids. In addition, this method would allow the purification of a mixture of fatty acids into single fatty acids such that they could be used in more industrial applications. Other methods to purify fatty acids include selective precipitation, liquid chromatography, or selective hydrolysis of trans-fatty acids from glycerol.¹¹⁹⁻¹²⁶ Although each method has found applications on small batches of fatty acids, none of them can separate complex

mixtures of fatty acids into individual components on the scale of millions of tons per year that is required for widespread applications.

Membranes are commonly used in industry to remove impurities from a mixture of molecules. Separations using membranes are a preferred method for large industrial applications because it is one of the simplest and least energy intensive methods of purification. Unfortunately, membranes do not readily separate fatty acids from each other because they are similar in size and polarity. Although *cis* and *trans* double bonds confer differences in overall shape to fatty acids, the ease of rotation about the numerous carbon-carbon sigma bonds leads to a large number of energetically assessable conformations for each fatty acid which increases the complexity of separating them with membranes.

We recently developed size-selective membranes based on highly cross-linked polydicyclopentadiene (PDCPD).^{90,127} These membranes were fabricated by polymerizing 5,000 molar equivalents of dicyclopentadiene with one molar equivalent of the Grubbs first generation catalyst to yield solid, dense membranes. These membranes do not have well-defined pores such as zeolites; rather, when they are swollen in organic solvents, they possess openings between the polymer chains that small molecules may diffuse through. The distribution in size of the openings is polydisperse and on the nanometer to sub-nanometer size scale. We investigated the flux of a large number of molecules through PDCPD membranes and discovered that the membranes were highly selective to retain molecules with cross-sectional areas above 0.50 nm² as shown in Figure 3.2, but molecules with cross-sectional areas below 0.38 nm² permeated the membranes.¹²⁷ The critical areas in Figure 3.2 were defined as the smallest rectangular cross-sectional areas for each molecule in its lowest energy state. These values were measured *in silico* as reported in prior publications.¹²⁷ The molecules that were retained had values for their flux that were at least four to five orders of magnitude lower than those for molecules that did permeate. These membranes did a poor job of separating

molecules based on their molecular weights as shown in Figure 3.2a, but when the critical area for each molecule was plotted against retention a clear difference was observed.

PDCPD membranes are a new type of size-selective membrane that separates organic molecules with molecular weights up to 600 g mol^{-1} based on their cross-sectional areas.

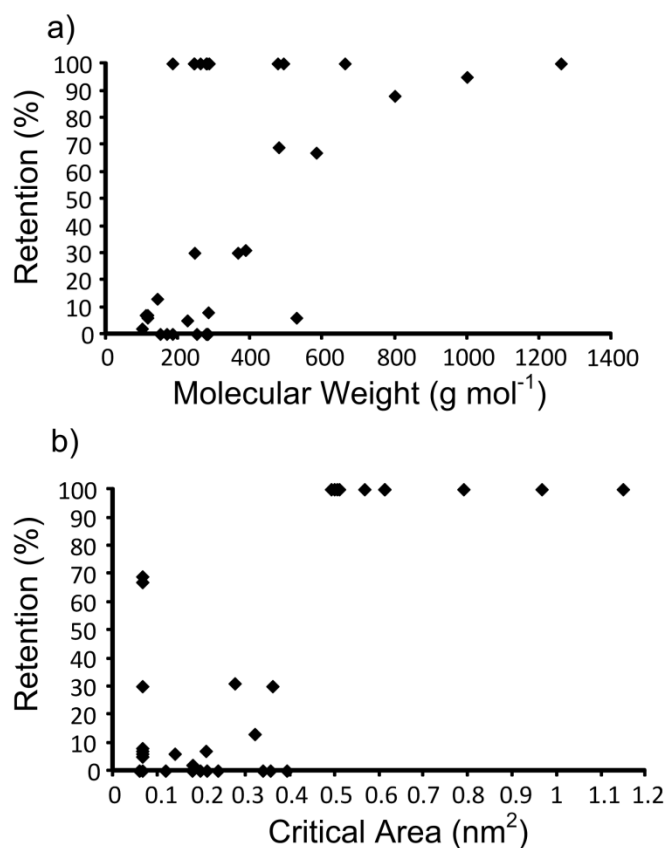


Figure 3.2 A retention of 100% indicated that the molecule did not permeate the membrane at any level and a retention of 0% indicated that the molecule readily permeated the membrane and was not retained. a) The plot of retention versus molecular weight for 35 samples is shown. b) The plot of retention versus critical area is shown for the molecules in part a).

In this article we show for the first time that membranes can be used to separate fatty acids. This is an important advance in this field because it was previously believed

that membranes were ineffective at separating fatty acids from each other due to their small sizes and fluxional structures. Membranes have been used to remove other impurities (i.e. proteins and glycerols) from fatty acids, but they had never been used to separate the individual components of fatty acids. In this article, we show that fatty acids are too small to be separated using PDPCPD membranes, but when they are coordinated with amines that increase their sizes, cis-fatty acid salts are selectively retained by PDPCPD membranes. In contrast, saturated and trans-fatty acid salts readily permeated the membranes and were not retained. This is the first example of the separation of fatty acids using membranes and a significant new method to isolate cis-fatty acids.

Experimental Procedures

Materials

Dicyclopentadiene, elaidic acid, oleic acid, stearic acid, linoleic acid, linolenic acid, vaccenic acid, petroselinic acid, triethylamine, tripropylamine, triisobutylamine, tributylamine, *p*-nitrobenzaldehyde, and solvents were purchased at their highest purity from Aldrich and Acros and used as received.

Characterization

^1H NMR spectra were acquired using a Bruker DPX-500 instrument at 500 MHz and referenced to TMS.

Fabrication of PDPCPD membranes

A 20 mg mL⁻¹ solution of Grubbs first generation catalyst was made using 1,2-dichloroethane. A sample of this solution (0.72 mL, 6.0 x 10⁻³ mmol of catalyst) was added to 12 mL of dicyclopentadiene heated to 40 °C. Heat was used to keep dicyclopentadiene (melting point 33 °C) a liquid. This solution was immediately placed between two glass slides with 100 μm thick paper as spacers along the edges. The sample

was heated to 50 °C for 2 h and then removed from the glass slides. All PDCPD membranes used in this project were fabricated according to this method.

Permeation of oleic acid and elaidic acid with different amines (Table 3.1)

A PDCPD membrane was added to the apparatus to study permeation. CH₂Cl₂:MeOH (v/v, 75:25, 25 mL) was added to the downstream side of the membrane and 25 mL of the same solvent was added to the upstream side of the membrane with 0.426 mmol of oleic acid, 0.426 mmol of elaidic acid, 0.852 mmol of amine, and 0.426 mmol of *p*-nitrobenzaldehyde as an internal standard. Solvent on both sides of the membrane was stirred continuously at room temperature. At 24, 48, and 72 h a 1 mL aliquot of solvent was removed from solvent on both sides of the membrane. The aliquots were used to determine the concentration and the absolute amounts of the oleic acid salt, elaidic acid salt, and *p*-nitrobenzaldehyde by ¹H NMR spectroscopy. The S_d/S_u values were found by the addition of known amounts of toluene to each aliquot as an internal standard. For each aliquot, the integration of the peak corresponding to toluene at 7-7.4 ppm was compared to the integration of the olefinic proton peak for oleic acid and elaidic acid at 5.34 and 5.38 ppm respectively to find the absolute amount of fatty acids in the aliquot.

Permeation of saturated and cis-fatty acid salts with triisobutylamine through PDCPD (Table 3.2)

A PDCPD membrane was added to the apparatus to study permeation. CH₂Cl₂:MeOH (v/v, 75:25, 25 mL) was added to the downstream side of the membrane and 25 mL of the same solvent was added to the upstream side of the membrane with 0.426 mmol of stearic acid, 0.426 mmol of unsaturated acid, 0.852 mmol of triisobutylamine, and 0.426 mmol *p*-nitrobenzaldehyde as an internal standard. Both sides of the membrane were stirred continuously at room temperature. At 24, 48, and 72 h a 1 mL aliquot of solvent was removed from both sides of the membrane. The aliquots were used to

determine the concentration and the absolute amounts of the stearic acid salt, unsaturated acid salt, and *p*-nitrobenzaldehyde by ^1H NMR spectroscopy. The S_d/S_u values were found by the addition of known amounts of toluene as an internal standard to each aliquot.

Permeation of stearic and oleic acid as triisobutylamine salts through PDCPD in different solvents (Table 3.3).

A PDCPD membrane was added to the apparatus to study permeation. Toluene or chloroform (25 mL) was added to the downstream side of the membrane and 25 mL of the same solvent was added to the upstream side of the membrane with 0.426 mmol of stearic acid, 0.426 mmol of oleic acid, 0.852 mmol of triisobutylamine, and 0.426 mmol *p*-nitrobenzaldehyde as an internal standard. Solvent on both sides of the membrane were stirred continuously at room temperature. At 24, 48, and 72 h, a 1 mL aliquot of solvent was removed from both sides of the membrane. The aliquots were used to determine the concentration and the absolute amounts of the stearic acid salt, oleic acid salt, and *p*-nitrobenzaldehyde by ^1H NMR spectroscopy. The S_d/S_u values were found by the addition of known amounts of tetraethylene glycol as an internal standard to each aliquot.

Partition coefficients of molecules in PDCPD (Table 3.4)

A PDCPD slab was cut into small rectangular pieces. A typical value for the dimension of the slab was 2.5 cm x 0.9 cm x 0.3 cm, and the weight was approximately 0.800 g. A fatty acid (0.213 mmol) and triisobutylamine (0.213 mmol) were dissolved in 12.5 mL of CH_2Cl_2 : MeOH (v/v, 75:25) solution. The weight of the PDCPD slab was measured, and it was immersed in the solution. The solution was stirred for 96 h. After 96 h, the PDCPD slab was pulled out of the solution and solvent was removed *in vacuo*. The weight of the slab was measured. The amount of molecule that partitioned into the slab was calculated based on the difference in weight of the slab before and after being swollen. The volume of the solvent was measured prior to removing it *in vacuo*. An

aliquot of the residue was added to a NMR tube. The absolute amount of the fatty acid in the solvent was determined by ^1H NMR spectroscopy by the addition of known amounts of tetraethylene glycol. The partition coefficient of the molecule was calculated by dividing the concentration of the molecule in PDCPD by the concentration of the molecule in the solvent.

Critical areas of fatty acids (Table 3.5)

The software used for these calculations was Spartan `08 V1.2.0. The model for each molecule was drawn in the software using a space filling model. The energy was minimized for each molecule using a semi-empirical AM1 to find the conformation with the lowest energy. Each molecule was thoroughly visualized to see which conformation had the lowest cross-sectional area. This method was also described in prior work.^{90,127}

Separation of a mixture of four fatty acids using multiple extractions

A PDCPD membrane was added to the apparatus to study permeation. CH_2Cl_2 (25 mL) was added to the downstream side of the membrane and 25 mL of the same solvent was added to the upstream side of the membrane with 0.426 mmol of stearic acid, 0.426 mmol of oleic acid, 0.426 mmol of linoleic acid, 0.426 mmol of linolenic acid, and 1.704 mmol of triisobutylamine. Solvent on both sides of the membrane were stirred continuously at room temperature. After 24, 48, and 72 h the downstream solvent was removed and replaced with fresh 25 mL CH_2Cl_2 . After 96 h, the downstream solvent was combined with the previous solvent removed from the downstream side of the membrane. After 96 h, the upstream solvent was removed and replaced with 25 mL of CH_2Cl_2 and 1.278 mmol of triethylamine to extract any fatty acid retained in the membrane. After 45 h, the solvent was replaced with 25 mL of CH_2Cl_2 for a second recovery cycle. The downstream and upstream solvents were combined separately to determine the absolute amounts of stearic acid salt, oleic acid salt, linoleic acid salt, and linolenic acid salt by ^1H

NMR spectroscopy. The absolute amounts of each fatty acid were found by the addition of known amounts of tetraethylene glycol to each aliquot.

Use of pressure to increase the flux through PDCCPD membranes (Table 3.6)

A PDCCPD membrane was immersed in 30 mL of CH₂Cl₂: MeOH (v/v, 90:10, 75:25, or 60:40) for 15 min. After 15 min, the membrane was added to a metal vessel to study flux. CH₂Cl₂:MeOH at the same v/v ratio (100 mL) was added to the upstream side of the membrane with 0.426 mmol of stearic acid, 0.426 mmol of oleic acid, and 0.852 mmol of triisobutylamine. The valve on the downstream side was opened. The pressure was increased to 90 psi in 10 min. After an induction period of a few hours where no solution permeated to the downstream side, the solution was collected on the downstream side in 15-20 min. An aliquot of solvent was used to determine the absolute amounts of stearic acid and oleic acid salts by ¹H NMR spectroscopy. The absolute amounts of the salts were found by the addition of known amounts of tetraethylene glycol to the aliquot. The same experiment was repeated with mixtures of toluene:hexane (v/v, 40:60, 35:65, or 30:70).

Results and Discussion

Choice of fatty acids and how the experiments were completed

The fatty acids shown in Figure 1 were used in this study. These fatty acids all possessed 18 carbons and represented some of the most common fatty acids found in vegetable oils. Included in this study were linolenic acid and linoleic acid which are two essential fatty acids that are needed within the body, but that humans are not able to synthesize.

PDCPD membranes were fabricated as described in the experimental section (Figure 3). These membranes were highly cross-linked by the Grubbs catalyst. Dicyclopentadiene has two carbon-carbon pi bonds; one is highly strained (approximately 25 kcal/mole of ring strain) and other is less strained (approximately 7 kcal/mole of ring strain). The ring opening metathesis polymerization of the highly strained pi bond yielded polymer and the ring opening of the less strained ring yielded cross-links.^{90,127-132} In prior work it was shown that 83% of the less strained pi bond was ring opened which led to a highly cross-linked matrix.^{90,127}

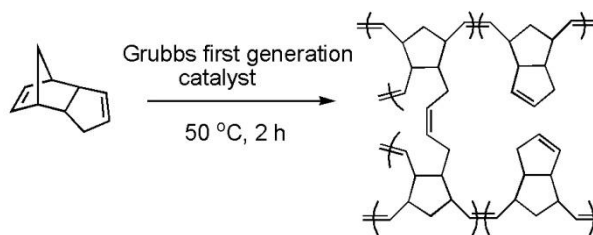


Figure 3.3 The polymerization of dicyclopentadiene by the Grubbs first generation catalyst yielded a highly cross-linked solid polymeric slab.

The experimental apparatus for studying the permeation of fatty acids is shown in Figure 4. A 100 micron-thick PDCPD membrane was fabricated and placed between two glass reservoirs. Solvent was added to either side of the membrane. On one side of the membrane molecules that were to be studied for their flux were added with the solvent. This side was defined as the upstream side of the membrane. On the downstream side of the membrane only solvent was added. The molecules diffused from the upstream side to the downstream side of the membrane. The solvent on both sides of the membranes were constantly mixed using stir bars to ensure uniform concentrations on each side of the membrane. After a period of time, typically 24 h, well-defined aliquots of solvent from both sides of the membranes were removed and the solvent was evaporated. An internal standard of toluene or tetraethylene glycol was added prior to analysis by ¹H NMR

spectroscopy to allow the absolute concentrations of each molecule downstream and upstream of the membranes to be measured.

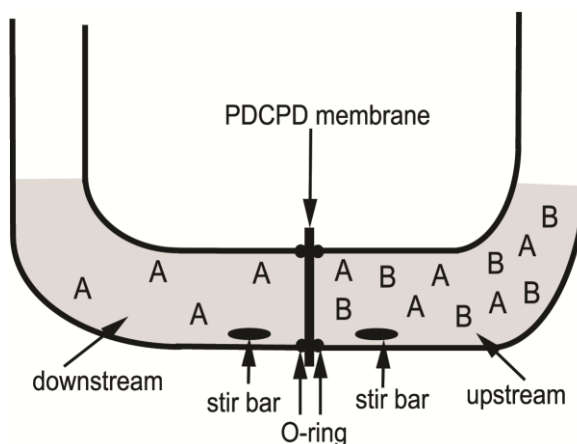


Figure 3.4 A schematic of the apparatus that was used in these experiments. Molecules A and B were initially added to the solvent upstream of the membrane and only molecule A permeated to the downstream solvent.

Separation of oleic acid and elaidic acid

The separation of oleic acid from elaidic acid was chosen as an initial test due to the similarities of these fatty acids. They possess identical molecular formulas and the double bond is located at the same position, but oleic acid is the cis isomer and elaidic acid is the trans isomer. A 75/25 (v/v) mixture of $\text{CH}_2\text{Cl}_2/\text{MeOH}$ was used because all fatty acids dissolved in this solvent and reasonable flux values were obtained.

A mixture of oleic acid, elaidic acid, and *p*-nitrobenzaldehyde as an internal standard were added to solvent on the upstream side of the membrane. The ratio of the concentration of each molecule in the solvent on the downstream side (S_d) to the upstream side (S_u) was measured every 24 h as reported in the experimental section. The S_d/S_u ratio was zero at the beginning of the experiment because the molecules were only added to the upstream side of the membrane. The S_d/S_u ratio was equal to one when a

molecule had diffused through the PDCPD membrane such that its concentration was the same on both sides of the membrane. Both oleic and elaidic acid readily permeated the PDCPD membrane at similar rates and were fully equilibrated after 72 h (entry 1 in Table 3.1). This result was expected based on the small cross-sectional areas of these fatty acids.

Table 3.1 Permeation of oleic acid and elaidic acid with different amines through PDCPD membranes.

Entry	Salt	Oleic acid (S_d/S_u)			Elaidic acid S_d/S_u		
		24 h	48 h	72 h	24 h	48 h	72 h
1	No salt	0.26	0.72	1.04	0.27	0.73	1.08
2	triethylamine	0.09	0.36	1.03	0.11	0.34	1.08
3	tripropylamine	0.01	0.09	0.17	0.13	0.58	1.08
4	triisobutylamine	0.017	0.05	0.07	0.20	0.68	1.01
5	tributylamine	0.0	0.0	0.0	0.0	0.0	0.0

A series of trisubstituted amines were added to the fatty acids to investigate their effect on the observed permeation. From prior work by our group, it was known that triethylamine, tripropylamine, and triisobutylamine readily permeated the membranes but that tributylamine did not permeate at any detectable level. The difference in permeation between triisobutylamine and tributylamine was surprising because these two molecules are constitutional isomers; yet, their flux differed by at least four to five orders of magnitude. The difference in flux was due to the smaller, compact shape of triisobutylamine (critical area of 0.38 nm^2) compared to tributylamine (critical area of 0.50 nm^2).

An amine was added to solvent on the upstream side of the membrane with the fatty acids to form a noncovalent bond (Figure 3.5). The fatty acid and the amine formed a salt pair by transfer of the hydrogen from the acid to the nitrogen. These salts were stable and persistent in a variety of organic solvents. The amines had compact shapes and larger cross-sectional areas than the fatty acids, so their addition increased the critical area of each fatty acid. It was hypothesized that the curvature of the cis-fatty acids would lead to a larger increase in their critical areas when compared to the saturated and trans-fatty acids. It was also hypothesized that the amine would increase the cross-sectional area of the fatty acids to reach the size range where PDCPD membranes were effective at separating molecules. The critical areas of each fatty acid and fatty acid salt are reported later in this article.

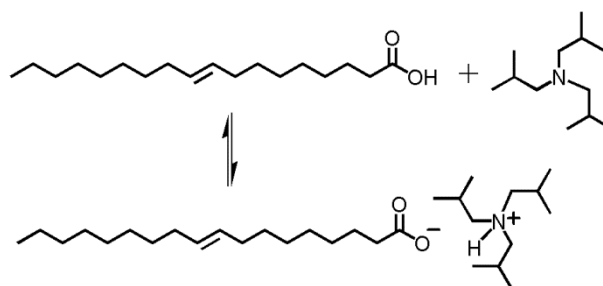


Figure 3.5 The addition of triisobutylamine led to formation of a stable salt with the fatty acids.

The results for the flux when a 1:1:2 molar ratio of oleic acid:elaidic acid:amine was added to the solvent on the upstream side of the membrane was shown in Table 3.1. Not surprisingly, the addition of triethylamine (critical area = 0.18 nm^2) had little impact on the flux of oleic and elaidic acid; both fatty acid salts equilibrated after 72 h. When tripropylamine (critical area = 0.32 nm^2) was added, the flux of oleic acid was slowed but elaidic acid equilibrated after 72 h. Better results were obtained when triisobutylamine

(critical area = 0.38 nm^2) was used. The value for S_d/S_u of oleic acid was only 0.07 after 72 h, but the elaidic acid was fully equilibrated.

Not surprisingly the use of tributylamine (critical area = 0.50 nm^2) kept both oleic and elaidic acid from permeating the membrane. Prior work showed that tributylamine did not permeate these membranes at any detectable level, so it was expected that the salts would not permeate. This experiment with tributylamine demonstrated that the fatty acids coordinated strongly to the amines because if the fatty acids dissociated from tributylamine, they would have readily permeated the membranes.

Separation of cis, trans, and saturated fatty acids.

Five additional fatty acids were studied for their ability to permeate PDCPD membranes. Stearic, linoleic, vaccenic, petroselinic, and linolenic acid all readily permeated the membranes and fully equilibrated within 72 h (Figure 6).

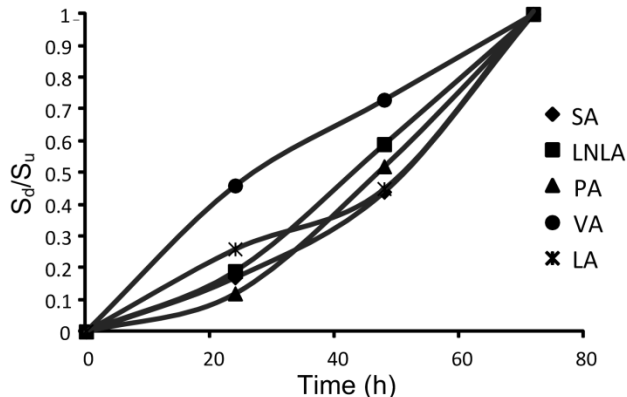


Figure 3.6 The values for S_d/S_u at 24, 48, and 72 h for stearic, linoleic, vaccenic, petroselinic, and linolenic acid are shown. The lines are meant for ease of viewing the data and do not represent a fit to any equation.

The results for the permeation of these five fatty acids were remarkably different when triisobutylamine was added to the solvent on the upstream side of the membrane

(Table 3.2). When triisobutylamine was used, stearic acid readily permeated the membranes but the other four fatty acids had greatly reduced permeation. To ensure that the diminished permeation of the cis-fatty acids was due to their structure rather than another effect, the flux of each cis-fatty acid was studied in the presence of both stearic acid and *p*-nitrobenzaldehyde. The permeation of *p*-nitrobenzaldehyde was known from prior work, so it provided an internal standard for the physical properties of the membranes. In these experiments, both *p*-nitrobenzaldehyde and the stearic acid salt with triisobutylamine readily permeated the membranes. Thus, the diminished permeation of the cis-fatty acid salts was not due to the membranes, but rather it was due to their structures.

Table 3.2 Permeation of cis-fatty acid salts with triisobutylamine through PDCPD membranes.

Entry	^a Fatty acids	Stearic acid			Unsaturated acid		
		(S _d /S _u)			(S _d /S _u)		
		24 h	48 h	72 h	24 h	48 h	72 h
1	Stearic acid and linoleic acid	0.24	0.67	1.04	0	0	0.035
2	Stearic acid and linolenic acid	0.21	0.78	1.04	0	0	0
3	Stearic acid and petroselinic acid	0.15	0.62	0.83	0.02	0.06	0.10
4	Stearic acid and vaccenic acid	0.4	0.65	1.00	0.03	0.07	0.11

^aOne molar equivalent of triisobutylamine to fatty acid was added to each experiment.

Two interesting sets of cis-fatty acids were studied in these experiments. Petroselinic, oleic, and vaccenic acid all possessed 18 carbons and one cis-olefin, but they differed in the location of the double bond (see Figure 3.1). Petroselinic, oleic, and vaccenic acid had 11, 8, and 6 sp³ hybridized carbons after the double bond. The

saturated ends of the fatty acids represented the “hooks” of the cis-fatty acids that led to their diminished flux through the membranes. All three of these fatty acids had similar flux through the membranes despite the difference in location of the cis bonds (entries 3 and 4 of Table 3.2 and entry 4 of Table 3.1).

In a second set of cis-fatty acids, the number of cis bonds differed. Oleic, linoleic, and linolenic acids all possessed one cis-bond at the 9 carbon, but linoleic acid had a second cis-bond at the 12 carbon and linolenic acid had two additional cis-bonds at the 12 and 15 carbons. The number of cis bonds had a small effect on the flux of a fatty acid, but all of the cis-fatty acids were retained by the PDPCPD membrane (entries 1 and 2 in Table 3.2 and entry 4 of Table 3.1).

In all prior experiments a mixture of 75/25 (v/v) of $\text{CH}_2\text{Cl}_2/\text{MeOH}$ was used as the solvent. To investigate if the difference in flux for cis-fatty acids resulted in part from a choice of solvent, chloroform and toluene were studied (Table 3.3). In these experiments the permeation of stearic acid and oleic acid salts were examined to investigate how rapidly the stearic acid salt permeated and whether the oleic acid salt permeated. In both experiments the stearic acid salt readily permeated the membranes but the oleic acid salt did not permeate. The flux of the stearic acid salt was faster when toluene and chloroform were used as solvent than with the $\text{CH}_2\text{Cl}_2/\text{MeOH}$ mixture. In the $\text{CH}_2\text{Cl}_2/\text{MeOH}$ mixture the value for S_d/S_u was 0.68 after 48 h (this value was the average of the four experiments shown in Table 2), but the value for S_d/S_u after 48 h was 0.98 and 0.92 in toluene and chloroform respectively.

Table 3.3 Permeation of stearic acid and oleic acid as triisobutylamine salts through PDCPD membranes in different solvents.

Solvent	Stearic acid			Oleic acid		
	(S_d/S_u)			(S_d/S_u)		
	24 h	48 h	72 h	24 h	48 h	72 h
Toluene	0.32	0.98	1.00	0.03	0.06	0.05
Chloroform	0.34	0.92	1.00	0.03	0.06	0.07

Partitioning coefficients for fatty acids and fatty acid salts

The equations that describe permeation can be complex, but the main concepts are straightforward.¹³³⁻¹⁴¹ For a molecule to permeate a membrane it must partition into the membrane, and it must have a nonzero rate of diffusion inside the membrane. The well-known equation $P = DS$ describes this relationship (P is the permeability, D is the rate of diffusion, and S is the solubility of a molecule in the membrane). The partitioning coefficient, PC (unitless), is defined as the ratio of the concentration of a molecule in a membrane divided by its concentration in solvent when a system is at equilibrium. The partitioning coefficients for every fatty acid salt with triisobutylamine were investigated for their ability to permeate into PDCPD slabs as described in the supporting information.

The partitioning coefficients of oleic and elaidic acid in the absence of any amine were almost identical (entries 1 and 2 in Table 3.4). This result was expected based on the similarities of these fatty acids. Interestingly, the partitioning coefficients of all seven fatty acid with triisobutylamine were also nearly identical (entries 3-9 in Table 3.4). This result was due to the similarities in size and composition of the fatty acid salts and that the charged parts of the salts were encapsulated by the isobutyl groups and the hydrophobic tails of the fatty acids. The different in permeation of the cis-fatty acid salts

compared to the saturated and trans-fatty acid salts was not their partitioning coefficients; rather, the differences were due to their rates of diffusion with the PDCPD matrix.

Table 3.4 Partitioning coefficients of fatty acids and fatty acid salts into PDCPD

Entry	Fatty acid	PC
^a 1	Oleic acid	1.07
^a 2	Elaidic acid	0.997
3	Elaidic acid salt	0.999
4	Oleic acid salt	1.00
5	Stearic acid salt	1.00
6	Linoleic acid salt	0.999
7	Linolenic acid salt	1.00
8	Petroselinic acid salt	1.00
9	Vaccenic acid salt	1.00

^aThe first two entries were measured as free acids without triisobutylamine. Entries 3-9 were measured with one molar equivalent of triisobutylamine present.

Measurement and comparison of critical areas

Differences in partitioning coefficients do not explain the differences in permeation of the fatty acid salts, so the differences in permeation must have been due to the differences in flux. In cross-linked polymer matrixes the diffusion, D , of a molecule depends exponentially on the energy of activation, E_a (kcal mol^{-1}) according to the equation $D = D_0 \exp(-E_a/RT)$.¹³⁵ Molecules that are much smaller than the pores in a matrix can diffuse rapidly because the polymer matrix does not have to rearrange to allow

them to diffuse. Molecules that are on the same size as the pores or larger than the pores diffuse slowly because the polymer matrix must deform and the value for E_a is large. In practice, the rate of diffusion in cross-linked polymers has been shown to be heavily dependent on the cross-sectional areas of molecules. For instance, in 1982 Berens and Hopfenberg plotted the log of diffusion versus the square of diameter for 18 molecules that permeated poly(vinyl chloride), polystyrene, and polymethylmethacrylate.¹⁴² The diffusion of He (diameter squared = $6.66 \times 10^{-2} \text{ nm}^2$) was ten orders of magnitude faster than the diffusion of neopentane (diameter squared = $3.36 \times 10^{-1} \text{ nm}^2$). PDCPD was a highly cross-linked polymer matrix and the rate of diffusion of molecule was expected to depend on their critical areas. In prior work it was shown that molecules above a critical area of 0.50 nm^2 did not permeate PDCPD membranes but molecules with cross-sectional areas below 0.38 nm^2 did permeate.

One challenge in the field of size-selective membranes is defining the critical area of a molecule. This is usually not attempted; rather, membranes are described as possessing a “molecular weight cutoff” that is used to determine whether a new molecule will permeate.¹⁴³⁻¹⁴⁹ The molecular weight cutoff is used although it is not meant to be a good predictor of what will permeate. It is well understood that molecular weight does not have a strong correlation with cross-sectional area. Rather, it provides a simple, unambiguous method to suggest which molecules may permeate a membrane. The molecular weight of a molecule can be determined within minutes, but the cross-sectional area is much harder to determine and dependent on the method used.

The critical areas for the molecules in this study were found using Spartan '08 V1.2.0. The free fatty acids were constructed and their energies were minimized in Spartan. Not surprising, the fatty acids were in the all-trans conformations. The fatty acids were rotated until the smallest rectangular cross-sectional area was found, and this value was labeled the critical area and reported in Table 5. The critical area was measured because this area was the smallest size for the pore that each molecule may diffuse

through. The procedure to find the critical areas for the fatty acids salts was similar. The energy of triisobutylamine was first minimized such that it could be docked in the same conformation with each fatty acid. Next, the energy of the fatty acid with the amine was minimized. The critical areas of the salts were found as described before.

Table 3.5 Critical areas of fatty acids.

Molecule	Critical area of free fatty acid (nm ²)	Critical area of fatty acid salt (nm ²)
Elaidic acid	0.12	0.38
Stearic acid	0.067	0.38
Oleic acid	0.21	0.59
Linoleic acid	0.34	0.97
Linolenic acid	0.36	0.94
Petroselinic acid	0.20	1.27
Vaccenic acid	0.24	0.47

In Figure 3.7 the seven fatty acid and fatty acids salts are shown in their energy minimized structures. The view on the right shows the orientation of the fatty acid salts that was used to find their critical area. The view on the left shows a side view of the fatty acids in the absence of amine to emphasize the curved structures of the cis-fatty acids. The cis-fatty acid salts had larger critical areas than the saturated and trans-fatty acid salts they were not completely eclipsed by the triisobutylamine. The omega ends of the cis-fatty acids were not eclipsed by triisobutylamine, and these ends were “hooks” that increased the critical areas of the cis-fatty acid salts.

It is important to note that there are other methods to measure critical areas. For instance, we defined the critical area as possessing a rectangular shape, but other shapes (i.e. sphere, square, oval, etc) can also be used and will give different values for the critical areas. The variation of the critical area depending on the method of its measurement is an important reason why many nanofiltration membranes use a molecular weight cutoff rather than a critical area cutoff. Although the absolute value for the critical areas may be debatable, it was clear from Figure 3.7 that cis-fatty acid salts had larger critical areas than the saturated and trans-fatty acid salts.

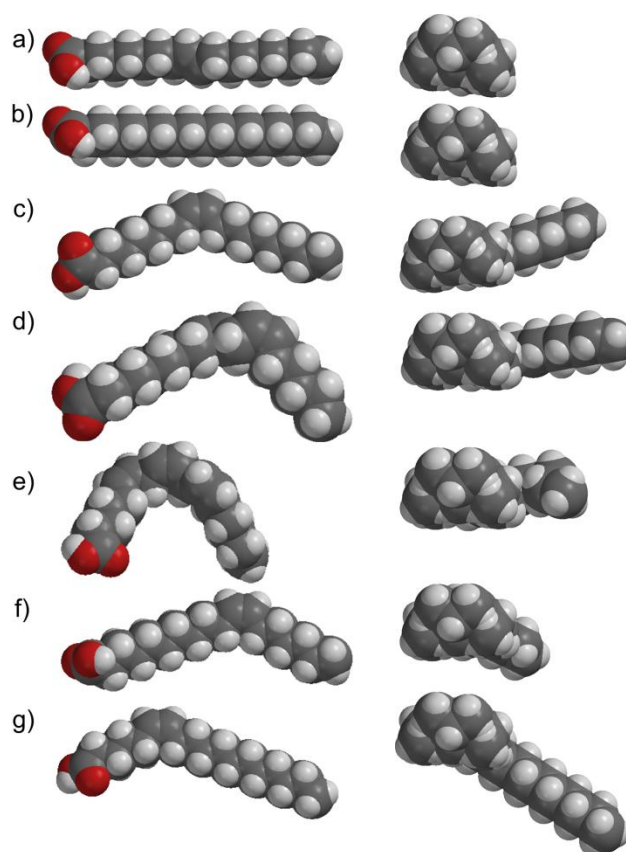


Figure 3.7 Energy-minimized space filling models for each fatty acid and fatty acid salt with triisobutylamine. One image shows the fatty acid to emphasize any curvature. The other image shows a view of the critical area of each fatty acid salt. These images for a) elaidic acid, b) stearic acid, c) oleic acid, d) linoleic acid, e) linolenic acid, f) vaccenic acid, and g) petroselinic acid are shown.

Separation and isolation of cis-fatty acids from saturated and trans-fatty acids

The PDCPD membranes effectively retained cis-fatty acids, but at the completion of the experiment the upstream solvent contained a high concentration of saturated and trans-fatty acids due to how these experiments were conducted. The saturated and trans-fatty acids equilibrated between the solvent upstream and downstream of the membranes; at the end of the separations approximately 50% of these fatty acids were found in the upstream solvent with the cis-fatty acids. Thus, only approximately half of the saturated and trans-fatty acids were removed from the cis-fatty acids. This amount is much lower than would be desired for many applications.

To increase the purity of cis-fatty acids in the upstream solvent as well as the purity of the saturated and trans-fatty acids in the downstream solvent, a series of separations were completed using CH_2Cl_2 as the solvent. CH_2Cl_2 was chosen rather than the $\text{CH}_2\text{Cl}_2/\text{MeOH}$ mixture due to the faster flux for fatty acid salts in CH_2Cl_2 . In these experiments, the downstream solvent was periodically removed and replaced with fresh solvent. Replacing the downstream solvent lowered the concentration of the fatty acids in the downstream solvent which lowered the amount of fatty acid that permeated from the downstream solvent to the upstream solvent. This experiment was similar to a continuous extraction that is common in industrial applications.

In one experiment, a 1:1:2 mixture of stearic acid:oleic acid:triisobutylamine was added to 25 mL of CH_2Cl_2 upstream of the membrane. On the downstream side 25 mL of CH_2Cl_2 was added. The upstream and downstream solvents were stirred for 24 h, and then the downstream solvent was removed and a fresh 25 mL of CH_2Cl_2 was added. The solvents were stirred for an additional 24 h, and then the downstream solvent was removed and replaced with fresh 25 mL of CH_2Cl_2 . The solvents were stirred for 24 h and then the upstream and downstream solvents were removed. All of the downstream solvents were combined, the solvent evaporated, and the residual was analyzed by ^1H

NMR spectroscopy. To extract any fatty acid within the PDPCD matrix, the membrane was extracted with CH_2Cl_2 and Et_3N twice as described in the experimental section. This solvent was combined with the upstream solvent and analyzed by ^1H NMR spectroscopy.

In this experiment, 90% of the stearic acid and only 13% of the oleic acid that were originally added to the apparatus were found in the downstream solvent. In contrast, 5% of the stearic acid and 86% of the oleic acid were found in the upstream solvent and membrane. For many applications purification of the cis-fatty acids is desired, and this experiment took a 1:1 molar ratio of stearic acid:oleic acid and to yield an isolated ratio of 1:17. Notably, 97% the fatty acids that were added to the apparatus were isolated at the end of the experiment. The fatty acids were not permanently trapped within the PDPCD membrane.

This experiment was repeated with four extractions rather than three as before, and the results were similar. Stearic acid (94%) and oleic acid (17%) were isolated from the downstream solvent, and stearic acid (3%) and oleic acid (81%) were isolated from the upstream solvent and membrane. Thus, the isolated ratio of stearic acid to oleic acid in the upstream solvent was 1:27. These results were very promising and demonstrated that the membranes could be used to separate oleic acid from stearic acid.

This experiment was repeated with a 1:1:1:1:4 molar ratio of stearic acid:oleic acid:linoleic acid:linolenic acid:triisobutylamine using CH_2Cl_2 as the solvent. This experiment was to simulate the separation of a small amount of a saturated fatty acid (stearic acid) from a mixture of three different cis-fatty acids. Four extractions were completed and the samples were analyzed as described in the supporting information. The downstream solvent possessed 92% of the stearic acid and only 5% of the cis-fatty acids that were originally added to the apparatus, but the upstream solvent and membrane had 4% of the stearic acid and 86% of the cis-fatty acids. Thus, most of the stearic acid was removed from the cis-fatty acids and the isolated ratio from the upstream solvent of stearic acid to cis-fatty acids was 1:22.

Use of pressure to increase flux

The cis-fatty acid salts were selectively retained while the saturated and trans-fatty acids salts readily permeated the membranes, but the values for flux were very low. No pressure was applied in these experiments, so the driving force for flux was based on differences in concentration of the molecules in solvent upstream and downstream of the membranes. Typical values for the flux of solvent through size selective membranes used in industry are around $10 \text{ L m}^{-2} \text{ h}^{-1}$, and these filtrations require less than an hour to complete.¹⁴³⁻¹⁴⁹ There are two important points about how the industrial separations are completed and interpreted. First, they required the use of pressure on one side of the membrane or the separations were very slow. The use of pressure is not only acceptable, it is almost mandatory such that the filtrations are quick. Second, the values for flux are typically reported for the solvent rather than the molecule of interest (i.e. the product of a reaction). If the concentration of a product is approximately 100x lower than that of the solvent, then values for the flux of the products in a solvent are approximately $0.1 \text{ L m}^{-2} \text{ h}^{-1}$. Separations using PDCCPD membranes required days to reach completion because no pressure was applied. An approximate value for the flux of a fatty acid through PDCCPD membranes was $10^{-10} \text{ L m}^{-2} \text{ h}^{-1}$ which was far too slow for industrial applications.

Because the flux was very slow for the fatty acids, the use of pressure was studied. A metal vessel was used to apply pressure to solvent upstream of the membrane. A membrane was placed horizontally within a metal vessel, and 100 mL of solvent with stearic acid, oleic acid, and triisobutylamine (1:1:2 molar ratio) were added to the solvent in the vessel. The reaction vessel was pressurized to 90 psi, and all of the solvent permeated within 20 min. It is important to note that that solvent was found on only one side of the membrane unlike in the experiments that did not use pressure. Initial experiments with mixtures of CH_2Cl_2 and methanol were unsuccessful due to the poor selectivity of the membrane (entries 1-3 in Table 3.6). Nearly all of the stearic acid salt

(93-97%) permeated the membrane and was found in the solvent downstream of the membrane, but 77-80% of the oleic acid salt was found in the downstream solvent.

Table 3.6 Use of pressure to increase the flux through PDCPD membranes.

Entry	Solvent	^a Amount permeated (%)	
		Stearic acid	Oleic acid
1	90/10 CH ₂ Cl ₂ /MeOH	97	78
2	75/25 CH ₂ Cl ₂ /MeOH	93	80
3	60/40 CH ₂ Cl ₂ /MeOH	95	77
4	40/60 toluene/hexanes	94	36
5	35/65 toluene/hexanes	99	22
6	30/70 toluene/hexanes	^b 0	^b 0

^aThese values refer to the fraction of each acid found in the downstream solvent relative to the amount of acid originally added to the upstream solvent. ^bThe fatty acid salts did not permeate the membranes.

When a mixture of toluene and hexanes were studied, the difference in flux was much higher. At an optimal concentration of 35/65 (v/v) of toluene/hexanes, 99% of the stearic acid was found in the solvent downstream of the membrane but only 22% of the oleic acid was found in the downstream solvent. Some selectivity was lost compared to the experiments without pressure, but the time required for permeation was only 20 min which yielded a flux of for the solvent of 39 L m⁻² h⁻¹. This value for the flux was similar to values reported for membranes used in industry and represented a large improvement for the use of PDCPD membranes.

The use of multiple membranes to increase the selectivity for permeation of one molecule is commonly used in industrial labs, and this method was successful here too.

To increase the separation of oleic acid from the stearic acid, the solvent downstream of the membrane was passed through a second PDCCPD membrane using pressure. When the downstream solvent from entry 5 of Table 6 was passed through a second membrane, the amount of stearic acid that permeated was 96% of the original amount. In contrast, the amount of oleic acid that permeated decreased to only 7.5% of the original amount. Thus, the 1:1 molar ratio of stearic acid to oleic acid that was originally added was concentrated to a 13/1 ratio of stearic acid to oleic acid after passing through two PDCCPD membranes.

This experiment was repeated to investigate the ratio of stearic acid to oleic acid upstream and downstream of the membranes. Briefly, a 1:1:2 molar ratio of stearic acid:oleic acid:triisobutylamine was passed through a PDCCPD membrane using a 35/65 (v/v) toluene/hexanes mixture. The downstream solvent was then passed through a second PDCCPD membrane under pressure. The downstream solvent after filtration through two PDCCPD membranes had 95% of the original amount of stearic acid and only 7% of the original amount of oleic acid. The remainder of the oleic and stearic acid had permeated into the membranes and was retained within them. The membranes were removed from the apparatus and swollen in CH_2Cl_2 with Et_3N to extract the fatty acids. The CH_2Cl_2 extracts were then combined, the solvent was evaporated, and the distributions of products were analyzed by ^1H NMR spectroscopy. The recovery of oleic acid from the membrane was high (89% of the original amount added) and only 3% of the stearic acid was recovered from the membranes.

These results indicated a high level of success both in the overall recovery of the fatty acids and in the separation of saturated and cis-fatty acids. Nearly all of the stearic acid (98%) and oleic acid (96%) that was used at the beginning of the experiment was accounted for at the end. Most of the stearic acid (95%) was found downstream of the membrane and the ratio of stearic acid to oleic acid was 13.6/1 in the downstream solvent. In contrast, most of the oleic acid (89%) was retained by the membranes and the

ratio of retained oleic acid to stearic acid was 30/1. These membranes were successful at separating a mixture of oleic acid/stearic acid.

Use of pressure to purify fatty acids derived from soybean oil

Soybean oil is one of the major sources of vegetable oils with over 35 million tons produced every year. Over 10 million tons of soybean oil are partially hydrogenated each year and used as food for humans and animals. The oil is partially hydrogenated because it has a high component of polyunsaturated cis-fatty acids (55% linoleic acid and 13% linolenic acid) that are prone to oxidation and lead to off-flavors or rancid food. The partial hydrogenation process introduces trans-fatty acids that were not present before, and these trans-fatty acids are highly undesired due to their negative effect on health. Furthermore, only a small fraction of soybean oil is used to produce fatty acids for industrial processes because they are isolated as mixtures of fatty acids. Fatty acids may find increased applications in industry if a method to readily purify them was developed.

The separation of fatty acids derived from soybean oil was completed with PDCCPD membranes under pressure. A mixture of 14% stearic acid, 18% oleic acid, 55% linoleic acid, and 13% linolenic acid was formulated from commercially available fatty acids. This mixture of fatty acids was added to 100 mL of hexanes:toluene (35/65, v/v) with one molar equivalent of triisobutylamine for every mole of fatty acid. This mixture was pressurized and allowed to permeate through two PDCCPD membranes in series. The downstream solvent was removed and the residual was analyzed by ^1H NMR spectroscopy. The PDCCPD membranes were soaked in CH_2Cl_2 with Et_3N to remove any fatty acids that had permeated into the matrix.

Nearly all of the stearic acid (94%) was found in the downstream solvent as expected based on its fast flux through PDCCPD membranes (Table 3.7). Only 3% of oleic

acid and 4% of the linolenic acid/linoleic acid permeated the membranes. The original mixture of fatty acids was only 14% by weight stearic acid, but after filtration through two PDCPD membranes the downstream solvent was 79% by weight stearic acid. Importantly, nearly all of the saturated fatty acid was removed from the unsaturated fatty acids. The fatty acids isolated from the PDCPD membranes contained less than 1% stearic acid. These membranes were very efficient at separating the saturated from unsaturated fatty acids.

Table 3.7 Separation of soybean oil through two PDCPD membranes under pressure.

	Initial amount (mmol)	Downstream solvent (mmol)	Upstream solvent (mmol)
Molecule			
Stearic acid	0.426	0.401	0.022
Oleic acid	0.547	0.018	0.505
Linolenic acid/ Linoleic acid	2.065	0.086	1.949

It was hypothesized that the linolenic and linoleic acids could be selectively retained while oleic acid permeated the membranes. This hypothesis was based on the differences in shapes of the cis-fatty acid salts. Specifically, linoleic and linolenic acid had higher curvatures than oleic acid, and it was hypothesized that an oleic acid salt would possess a higher flux through PDCPD than the polyunsaturated acid salts (see Figure 3.7 for the energy minimized structures of these fatty acids)

To test this hypothesis, the composition of fatty acids that permeated the two PDCPD membranes as shown in Table 3.7 were made into salts by the addition of one

molar equivalent of Et₃N. The cis-fatty acid salts had very low flux when triisobutylamine was used, so smaller amines were investigated to find an amine salt where oleic acid permeated but linoleic and linolenic acid salts were retained. All of the fatty acid salts permeated the membrane after the application of pressure and no separation between oleic acid and the polyunsaturated fatty acid salts was found when Et₃N was used. This experiment was repeated with the same ratio of fatty acids salts that permeated the membranes as shown in Table 3.7 but with Pr₃N to form the salts. Here, pressure was applied across the membrane to reach fast values for the flux.

The oleic acid salt permeated the membrane and 0.33 mmoles were found in the downstream solvent, but only 0.43 mmoles of the polyunsaturated fatty acid salts permeated. The original mixture of fatty acids had a 1:3.8 ratio of oleic acid:polyunsaturated fatty acids but after permeation the ratio was 1:1.3. In the upstream solvent and the membrane, the ratio of oleic acid: polyunsaturated fatty acids was 1:7.3. Although this experiment did not lead to complete separation of oleic acid from linoleic and linolenic acid, it demonstrated that their salts possessed different flux. It may be possible, with some optimization, to find an amine where that allows the oleic acid salt to permeate as linoleic and linolenic acid salts are retained.

Conclusions

The addition of amines led to the selective retention of the cis-fatty acid salts due to two effects. First, the amines increased the critical areas of the fatty acids to the size range where PDPCD membranes could separate them. The free fatty acids were too small to be retained by the membranes, but the fatty acid salts were larger and in the size range where PDPCD membranes retain molecules. Second, the addition of the amines led to a larger difference in critical areas of the salts compared to the free fatty acids. The critical areas for the free fatty acids fell within a narrow range (0.067 to 0.36 nm²), but the critical areas for the fatty acid salts fell within a large range (0.38 to 1.27 nm²).

It was surprising and unexpected that the formation of a noncovalent, reversible interaction between a fatty acid and an amine led to a large difference in permeation. The hooks on the cis-fatty acids were distant from the amines which were the largest, bulkiest part of the salts. Furthermore, fatty acids have large numbers of C-C single bonds that rotate at room temperature and lead to a wide variety of different conformations – and critical areas – for each fatty acid. It would have been reasonable to assume that the flexibility of the fatty acids coupled with the distance between the hooks and the amine would have led to little or no effective difference in critical areas or flux between the fatty acid salts. Yet, the addition of amines led to a difference in critical areas and a significant difference in permeation.

The separation of fatty acids using membranes is an important advancement in this field. Over 140 million tons of vegetable oils are produced each year, but over 96% of it is used for food, feed for animals, or biodiesel. There are surprisingly few other industrial applications of fatty acids despite their low cost and abundance. The reason for the limited industrial applications to turn fatty acids into more valuable materials is that they are isolated as mixtures and it is not possible to separate these mixtures into individual components on a large, industrial scale. Currently, any industrial application of fatty acids requires using a mixture of fatty acids (such as those derived from soybean oils). Our method to separate fatty acids using membranes is an important advance because membranes are widely used in industry and can be used to purify large quantities of a molecule. The purification of fatty acids by organic nanofiltration membranes may lead to methods to purify fatty acids on the millions of tons per year size scale which will make fatty acids an attractive starting material for industrial applications. This article is the first to describe how to purify fatty acids using membranes and represents a new approach to solving a critical problem.

CHAPTER 4
SITE-ISOLATION OF ORGANIC CATALYSTS USING
NANOPOROUS POLYDICYCLOPENTADIENE MEMBRANES

Introduction

Organocatalysis is defined as the acceleration of chemical reactions through the addition of a substoichiometric quantity of an organic compound. Applications of organic molecules as enantioselective catalysts has emerged as a major field in organic chemistry in the last decade.^{150,151} Enantioselective organocatalysis has received significant attention in recent years and has become very important in the synthesis of chiral molecules. Even though Hajos first reported the use of organic molecules as catalysts back in 1974³¹ (Figure 4.1), the use of organic molecules to catalyze organic reactions remained unexplored for a long time after that. In the 2000s organocatalysts emerged due to their applications in a large number of asymmetric reactions.^{33,34,152-155}

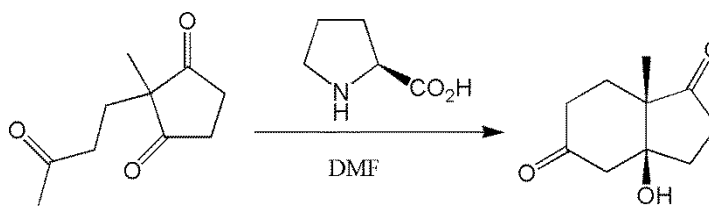


Figure 4.1 Proline catalyzed aldol reaction.

Organic catalysts have several advantages over inorganic and organometallic catalysts. The most important one is that it does not have any metals, so there is no need to remove any metals from the final product as with inorganic catalysts like palladium catalysts. From that perspective, these catalysts are much less toxic as compared to the organometallic catalysts which make the synthetic process greener. Organic catalysts are not sensitive to moisture and oxygen which makes them much easier to use as compared to organometallic catalysts like $\text{Pd}_2(\text{dba})_3$ and many other catalysts which are very

sensitive to oxygen. These catalysts are readily available and are not overly expensive. For example, L-proline which is widely used as an organic catalyst costs \$74 per mole, whereas Pd(OAc)₂ costs \$8,980 per mole. Thus, organic catalysts are an attractive option for use in organic reactions.

Organic catalysts can be broadly classified into four major classes. The first one is represented by biomolecules (e.g. proline, threonine, phenylalanine). The second class is represented by imidazolidinone based organic catalysts. The third major class is based on hydrogen bonding including derivatives of binol and thiourea. The final class of organic catalyst is based on quaternary ammonium salts. One of the important motifs in the first two classes of organocatalysts is a secondary amine functional group that catalyzes reactions by two vastly different mechanisms. One is the enamine mechanism where the active catalyst is an enamine nucleophile.¹⁵⁶ The second method is the iminium mechanism where the active catalyst is an iminium electrophile.³³

Organic catalysts based on non-covalent interactions like hydrogen bonding are used in low catalyst loadings (down to 0.001 mol%) in organic reactions. On the other hand, an organic catalyst which covalently binds to substrates needs high catalyst loadings (loadings of proline are typically 20-30%).¹⁵⁷ Because of such high loadings of catalyst for an organic reaction, it is very important that these catalysts are separated from the organic product at the end of the reaction and recycled for multiple cycles to make the process cost-effective.

Organic catalysts are similar to the organic products in terms of structure, so their separation is not trivial. Much research has been done in the past few years to develop ways of easily separating these catalysts from organic products. The method used by many researchers is to link an organocatalyst to a polymer support.^{155,158-161} The method allows easy separation of the catalysts from the products and facilitates their recycling for multiple cycles. Siegel showed that poly(methylhydrosiloxane) (PMHS) supported organic catalysts used in Diels-Alder reaction of dienes with α,β -unsaturated aldehydes

gave products in high yield and high enantiomeric excess.¹⁶² These catalysts were also recycled for five cycles without any loss of catalytic activity. The MacMillan organocatalyst was immobilized onto polystyrene and Fe₃O₄ magnetic nanoparticles through copper-catalyzed alkyne azide cycloaddition reactions.¹⁶³ The immobilized catalysts were used in Friedel-Crafts alkylation reactions. These catalysts could be recycled for 6 cycles without any loss of catalytic activity. Another method of separation is synthesizing bifunctional organic catalysts containing acid and basic sites with ionic liquid characteristics that makes the catalyst selective as well as recyclable.¹⁶⁴

In this chapter we describe a method to separate organic catalysts from organic products using an organic solvent nanofiltration membrane based on polydicyclopentadiene (PDCPD). This is the first report of the use of a membrane to retain commercially available organic catalysts from products without modifying the structure of a catalyst. The separation of commercially available organic catalysts without modifying their structures would make them a better choice for use in organic reactions as compared to catalysts attached to immobilized supports. When the catalyst is attached to a polymer support, the structure of the active catalyst is changed and the catalyst is transformed from a homogeneous to a heterogeneous catalyst. Membranes are commonly used in industry to remove impurities from a mixture of molecules. Separations using membranes are a preferred method for industrial applications as it is a simple and low energy intensive method to purify molecules.

We recently developed size-selective membranes composed of highly cross-linked polydicyclopentadiene (PDCPD).^{90,127} These membranes were fabricated by ring opening metathesis polymerization of dicyclopentadiene using Grubbs first generation catalyst at a monomer to catalyst ratio of 5000:1. These membranes do not have well-defined pores but after swelling in organic solvents, they possess openings through which molecules may diffuse through. The distribution in size of these openings is not uniform, and they are on nanometer to sub-nanometer scale. We studied the flux of a large number

of molecules through PDCPD membranes and discovered that they selectively retained molecules having critical area higher than 0.50 nm^2 but allowed permeation of molecules with critical areas below 0.38 nm^2 . The critical areas were defined as the smallest cross-sectional area for each molecule in its lowest energy state. We observed that PDCPD membranes are a new type of size-selective membrane that separates organic molecules with molecular weights of less than equal to 600 g mol^{-1} based on their cross-sectional areas.

In this work we show that for the first time membranes can be used to separate organic catalysts from other molecules. This is an important advancement in the separation of organic catalysts from organic products. This method does not require the modification of the structure of organic catalysts. In this work, we show that organic catalysts in the commercially available form can be retained by PDCPD membranes, and therefore can be separated from organic products using this method.

Experimental

Materials

Dicyclopentadiene, octylamine, diphenylpropionic acid, triphenylpropionic acid, MacMillan catalyst, L-proline, O-tert-butylthreonine, tetrabutylammonium hydroxide, *p*-dinitrobenzene, and solvents were purchased at their highest purity from Aldrich and Acros and used as received.

Characterization

^1H NMR spectra were acquired using a Bruker DPX-500 at 500 MHz and referenced to TMS.

Fabrication of PDCPD membranes

A 20 mg mL^{-1} solution of Grubbs first generation catalyst was made using 1,2-dichloroethane. A sample of this solution (0.72 mL , $6.0 \times 10^{-3} \text{ mmol}$ of catalyst) was

added to 12 mL of dicyclopentadiene heated to 40 °C. Heat was used to keep dicyclopentadiene (melting point 33 °C) a liquid. This solution was immediately placed between two glass slides with 100 µm thick paper as spacers along the edges. The sample was heated to 50 °C for 2 h and then removed from the glass slides. All PDCPD membranes used in this project were fabricated according to this method.

Permeation of octylamine, MacMillan catalyst and
carboxylic acids through PDCPD (Table 4.1 and Figure
4.5)

A PDCPD membrane was added to the apparatus to study permeation. CH₂Cl₂ (25 mL) was added to the downstream side of the membrane and 25 mL of the same solvent was added to the upstream side of the membrane with 1 mmol of the molecule and 1.0 mmol of *p*-dinitrobenzene as an internal standard. Solvent on both sides of the membrane were stirred continuously at room temperature. At 24, 48, and 72 h a 1 mL aliquot of solvent was removed from solvent on both sides of the membrane. The aliquots were used to determine the concentration of the molecule and *p*-dinitrobenzene by ¹H NMR spectroscopy. The S_d/S_u values were found by the addition of known amounts of tetraethylene glycol to each aliquot to use the known concentration of tetraethylene glycol to calculate the concentration of the molecule of interest.

Permeation of octylamine and MacMillan catalyst
salts with carboxylic acids through PDCPD (Table 4.2 and
Figure 4.6)

A PDCPD membrane was added to the apparatus to study permeation. CH₂Cl₂ (25 mL) was added to the downstream side of the membrane and 25 mL of the same solvent was added to the upstream side of the membrane with 1 mmol of the octylamine or MacMillan catalyst, 1 mmol of the carboxylic acid and 1.0 mmol of *p*-dinitrobenzene as an internal standard. Solvent on both sides of the membrane were stirred continuously at

room temperature. At 24, 48, and 72 h a 1 mL aliquot of solvent was removed from solvent on both sides of the membrane. The aliquots were used to determine the concentration of the molecule and *p*-dinitrobenzene by ^1H NMR spectroscopy. The S_d/S_u values were found by the addition of known amounts of tetraethylene glycol to each aliquot to use the known concentration of tetraethylene glycol to calculate the concentration of the molecule of interest.

Permeation of L-proline, *O*-*tert*-butylthreonine and *p*-dinitrobenzene through PDCPD (Figure 4.8)

A PDCPD membrane was added to the apparatus to study permeation. CH_2Cl_2 : MeOH (v/v, 9:1 for proline, 8:2 for *O*-*tert*-butylthreonine, 25 mL) was added to the downstream side of the membrane and 25 mL of the same solvent was added to the upstream side of the membrane with 1 mmol of the molecule and 1.0 mmol of *p*-dinitrobenzene as an internal standard. Solvent on both sides of the membrane were stirred continuously at room temperature. At 24, 48, and 72 h a 1 mL aliquot of solvent was removed from solvent on both sides of the membrane. The aliquots were used to determine the concentration of the molecule and *p*-dinitrobenzene by ^1H NMR spectroscopy. The S_d/S_u values were found by the addition of known amounts of tetraethylene glycol to each aliquot to use the known concentration of tetraethylene glycol to calculate the concentration of the molecule of interest.

Synthesis of L-proline and *O*-*tert*-butylthreonine salts with tetrabutylammonium hydroxide

Proline or *O*-*tert*-butylthreonine (1 mmol) was dissolved in 20 mL MeOH. Tetrabutylammonium hydroxide (1 mmol) was dissolved in 8 mL MeOH. The solutions were combined and stirred for 20 min to allow the reaction to happen. After 20 min, MgSO_4 was added to the solution to remove the water formed during the reaction. The residue was removed by gravity filtration. The solvent was removed *in vacuo*.

Permeation of tetrabutylammonium salts of L-proline or *O-tert*-butylthreonine salts through PDCPD

(Figure 4.9b)

A PDCPD membrane was added to the apparatus to study permeation. CH₂Cl₂: MeOH (v/v, 9:1 for proline salt, 8:2 for *O-tert*-butylthreonine salt, 25 mL) was added to the downstream side of the membrane and 25 mL of the same solvent was added to the upstream side of the membrane with 1 mmol of the salt and 1.0 mmol of *p*-dinitrobenzene as an internal standard. Solvent on both sides of the membrane were stirred continuously at room temperature. At 24, 48, and 72 h a 1 mL aliquot of solvent was removed from solvent on both sides of the membrane. The aliquots were used to determine the concentration of the molecule and *p*-dinitrobenzene by ¹H NMR spectroscopy. The S_d/S_u values were found by the addition of known amounts of tetraethylene glycol to each aliquot to use the known concentration of tetraethylene glycol to calculate the concentration of the molecule of interest.

Critical areas of molecules (Table 3)

The software used for these calculations was Spartan '08 V1.2.0. The model for each molecule was drawn in the software using a space filling model. The energy was minimized for each molecule using a semi-empirical AM1 to find the conformation with the lowest energy. Each molecule was thoroughly visualized to see which conformation had the lowest cross-sectional area. This method was also described in prior work.

Results and Discussion

How the experiments were completed

PDCPD membranes were fabricated as described in the experimental section (Figure 4.2). PDCPD was cross-linked by the first generation Grubbs catalyst.

Dicyclopentadiene has two five membered rings and each of them contain one carbon-

carbon pi bond. One of the pi bonds is more strained than the other. The ring opening metathesis polymerization of the highly strained pi bond yielded polymer and the ring opening of the less strained pi bond gave rise to the cross-links. In prior work it was shown that the degree of cross-linking for the PDCPD membrane was as high as 83%.⁹⁰

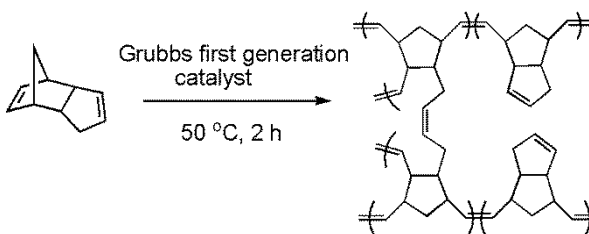


Figure 4.2 The polymerization of dicyclopentadiene by the Grubbs first generation catalyst yielded a highly cross-linked polymer.

The experimental apparatus for studying the permeation of organic catalysts is shown in figure 4.3. A 100 μm thick PDCPD membrane was fabricated and placed between two glass compartments. The glass compartments on either side of the membrane were filled with solvent. The compartment where the molecules were added was defined as the upstream side. The compartment where only solvent was added was defined as the downstream side. The molecules partitioned into the polymer, diffused through the polymer, and were found on the downstream side. The solvent on both sides of the membrane were constantly mixed using stir bars to ensure uniform concentrations on each side of the membrane. After a period of time, typically 24 h, well defined aliquots of solvent were removed from both sides of the membrane and the solvent was evaporated. An internal standard of tetraethylene glycol was added prior to analysis by ^1H NMR spectroscopy to allow the absolute concentrations of each molecule in the downstream and upstream solvents to be measured.

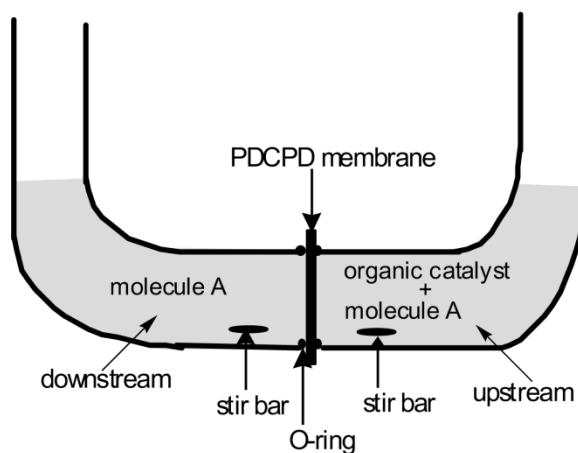


Figure 4.3 A schematic of the apparatus that was used for the permeation experiments. Organic catalyst was retained by the membranes, whereas molecule A permeated through the membranes.

Retention of octylamine

The study of retention of octylamine was chosen because octylamine has an amine functional group which is also present in imidazoline based organic catalysts. The initial experiments were to prove the hypothesis that amines can be retained by PDCPD membranes.

A mixture of octylamine and *p*-dinitrobenzene as an internal standard were added to the solvent on the upstream side of the membrane. The ratio of concentration of each molecule in the solvent on the downstream side (S_d) to the upstream side (S_u) was measured every 24 h. The S_d/S_u ratio was zero at the beginning of the experiment as the molecules were only added to the upstream side. The S_d/S_u ratio was equal to one when a molecule diffused such that the concentration was same on either side of the membrane. Both octylamine and *p*-dinitrobenzene equilibrated after 72 h (entry 1 in Table 4.1). This result was expected due to the small cross-sectional area of these molecules.

From prior work in our group, it was known that diphenylamine readily permeated the membrane but triphenylamine did not permeate at any detectable level.

Similarly, in our present work we observed that diphenylpropionic acid readily permeated the membrane after 48 h, but triphenylpropionic acid was not detected on the downstream side after 48 h (entry 2 and 3 respectively). The difference in permeation between diphenylpropionic acid and triphenylpropionic acid was due to the smaller cross-section area of diphenylpropionic acid (0.34 nm^2) as compared to triphenylpropionic acid (0.65 nm^2).

Table 4.1 Permeation of octylamine and carboxylic acids through PDCPD membranes.

Entry	Molecule	Molecule S_d/S_u			p-dinitrobenzene S_d/S_u		
		24 h	48 h	72 h	24 h	48 h	72 h
1	n-octylamine	0.77	0.75	1.00	0.88	0.99	1.08
2	diphenylpropionic acid	0.58	0.87	--	0.99	1.19	--
3	triphenylpropionic acid	0.00	0.00	--	0.49	0.93	--

A carboxylic acid was added to solvent on the upstream side of the membrane with octylamine to form a noncovalent bond (figure 4.4). Octylamine and the carboxylic acid formed a salt pair by transfer of the hydrogen from the acid to the nitrogen. These salts were stable and persistent in organic solvents. Both diphenylpropionic acid and triphenylpropionic acid had larger cross-sectional areas than octylamine, so their addition increased the critical area of octylamine. It was hypothesized that the addition of carboxylic acid would increase the cross-sectional area of octylamine to reach the size range where it can be effectively separated from other molecules by PDCPD membranes.

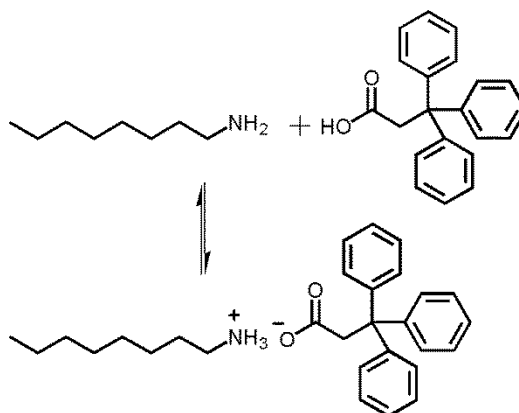


Figure 4.4 The addition of triphenylpropionic acid led to formation of a stable salt with octylamine.

The results for the flux when a 1:1 molar ratio of octylamine:carboxylic acid was added to the solvent on the upstream side of the membrane was shown in Table 4.2. The addition of diphenylpropionic acid to octylamine formed a salt which equilibrated after 72 h. On the other hand, addition of triphenylpropionic acid made the flux of octylamine so slow that none of it was detected on the downstream side after 72 h.

Table 4.2 Permeation of octylamine salts with carboxylic acids through PDCPD membranes.

amine/acid	amine/acid S_d/S_u			<i>p</i> -dinitrobenzene S_d/S_u		
	24 h	48 h	72 h	24 h	48 h	72 h
n-octylamine/ diphenylpropionic acid salt	0.23	0.68	1.00	0.79	0.99	0.99
n-octylamine/ triphenylpropionic acid salt	0.00	0.00	0.00	0.58	0.86	0.961

Not surprisingly the use of triphenylpropionic acid (critical area = 0.65 nm^2) stopped octylamine from permeating through PDCPD, whereas the use of

diphenylpropionic (critical area = 0.34 nm^2) acid did not affect the permeation of octylamine.

Retention of MacMillan organocatalyst

The lack of permeation of octylamine with triphenylpropionic acid present proved that amines can be retained by the PDCPD membranes. The MacMillan organocatalyst is similar to octylamine due to the fact that both the molecules have an amine. As shown in Figure 4.5a, MacMillan catalyst and diphenylpropionic acid had similar rates of permeation through PDCPD, but triphenylpropionic acid did not permeate through PDCPD even after 48 h.

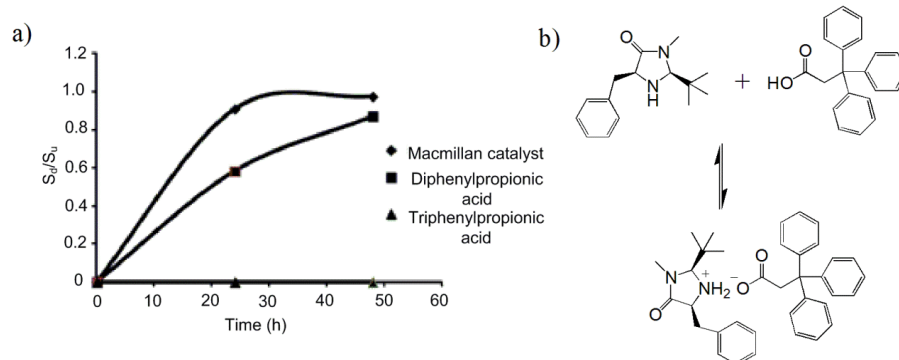


Figure 4.5 Study of Macmillan catalyst and carboxylic acids. a) Permeation of MacMillan catalyst and carboxylic acids through PDCPD membranes (b) The addition of triphenylpropionic acid to MacMillan catalyst formed a stable salt.

When equimolar amount of carboxylic acid was added to the MacMillan catalyst, salts were formed by the transfer of the hydrogen from the acid to the nitrogen as shown by the triphenylpropionic acid salt of the MacMillan catalyst in Figure 4.5b. As shown in figure 4.6, the salt with diphenylpropionic acid permeated through PDCPD and was equilibrated on both sides of the membrane after 72 h. The salt of the MacMillan catalyst

with triphenylpropionic acid did not diffuse through the PDCPD membrane to the downstream side even after 72 h. In both of the experiments, *p*-dinitrobenzene permeated through PDCPD. This result proved that the slow rate of permeation of the triphenylpropionic acid salt was not due to the membrane rather, it was due to the salt.

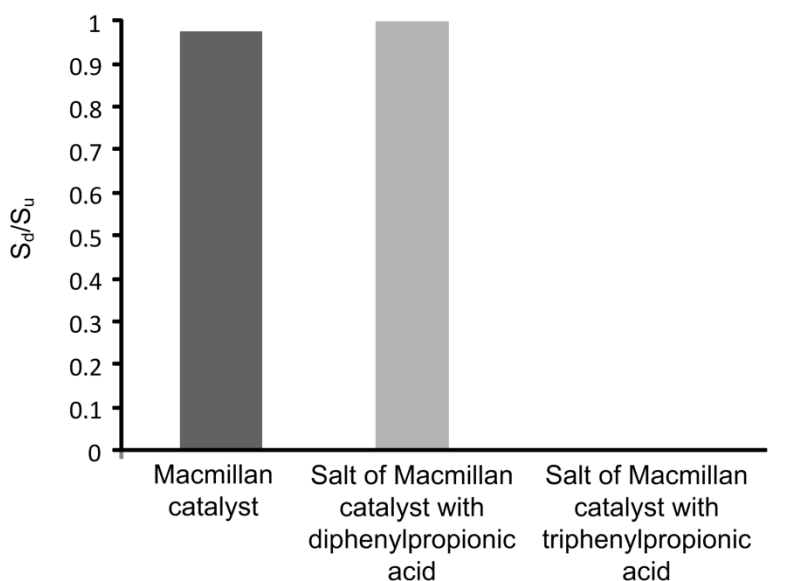


Figure 4.6 S_d/S_u of permeation studies of salts of the MacMillan catalyst with carboxylic acids through PDCPD membranes after 72 h.

Thus, the addition of triphenylpropionic acid resulted in the formation of a salt with MacMillan catalyst. This salt had a much slower rate of diffusion through the polymer as compared to other organic molecules such as *p*-dinitrobenzene and molecules studied in our previous work. This method can be used to separate the MacMillan catalyst from organic products after a reaction has been completed. This would also allow recycling of these expensive MacMillan organocatalysts.

Retention of amino acids

Amino acids are organic compounds that consist of amines and carboxylic acids. The amino acids we studied are L-proline and *O*-*tert*-butylthreonine as shown in Figure 4.7. These amino acids are used as organic catalysts for both intramolecular and intermolecular aldol reactions.

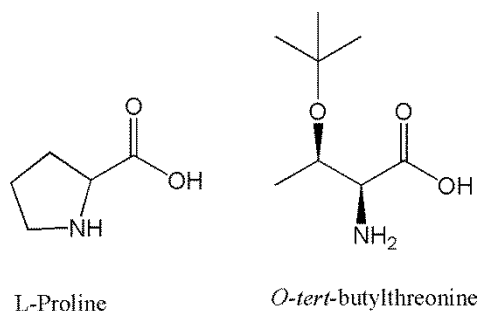


Figure 4.7 Amino acid based organic catalysts used in this study.

In neutral conditions L-Proline and *O*-*tert*-butylthreonine exist as zwitterions with a positive charge on the nitrogen and the negative charge on the oxygen of the carboxylate group. In our prior flux experiments we used dichloromethane as the solvent on either side of the membrane. Both of these organic catalysts had poor solubilities in dichloromethane but they had good solubilities in methanol. The experiment for L-proline was carried out in 9:1 CH₂Cl₂: MeOH and the experiment for *O*-*tert*-butylthreonine was carried out in 8:2 CH₂Cl₂: MeOH. The idea was to use a minimal amount of methanol to dissolve these molecules because it was shown in prior work that methanol was not a good swelling solvent for PDCPD. The results of the flux of L-proline and *O*-*tert*-butylthreonine (Figure 4.8) showed that while *p*-dinitrobenzene equilibrated on both sides of PDCPD membrane after 72 h, the rate of permeation through a PDCPD membrane was very slow for both of these organic catalysts. The S_d/S_u for L-proline after 72 h was 0.266 and for *O*-*tert*-butylthreonine it was 0.25.

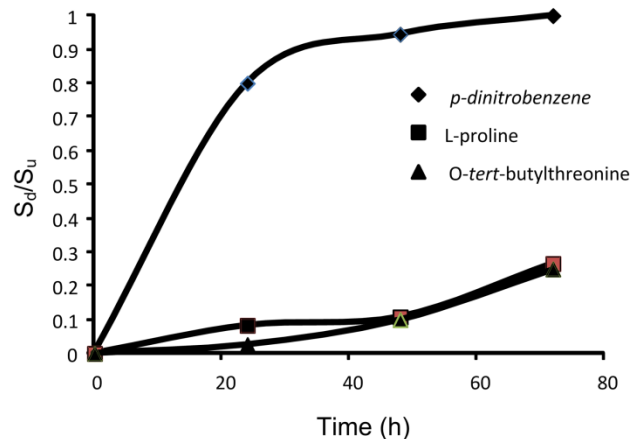


Figure 4.8 Permeation of proline and O-*tert*-butylthreonine through PDCPD membranes.

When an equimolar amount of tetrabutylammonium hydroxide was added to the amino acid, a noncovalent bond was formed as shown in Figure 4.9a. The amino acid and the base formed a salt pair that was stable in organic solvents. From our prior work it was known that tributylamine did not permeate through a PDCPD membrane. It was hypothesized that tetrabutylammonium hydroxide by itself would not permeate PDCPD and, when it formed a salt with the amino acids, it would stop their permeation. It was also hypothesized that by adding tetrabutylammonium hydroxide to these amino acids they could be separated from organic products by PDCPD membranes.

The results for the flux when a 1:1 mole ratio of tetrabutylammonium hydroxide was added to the solvent on the upstream side of the membrane has been shown in Figure 4.9b. This result showed us that without the addition of the base, the permeation of the amino acids was slow. This result also showed that the addition of tetrabutylammonium group increased the cross-sectional area of the salt enough to stop its permeation across the PDCPD membrane on to the downstream side after 72 h. In each of these experiments *p*-dinitrobenzene equilibrated on both sides of the membrane after 72 h.

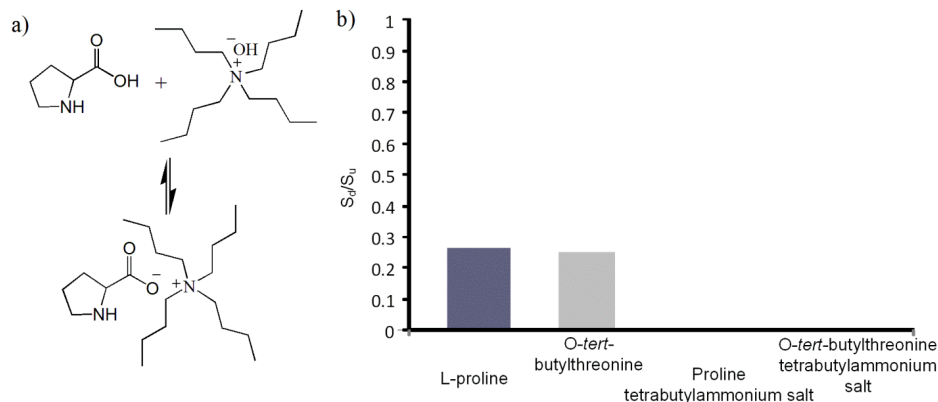


Figure 4.9 Retention of amino acids. a) The addition of tetrabutylammonium hydroxide led to formation of stable salt with proline (b) S_d/S_u of permeation studies of tetrabutylammonium salts of proline and *O*-tert-butylthreonine through PDCPD membranes.

The above experiment showed that the addition of tetrabutylammonium hydroxide can be used to retain organic catalysts such as proline and *O*-tert-butylthreonine from organic products. This method may lead to recycling of L-proline and *O*-tert-butylthreonine.

Measurement of critical area and the reason of retention of molecules using PDCPD membranes

The permeation of a molecule across a polymer membrane depends on two important factors. The molecule must partition into the polymer membrane first, and after partitioning into the membrane it must have a considerable rate of diffusion inside the polymer. The well known equation $P = DS$ describes this relationship (P is the permeability, D is the rate of diffusion and S is the solubility of a molecule in the membrane). The partitioning coefficient is defined as the ratio of the concentration of a molecule inside a polymer divided by its concentration in the solvent when the system is at equilibrium. Our prior work showed that the triisobutylamine salts of fatty acids had similar partition coefficients in PDCPD as compared to fatty acids. It was hypothesized

that the partition coefficient of octylamine and the MacMillan catalyst would be similar to the partition coefficients of their salts with diphenylpropionic acid and triphenylpropionic acid. The charges on the salts should be encapsulated by the hydrophobic phenyl rings of the acid. The slow rate of permeation of proline (critical area = 0.137 nm^2) can be hypothesized due to slower partitioning of the amino acid into a PDCPD membrane. We hypothesized that the tetrabutylammonium salt of proline would have similar partition coefficients to proline.

If partition coefficients were not the reason for different rates of permeation between the diphenylpropionic acid salt of MacMillan catalyst and the triphenylpropionic acid salt of MacMillan catalyst, diffusion was the likely reason. Molecules that are smaller than the pores inside a polymer matrix can easily diffuse through the polymer, whereas molecules that are larger than the pores diffuse much slower through the polymer matrix. PDCPD was a highly cross-linked polymer and the rate of diffusion of molecules depended on their critical areas. In prior work, it was shown that molecules having a critical area of $\geq 0.50 \text{ nm}^2$ did not permeate PDCPD membranes but molecules having a cross-sectional area $\leq 0.38 \text{ nm}^2$ did permeate.

The critical areas for the molecules in this study were calculated using Spartan '08 V1.2.0. The molecules were built and their energies were minimized using Spartan. The molecules were rotated until the smallest rectangular cross-sectional area was found, and this value was labeled the critical area and reported in Table 4.3. The critical area was measured because it was the smallest area for the pore that each molecule could diffuse through. For the salts, the energy of the carboxylic acids were minimized and docked in the same conformation with each molecule. The critical areas of the salts were calculated as described above.

Table 4.3 Critical areas of molecules used in this study

Molecule	Critical Area (nm ²)
n-octylamine	0.07
diphenylpropionic acid	0.34
triphenylpropionic acid	0.65
n-octylamine ^a	0.418
n-octylamine ^b	0.718
MacMillan catalyst	0.36
MacMillan catalyst ^a	0.424
MacMillan catalyst ^b	0.837
proline	0.137
proline salt ^c	0.699
tetrabutylammonium hydroxide	0.558

^asalt formed with diphenylpropionic acid. ^bsalt formed with triphenylpropionic acid. ^csalt formed with tetrabutylammonium hydroxide

It is important to note that there are other methods to measure critical areas such as different shapes (i.e. sphere, square, oval, etc) can be used and that will give different values for the critical areas. An important thing to note is that the addition of triphenylpropionic acid made the critical area of the salts of octylamine and MacMillan catalyst greater than 0.5 nm² and therefore these salts had very slow rate of diffusion inside PDCPD. Similarly, tetrabutylammonium hydroxide made the critical area of amino acid salts greater than the 0.5 nm². This explains the very slow rate of diffusion and permeation of these salts across a PDCPD membrane.

Conclusions

The addition of triphenylpropionic acid and tetrabutylammonium hydroxide led to retention of important organic catalysts such as the MacMillan catalyst and L-proline respectively. The selective retention of organic catalysts used in this study from organic products was because the acid and the base increased the critical areas of the organic catalysts to the size range ($>0.5 \text{ nm}^2$) where PDCPD membranes could retain them. The catalysts by themselves were too small to be retained by the membrane, but the salts were in the range where PDCPD retains molecules. The formation of a noncovalent, reversible interaction between the catalysts and the acid or the base led to a large difference in their permeation across PDCPD membranes.

This method of retention of organic catalysts using membranes is an important advancement in the research of separation of organic catalysts from organic products. Membranes are widely used in industry for various applications to remove impurities from a final product. The method of retention of organic catalysts using polymer membranes would be exciting because this method can be used to separate commercially available organic catalysts without modifying their structure with extra synthetic steps. This method of separation would also allow recycling of these catalysts for multiple cycles which would make the process cost effective.

CHAPTER 5

CONCLUSIONS AND RECOMMENDATIONS FOR FUTURE WORK

Conclusions

This thesis summarizes the development of a novel organic solvent nanofiltration membrane based on polydicyclopentadiene (PDCPD). The polymer membrane was highly cross-linked and the degree of crosslinking was measured using infrared spectroscopy. Approximately 84% of the monomer reacted to form cross-links. This thesis focused on the separation of many molecules by PDCPD using various methods. In the initial work, we used PDCPD thimbles, and we moved to thin, flat membranes as the project progressed. The separation of molecules was based on the concept that molecules with large cross-sectional areas diffused very slowly through the highly cross-linked PDCPD matrix and were therefore retained by the membrane.

Macroscopic, hollow thimbles were fabricated from dicyclopentadiene with Grubbs second generation catalyst at monomer: catalyst ratio of 10000:1. Palladium catalyzed Buchwald-Hartwig and Sonogashira reactions were completed on the interior of the thimbles followed by extraction of the products on to the exterior. In all the reactions, palladium was site-isolated such that a maximum of 0.1% of the palladium added to the interior leached to the exterior of the thimble. Palladium was retained by the membranes at $\geq 99.9\%$ levels in Buchwald-Hartwig and Sonogashira coupling reactions.

The thimbles were investigated for the permeation of organic molecules. It was observed that molecules with critical areas of $>0.50 \text{ nm}^2$ did not permeate through these thimbles, but all molecules that permeated had critical areas $<0.38 \text{ nm}^2$. Critical area was defined as the smallest cross-sectional area of the molecule in its lowest energy state. The permeation of molecules through these thimbles had no correlation with the molecular weight of the molecules.

In an extension to previous work, membranes were fabricated from the ring opening metathesis polymerization of dicyclopentadiene with the Grubbs first generation catalyst at a monomer: catalyst ratio of 5000: 1. The permeability of organic molecules through these membranes was studied. These studies showed that PDCPD membranes were a new type of size-selective membrane that separated organic molecules with molecular weights up to 600 g mol^{-1} based on their cross-sectional areas. Both polar and apolar molecules with molecular weights from 101 to 583 g mol^{-1} permeated these membranes with values for flux of 10^{-5} to $10^{-6} \text{ mol cm}^{-2} \text{ h}^{-1}$. Molecules which did not permeate had 10^4 to 10^5 times slower flux than the molecules which did permeate.

We explored the separation of cis fatty acids from saturated and trans-fatty acids by nanoporous polydicyclopentadiene membranes based on the difference of critical areas of these molecules. Mixtures of fatty acids could not be separated by PDCPD membranes, but on addition of triisobutylamine the cis-fatty acids had much slower permeation than the trans and saturated fatty acids. The critical area of the salts of cis-fatty acids was greater than the critical area cut-off (0.50 nm^2), whereas the salts of trans and saturated fatty acids had smaller critical areas and they readily permeated the PDCPD membranes. The use of pressure accelerated the separation of cis-fatty acids from saturated and trans-fatty acids. Under a pressure of 90 psi, for a solvent mixture of 35/65 (v/v) toluene/hexanes, the permeation of solvent was approximately $39 \text{ L m}^{-2} \text{ h}^{-1}$. This value of flux of solvent was similar to values reported for permeation through membranes used in the industry.

In an extension to the above work, PDCPD membranes were used to separate organic catalysts based on imidazolinone and amino acid. The MacMillan catalyst was separated from an organic molecule by forming a salt with triphenylpropionic acid and that stopped its permeation through PDCPD membranes. Proline and *O-tert*-butylthreonine formed salts with tetrabutylammonium hydroxide and both of these salts were selectively retained by the membranes. All of these salts had critical areas greater

than the cut-off (0.50 nm^2) and that is the major reason for the slow diffusion of these molecules through the highly cross-linked PDCPD matrix. Thus, this was a new method to separate organic catalysts using polymer membranes without immobilizing the catalysts.

Recommendations for Future Work

It can be envisioned that in the future cis-fatty acids can be separated from each other such that the monounsaturated will be separated from the polyunsaturated fatty acids by nanoporous PDCPD membranes. In our prior work we saw that by using triethylamine, there was no separation between oleic acid and the polyunsaturated acid. But with tripropylamine there was some difference in the rate of permeation of salts of oleic and polyunsaturated fatty acids through PDCPD, but not enough to completely separate the oleic acid from linoleic and linolenic acid. The original mixture of fatty acids had a 1:3.8 molar ratio of oleic acid: polyunsaturated acid but after permeation the ratio was 1:1.3. In the upstream solvent and the membrane, the ratio was 1:7.3. Thus it can be envisioned that by optimizing the size of amines as shown in Fig 5.1 the oleic acid can be separated from the linoleic and linolenic acids.

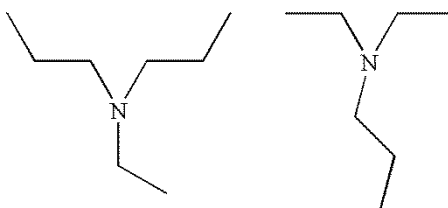


Figure 5.1 Different trisubstituted amines which can be tried to study the permeation of oleic acid and polyunsaturated acids through PDCPD membranes.

In future, the separation of cis-fatty acids from saturated and trans-fatty acids in vegetable oils like soybean oil can be investigated using membranes composed of

copolymers of dicyclopentadiene with cyclooctene. The highly cross-linked PDCPD membranes will most likely not allow the permeation of vegetable oils. It can be hypothesized that the membranes based on the copolymers will have larger pores than PDCPD membranes because cyclooctene increases the distance between the cross-links. It can be envisioned that by optimizing the amount of cyclooctene, the membranes will have the right properties to separate vegetable oils.

APPENDIX
SELECTIVE FLUX OF ORGANIC LIQUIDS AND SOLIDS USING
NANOPOROUS MEMBRANES OF POLYDICYCLOPENTADIENE

Abstract

Membranes were fabricated from the ring opening metathesis polymerization of dicyclopentadiene with the Grubbs first generation catalyst, and the permeability of twenty-one molecules through them was studied. Both polar and apolar molecules with molecular weights from 101 to 583 g mol⁻¹ permeated these membranes with values for flux of 10⁻⁵ to 10⁻⁶ mol cm⁻² h⁻¹ but selected molecules did not permeate them and had flux 10⁴ to 10⁵ times slower. The difference in flux was large between molecules that permeated and those that did not permeate, but no trend was observed that correlated flux with molecular weight or hydrophobicity. Rather, molecules that did not permeate the membranes had large cross-sectional areas that led to low rates of diffusion within the highly cross-linked polydicyclopentadiene membranes. The degree of cross-linking within the polydicyclopentadiene membranes was measured using infrared spectroscopy and approximately 84% of the dicyclopentadiene monomer had reacted to form cross-links. These are the first organic solvent nanofiltration membranes that separate molecules with molecular weights from 100 to 600 g mol⁻¹ based on cross-sectional areas.

Introduction

Membranes are one of the most common and economically efficient methods to purify active pharmaceutical ingredients (API) in industry and provide a critical alternative to distillations, recrystallizations, and column chromatography. Distillations require that an API be stable to elevated temperatures and require significant amounts of energy to complete. Recrystallizations often result in APIs with high purities, but not every molecule can be recrystallized and the recrystallization conditions are often

difficult to optimize and scale up to an appropriate level.^{165,166} In addition, the formation of multiple crystalline isomorphs is poorly understood and results in APIs with different delivery characteristics in the body.¹⁶⁷⁻¹⁷² Column chromatography is often used in the early discovery and development of APIs due to its simplicity and success, but it is not widely used for large scale production of APIs due in part to the large volumes of solvents that are used which necessitate further purification. In contrast, the use of nanoporous membranes to purify APIs can be readily scaled up to purify large quantities of product, use little energy, and does not require large amounts of solvent.^{83,173-176} The use of nanoporous membranes in industry is common in aqueous separations or to purify gasses by pervaporation, but nanoporous membranes are used less commonly with organic solvents. A breakthrough was realized in 1990 when nanoporous membranes based on “organic solvent nanofiltration” (OSN) membranes were used in an ExxonMobil refinery to separate oil from dewaxing solvents.¹⁷⁷ The next generation of OSN membranes based on cross-linked polyaniline, polyimides, and other polymers and sold as StarMem, Duramem, and PuraMem have been developed that function in a wide range of organic solvents and separate organic molecules dissolved in organic solvents.^{83,92,173,175,176,178-180}

All OSN membranes report values for the “molecular weight cutoff” (MWCO) that correspond to the molecular weight where molecules transition from having high to low values of permeation.^{179,180} Simply, molecules below the MWCO permeate the membranes but molecules above the MWCO have significantly reduced permeation and are retained. The use of membranes that feature a MWCO has limitations for the separation of catalysts from APIs because the ligands on a catalyst often have molecular weights that are similar to that of the product. Thus, ligands such as PPh₃ (MW: 262 g mol⁻¹), PCy₃ (MW: 280 g mol⁻¹), and binol (MW: 286 g mol⁻¹) can be very challenging to separate from APIs with similar molecular weights or impossible to separate if an API has a higher molecular weight. In this article we report the first nanoporous membranes

composed of polydicyclopentadiene (PDCPD) that separate many common ligands for metals from other molecules that possess molecular weights lower and higher than those of the ligands (Figure A.1a). These ligands include phosphines, trisubstituted amines, binol, and salen. The separation is due to the large cross-sectional area of ligands which hinders their diffusion through heavily cross-linked PDCPD. In contrast to the ligands which do not permeate these membranes at any level, molecules with low to high molecular weights permeate them if their cross-sectional areas are below a critical threshold. The significance of this work is that PDCPD membranes retain key molecules that are common ligands for metals while allowing molecules with molecular weights over three times as high to permeate. No OSN membranes have this property for molecules with molecular weights of 100-600 g mol⁻¹.

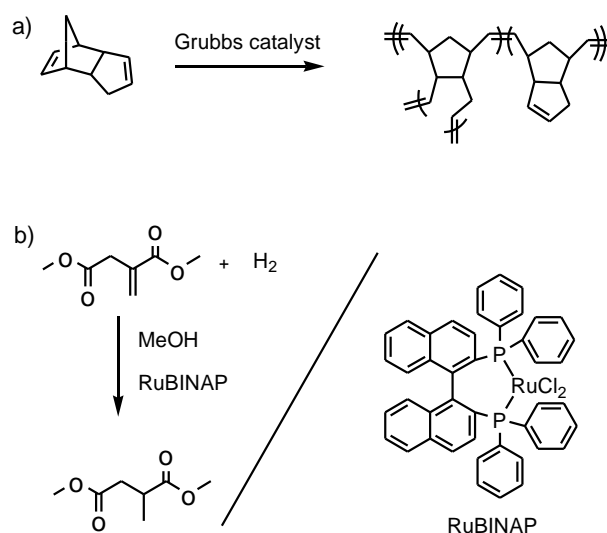


Figure A.1 a) Polydicyclopentadiene was synthesized by polymerizing dicyclopentadiene with the Grubbs first generation catalyst at monomer to catalyst loadings of 5,000:1. b) Despite the large difference in molecular weight between RuBINAP and the product of the reaction, RuBINAP was only site-isolated at 98% using an OSN membrane.

The state-of-the-art membranes to separate catalysts from the products of reactions are based on highly cross-linked organic polymers that function in a range of organic solvents. For instance, in the reaction shown in Figure A.1b the RuBINAP catalyst (molecular weight 795 g mol^{-1}) was retained by OSN membranes at levels of approximately 98% for multiple cycles and was active for long periods of time.⁸⁰ The product was allowed to permeate the membranes and was isolated on the side of the membrane opposite of the catalyst. Part of the success of this project was the high molecular weight of the catalyst compared to the product (molecular weight 160 g mol^{-1}) which allowed the catalyst to have a molecular weight significantly higher than the MWCO of the membrane (220 g mol^{-1}).

In other work, the flux of trialkylamines (i.e. NR_3 where R is methyl, ethyl, propyl, etc) through commercially available OSN membranes (StarMemTM membranes) were studied. This study described perplexing results because even though the molecular weight cutoff was 220 g mol^{-1} , only 19% of tridodecylamine (molecular weight 522 g mol^{-1}) was retained (81% permeated the membrane). Also, when the system was studied using cross-flow, the rejection rate for all of the trialkylamines was much poorer than expected. The authors concluded that the use of a molecular weight cutoff for trialkylamines and the StarMem membranes was not useful and gave misleading predictions.⁹²

OSN membranes have an important role in the chemical industry, but they have two limitations that hinder applications in many commercial syntheses of small molecules.^{83,175,176,178,179,181,182} First, to be effective there must be a large difference between the molecular weight of the catalyst and the organic product. The molecular weights of many common ligands range from a couple to several hundred grams per mole and would not provide enough difference in molecular weight to separate them from products with similar or higher molecular weights. Second, the MWCO of a membrane is defined as the molecular weight at which 90 to 98% of the solute is rejected; thus,

significant amounts of a molecule may pass through these membranes even if the molecular weight is larger than the cutoff.

Other membranes composed of nanopores etched in polycarbonate, zeolites, and metal-organic frameworks have been fabricated by others that can separate organic molecules. Zeolites are well known for distinguishing molecules based on size, but they are not used as membranes for molecules with the dimensions described in this proposal. Nanopores etched in polycarbonates have found some success, but the molecular size cutoffs are typically not sharp and the membranes suffer from low flux, fouling, and degradation with time.¹⁸³⁻¹⁸⁶ Metal-organic frameworks have been developed that use porphyrins to define pores, but all of these examples require either water as the solvent or only separate gasses.¹⁸⁷⁻¹⁹⁴ Although promising, none of these other approaches have the selectivities and properties of PDCPD membranes as described in this report.

In this article we report the first use of PDCPD as membranes and the very low flux of common organic ligands through these membranes. PDCPD synthesized from the polymerization of commercially available dicyclopentadiene and the Grubbs catalyst is a relatively new material.^{132,195-198} This polymer is heavily cross-linked and forms a solid, hard material that, when synthesized by other catalysts, is used in the fabrication of the hoods of semitrucks and snowmobiles. This article reports that although it is a hard polymer, it will readily swell in organic solvents and allow molecules to permeate through it. This is the first reported use of PDCPD as a membrane for liquid separations. We will describe how molecules with a variety of polar functional groups and differing molecular weights permeate PDCPD membranes while other molecules do not permeate.

The difference in permeation is based on cross-sectional area of each molecule.^{133-137,139-141,199-201} Molecules that have cross-sectional areas larger than a critical value do not permeate the membranes while those below the critical value do permeate them. Both polar and apolar molecules permeate if their cross-sectional area is below the critical value. This criterion for separation is based on the highly cross-linked matrix of PDCPD

that results in a set of pores that allow the polymer to have unique properties for molecules with molecular weights between 100-600 g mol⁻¹. These are the first membranes to separate organic molecules with these molecular weights based on the large cross-sectional areas of many common ligands for metals. This paper will describe the permeation of over 20 different molecules, their chemical and physical properties, and the degree of cross-linking within PDCPD.

Experimental

Characterization and measurements

¹H NMR spectra were acquired on a Bruker DPZ-300 NMR at 300 MHz or a Bruker DRX-400 NMR at 400 MHz and referenced to TMS. The concentration of Co(salen) was acquired on a Varian Cary 100 Scan UV-Visible spectrophotometer and Varian 720-ES ICP-OES (inductively coupled plasma-optical emission spectrometer). The thicknesses of the membranes were determined using a Micromaster microscope at the highest magnification. Infrared spectra were acquired on a Bruker Tensor 27. A room temperature DTGS (deuterated triglycine sulfate) detector was used. All chemicals were purchased at their highest purity from Aldrich or Acros and used as received.

Calibration of UV-VIS spectrophotometer

CoII(salen) (23 mg, 0.039 mmol) was dissolved in toluene (0.5 mL) prior to the addition acetic acid (0.01 mL, 0.18 mmol). The mixture was stirred at room temperature for 1 h to yield Co^{III}(salen) with an acetate counterion. Here Co^{III}(salen)OAc is referred to as Co(salen) for the rest of this report. Toluene and the excess acetic acid were removed under vacuum. The Co(salen) was dissolved in CH₂Cl₂ (10 mL) and stirred at room temperature for 24 h. The solvent was removed and Co(salen) was redissolved in CH₂Cl₂ (10 mL) to yield a 0.00386 M solution. This solution was diluted to make standard solutions to calibrate the instrument. The intensity of the peak at 410 nm in each

of the spectra was measured and plotted against concentration to create a calibration curve.

Calibration of ICP-OES

Standards for Co were made by diluting a standard solution containing 9908 ppm of Co in 1-2 wt. % of HNO₃ with water. The concentrations of the standards were 0.248 ppm, 0.495 ppm, 0.990 ppm, 1.99 ppm, 4.95 ppm, 7.93 ppm, 15.8 ppm, and 39.6 ppm. The standards were used to calibrate the ICP-OES before running the samples for Table 2. A 1 ppm solution of Y was used as an internal standard.

Optical spectroscopy

The thickness of a membrane was determined by cutting a section of a membrane and placing it under the microscope. The section of membrane was held vertically with tweezers and the edge was imaged at the highest magnification. An optical micrograph was taken and the thickness was measured.

Synthesis of PDCPD membranes at a 5,000:1

dicyclopentadiene:Grubbs catalyst ratio

A 20 mg/mL solution of Grubbs first generation catalyst was made using 1,2-dichloroethane. A sample of this solution (0.246 mL, 6.0×10^{-3} mmol of catalyst) was added to 4 mL of dicyclopentadiene heated to 40 °C to melt it. The melting point of dicyclopentadiene is 33 °C. This solution was immediately placed between two glass slides with 100 µm thick paper as spacers along the edges. The sample was heated to 50 °C for 2 h and then removed from the glass slides.

Synthesis of PDMS membrane

These membranes were fabricated similar to methods described in prior work.^{75,77,202} Sylgard 184 was mixed with a curing agent in a 10:1 ratio and degassed. The PDMS was poured over a flat glass slide while allowing any excess to flow over the

side. The glass had been coated with a monolayer of trichloro(1H, 1H, 2H, 2H-perfluorooctyl)silane prior to its use. The PDMS was cured in a 65 °C oven for 24 h. The PDMS membrane was delaminated from the glass side by swelling in dichloromethane.

Permeation of Co(salen) through PDCPD membranes (Table A.2)

Co(salen) was synthesized with acetic acid and toluene as described before. A PDCPD membrane was added to the glass apparatus to study permeation. CH₂Cl₂ (25 mL) was added to the downstream side of the membrane. CH₂Cl₂ (25 mL) with Co(salen) (0.038 mmol) was added to the upstream side of the membrane. Both sides of the membrane were stirred continuously at room temperature. Aliquots (4 mL) were removed from both sides of the membrane at 24 and 48 h.

The concentration of Co(salen) was determined by UV-Vis spectroscopy or ICP-OES using the calibration curves that were determined as previously described. Samples for ICP-OES were prepared by first drying each aliquot and burning off all the organic materials with a Bunsen burner. The Co was dissolved in 1 mL of a 3:1 solution of concentrated HCl and concentrated HNO₃. The aliquot from upstream side of the membrane was diluted with 10 mL of water. The aliquot from the downstream side of the membrane was diluted with 5 mL of water. The samples were run through ICP-OES after it was calibrated on the same day as the measurements.

Permeation of Co(salen) through PDCPD membranes treated with ethyl vinyl ether (Table A.2 entries 6-8)

Co(salen) was synthesized with acetic acid and toluene as described before. CH₂Cl₂ (25 mL) and ethyl vinyl ether (5 mL, 52 mmol) were added to the downstream side of the membrane and CH₂Cl₂ (25 mL) and ethyl vinyl ether (5 mL, 52 mmol) with Co(salen) (0.038 mmol) were added to the upstream side of the membrane. Both sides of the membrane were stirred continuously at room temperature. At 24 and 48 h aliquots (4

mL) of solvent were removed from both sides of the membrane. The aliquots were used to determine the concentration Co(salen) by UV-Vis spectroscopy as previously described.

Permeation of Co(salen) through a PDMS membrane

(Table A.1)

Co(salen) was synthesized with acetic acid and toluene. A PDMS membrane was added to the apparatus to study permeation. CH₂Cl₂ (25 mL) was added to the downstream side of the membrane. CH₂Cl₂ (25 mL) with Co(salen) (0.038 mmol) were added to the upstream side of the membrane. Both sides of the membrane were stirred continuously at room temperature. At 2, 4, and 6 h aliquots (4 mL) were removed from both sides of the membrane. The aliquots were used to determine the concentration Co(salen) by UV-Vis spectroscopy as previously described.

Swelling of PDCPD by various solvents (Table A.3)

Commercially available dicyclopentadiene (24 mL, 0.177 mol) was heated in a glass vial at 35 °C for 10 minutes to melt it. The Grubbs catalyst (15 mg, 0.017 mmol) was mixed with dichloromethane (0.5 mL), added to the dicyclopentadiene, and thoroughly mixed. The solution was heated in a water bath at 50 °C for 1.5 h. The slab of PDCPD was removed from the vial and swelled in dichloromethane mixed with ethyl vinyl ether. The slab of PDCPD was cut into 12 small cubes. All the cubes were dried in air and then under vacuum.

The weights of cubes of PDCPD were measured. Each cube was placed in a glass vial with 10 mL of solvent to completely immerse the cube for 24 h. Next, the cubes were removed from the vials and briefly wiped with kimwipes to remove solvent from their surfaces. The weights of the swollen PDCPD cubes were measured. The swollen weight was divided by the dry weight of PDCPD to calculate how well each solvent swells PDCPD.

Permeation of organic molecules through PDCCPD
membranes with different solvents (Tables A.4 and A.5)

A membrane – made with a monomer:catalyst loading of 5000:1 – was added to the apparatus to study permeation. CH_2Cl_2 , toluene, or THF (25 mL) was added to the downstream side of the membrane and 25 mL of the same solvent was added to the upstream side of the membrane with 3 mmol of the substrate and 1 mmol hexadecane as an internal standard. Both sides of the membrane were stirred continuously at room temperature. At 24 and 48 h a 1 mL aliquot was removed from both sides. The aliquot was used to determine the concentration of the substrate and hexadecane by ^1H NMR spectroscopy. The concentrations were found by the addition of known amounts of tetraethylene glycol to each aliquot and comparing the known concentration of tetraethylene glycol with the concentration of the molecule of interest.

Rate of flux of hexadecane through a 5000/1
PDCCPD membrane

A membrane – made with a monomer:catalyst loading of 5000:1 – was added to the apparatus to study permeation. CH_2Cl_2 (20 mL) was added to the upstream and downstream sides of the membrane. The membrane was allowed to equilibrate for 30 min. CH_2Cl_2 (5 mL) was added to the downstream side of the membrane and CH_2Cl_2 (5 mL) was added to the upstream side of the membrane with hexadecane (1 mmol). Both sides of the membrane were stirred continuously at room temperature. At 1, 2, and 3 h a 1 mL aliquot was removed from both sides. An ^1H NMR spectrum was taken of each aliquot using tetraethylene glycol as an internal standard as described previously.

Flux is the amount of material in moles that progress through a unit area of a membrane per unit time. The mmole of hexadecane on the downstream side as determined by ^1H NMR spectroscopy was plotted against time. The slope of the graph

was divided by the area of the membrane (7.07 cm²) resulting in the flux of hexadecane. The aliquots were obtained early when flux can be approximated as unidirectional.

Density of cross-links of PDCPD membranes

IR spectroscopy was used to determine the density of cross-links in PDCPD. Dicyclopentadiene (5%, 10%, 15% and 20% by volume solutions) in dioxane was used to find a calibration curve. The IR spectrum of each solution was measured using a cell with a fixed pathlength of 100 μm . The intensity of the peak at 704 cm^{-1} in each of the IR spectra was measured and plotted against concentration to yield the calibration curve.

A 20 mg/mL solution of the Grubbs first generation catalyst in 1,2-dichloroethane was made. Commercially available dicyclopentadiene (4 mL, 0.029 mmol) was heated to 40 °C. The catalyst solution (0.246 mL, 6.0×10^{-3} mmol of catalyst) was added to dicyclopentadiene. A sample of this solution was added to the top of a glass slide and was pressed by down by another glass slide. This set up was heated to 50 °C for 2 h. The glass slides were removed from the PDCPD membranes and the thicknesses were measured using an optical microscope as described previously.

Eleven PDCPD membranes were fabricated and the IR spectrum of each was obtained. The intensity of the peak at 704 cm^{-1} for each of the membranes was fitted to the calibration curve and the density of unreacted cyclic olefin in PDCPD was calculated. The membranes were immersed in methylene chloride in glass vials for an hour. The dichloromethane was decanted off and any remaining solvent in the membrane was removed *in vacuo* for 12 h. The IR spectra were measured for all of the membranes. The intensity of the peak at 704 cm^{-1} for each of these membranes was fitted to the calibration curve and the density of unreacted cyclic olefin in PDCPD was calculated.

Isolation of cholesterol from tricyclohexylphosphine,
triphenylphosphine, and tributylamine (Figure A.6)

A membrane – made with a monomer:catalyst loading of 5000:1 – was added to the apparatus to study permeation. CH_2Cl_2 (23 mL) was added to the downstream side of the membrane and CH_2Cl_2 (25 mL) was added to the upstream side of the membrane with cholesterol (3 mmol), tricyclohexylphosphine (2 mmol), triphenylphosphine (2 mmol), and tributylamine (3 mmol). The solutions on the downstream and upstream sides of the membranes were continuously stirred. A 2 mL aliquot was removed from the upstream side immediately after it was added to the apparatus. The solvent was removed and a ^1H NMR spectrum was obtained. At 48 h aliquots (5 mL) were removed from both sides of the membrane. The solvent was removed and ^1H NMR spectra were obtained.

Isolation of nitrobenzaldehyde from binol

A membrane – made with a monomer:catalyst loading of 5000:1 – was added to the apparatus to study permeation. CH_2Cl_2 (50 mL) was added to the downstream side of the membrane and CH_2Cl_2 (25 mL) was added to the upstream side of the membrane with binol (0.264 g) and nitrobenzaldehyde (0.484 g). The solvent on both sides of the membrane were stirred continuously at room temperature. At 24 h the solvent from the downstream side was removed and evaporated to recover nitrobenzaldehyde (0.249 g). The solvent was replaced with CH_2Cl_2 (50 mL). At 48 h the solvent was removed from the downstream side and evaporated to recover nitrobenzaldehyde (0.186 g). Also at 48 h, the solvent from the upstream side was removed and evaporated to recover nitrobenzaldehyde (50 mg) and binol (0.046 g). CH_2Cl_2 (25 mL) was added the upstream side and stirred for 24 h. The solvent was removed and evaporated to yield 0.103 g of binol. The membrane was removed from the apparatus, cut into pieces, and placed into a flask with CH_2Cl_2 (50 mL) for 24 h. The CH_2Cl_2 was evaporated to yield an additional

0.033 g of binol. The total recovery of nitrobenzaldehyde from solvent downstream of the membrane was 90% with <3% binol contamination. The total recovery of binol from solvent upstream of the membrane was 69%.

Recycling of a PDCCPD membrane

A PDCCPD membrane was added to the apparatus to study permeation. CH_2Cl_2 (50 mL) was added to the downstream side of the membrane and CH_2Cl_2 (15 mL) was added to the upstream side of the membrane with binol (0.286 g, 1 mmol) and nitrobenzaldehyde (0.151 g, 1 mmol). At 24 and 48 h the solvent from the downstream side was removed and evaporated to recover nitrobenzaldehyde. The solvent was replaced with fresh CH_2Cl_2 (50 mL). At 72 h the solvent on the upstream and downstream sides of the membrane were removed and evaporated to recover binol and nitrobenzaldehyde. Fresh CH_2Cl_2 (30 mL) was added upstream of the membrane to extract binol from the membrane. At 84 h solvent upstream of the membrane was removed and evaporated to recover binol. This completed cycle 1 and cycles 2 and 3 were completed with the same PDCCPD membrane. In cycle 1, 99% of the nitrobenzaldehyde and 40% of the binol were recovered, in cycle 2 79% of the nitrobenzaldehyde and 4% of the binol were recovered, and in cycle 3 72% of the nitrobenzaldehyde and 82% of the binol were recovered.

Measurement of the critical dimension and critical area

The software used for these measurements was Spartan '08 V1.2.0. Each molecule was drawn in the software using a ball and spoke representation and its energy was minimized by finding the equilibrium geometry at ground state with a semi-empirical method using AM1 parameters. The surface area and molecular volume were calculated based on a space filling model. The space filling model chosen was a 3D molecular model with atoms represented by spheres whose radius is assumed to be the Van der Waals radius determined by the electron density cut-off at $0.002 \text{ electrons}/\text{\AA}^3$.

Each molecule was analyzed to find the conformation with the lowest rectangular, cross-sectional area. The two dimensions of the rectangle were measured and the longer dimension was labeled the critical dimension and the area was labeled as the critical area.

Results and Discussion

Fabrication of PDCPD membranes and the apparatus to measure permeation

Membranes composed of PDCPD were readily fabricated by the polymerization of commercially available dicyclopentadiene using the Grubbs first generation catalyst at molar ratios of >4,000:1 dicyclopentadiene:Grubbs catalyst (Figure A.1a). The Grubbs catalyst was added to dicyclopentadiene, mixed thoroughly, and placed between two glass slides separated by approximately 100 microns. These membranes were robust and could be manipulated by hand.

In the experiments described in this report, the membranes were placed in an apparatus between two reservoirs of solvent (Figure A.2). The membranes were kept in place using O-rings on either side and held in place using a clamp. The solvent on either side of the membrane was agitated using stir bars and a magnetic stir plate to eliminate any boundary effects that might influence these experiments. In most experiments the permeation of a molecule through the membrane was studied by adding it to solvent on only one side of the membrane. This was called the “upstream” side of the membrane. Many molecules permeated through the membranes and were also found in the solvent “downstream” of the membrane.

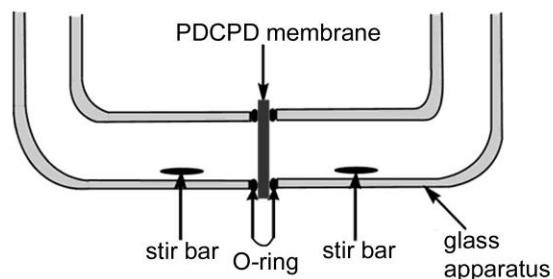


Figure A.2 A cross-sectional schematic of the apparatus used to measure permeation through PDCPD membranes.

Permeation of Co(salen) using membranes composed of
PDCPD or polydimethylsiloxane

Preliminary work indicated that membranes composed of PDCPD would not allow molecules above a critical cross-sectional area to permeate. To investigate the composition of PDCPD membranes that would retain selected molecules based on their cross-sectional area, the permeation of Co(salen) was studied due to its large cross-sectional area of 1.15 nm^2 . To contrast the results with PDCPD membranes, the permeation of Co(salen) and hexadecane through membranes composed of polydimethylsiloxane (PDMS) were also studied. PDMS was chosen based on our prior work to site-isolate water, Grignard reagents, butyl lithium, PdCl₂, and other catalysts and reagents.^{75-77,202-204} In this prior work, PDMS successfully retained a wide variety of reagents and catalysts based on their low solubility in hydrophobic PDMS.

A membrane composed of PDMS was fabricated with a thickness of 450 microns and equilibrated with CH₂Cl₂ on both sides of the membrane. Co(salen) and hexadecane were added upstream of the membrane and the concentration of Co(salen) and hexadecane upstream (S_u) and downstream (S_d) of the membrane were measured at 2, 4, and 6 h (Table A.1). In prior work little evidence was observed for the ability of PDMS membranes to distinguish molecules based on their cross-sectional areas, and in

experiments with Co(salen) and hexadecane, both molecules permeated the membranes at similar rates.

Table A.1 Permeation of Co(salen) and hexadecane using PDMS membranes and CH₂Cl₂ as the solvent.

Molecule	S _d /S _u at 2 h	S _d /S _u at 4 h	S _d /S _u at 6 h
Co(salen)	0.03	0.07	0.13
hexadecane	0.17	0.52	0.61

PDCPD membranes were fabricated with different loadings of dicyclopentadiene:Grubbs catalyst as shown in Table A.2 to determine the ratio that led to retention of Co(salen). In all of these experiments the concentration of Co(salen) was studied by UV-VIS spectroscopy rather than ¹H NMR spectroscopy because the UV-VIS spectrometer allowed lower concentrations of Co(salen) to be measured and because Co(salen) was paramagnetic. At high loadings of 50,000:1 dicyclopentadiene:Grubbs catalyst the polymerization was incomplete and the polymer membrane was tacky and not robust. At loadings of dicyclopentadiene:Grubbs catalyst below 4,000:1 the polymerization was too rapid and the solution hardened before it could be cast into a thin film.

PDCPD membranes synthesized with molar ratios of 4,000 to 20,000 dicyclopentadiene to one Grubbs catalyst resulted in controlled polymerizations and well-defined membranes. These membranes were used to study whether Co(salen) permeated them using CH₂Cl₂ as the solvent. In each of these experiments Co(salen) was not detected by UV-VIS spectroscopy downstream of the membrane at 24 or 48 h (Table A.2). To provide further evidence for the retention of Co(salen), the concentration of Co downstream and upstream of the membranes were measured by ICP-OES at 48 h for

entries 4 and 5. In these experiments, <0.5% of the Co was found downstream of the membrane which demonstrated that it did not permeate.

Table A.2 Permeation of Co(salen) using PDCPD membranes fabricated with different catalyst loadings.

Entry	Dicyclopentadiene: Grubbs catalysts	Ethyl vinyl ether	^a Thickness (μm)	^b S_d/S_u at 24 h	^b S_d/S_u at 48 h
1	^c 50000/1	^d none	Na	Na	Na
2	20000/1	none	110	$\leq 0.004^e$	$\leq 0.005^e$
3	10000/1	none	110	$\leq 0.005^e$	$\leq 0.006^e$
4	5000/1	none	110	$\leq 0.006^e$	$\leq 0.007^e$
5	4000/1	none	100	$\leq 0.005^e$	$\leq 0.007^e$
6	10000/1	^f 10 mL	120	0.49	0.35
7	5000/1	^f 10 mL	88	0.05	0.06
8	4000/1	^f 10 mL	110	0.04	0.08
9	5000/1	^g none	98	$\leq 0.006^e$	$\leq 0.009^e$

^aThe thickness of the membrane. ^bThe ratio of the downstream (S_d) concentration of Co(salen) to the upstream (S_u) concentration. ^cIncomplete polymerization after 47 h at 50 °C. ^dNo ethyl vinyl ether was added to the solvent on either side of the membrane. ^eNo Co(salen) was detected in the solvent downstream of the membrane. ^fEthyl vinyl ether was added to the solvent on each side of the membrane. ^gTHF was added to the solvent on either side of the membrane in the same concentration as ethyl vinyl ether from entries 6-8.

In entries 2-5 in Table 2 less than 30% of the Co(salen) permeated into the PDCPD matrix after 48 h, the remainder was found in the solvent upstream of the membrane. Thus, the Co(salen) was soluble in the PDCPD membrane and readily

partitioned into it, so its slow permeation through the membrane was due to a very low rate of diffusion in the PDCPD matrix. In a later section it will be shown that molecules can be extracted from the PDCPD membrane and do not remain “trapped” in the PDCPD matrix.

These membranes were further studied for the effect of ethyl vinyl ether on the permeation of Co(salen). When dicyclopentadiene is polymerized with the Grubbs catalyst, the strained bicyclic olefin reacts rapidly to yield a polymer and the other olefin reacts at a slower rate to yield cross-links in the PDCPD matrix.^{128,130,132,196,205-207} We hypothesized that the membranes underwent further cross-linking when swollen in organic solvent prior to being used as membranes because they were fabricated in the absence of solvent and initially yielded hard, solid materials that hindered the diffusion of the Grubbs catalyst. To investigate whether the Grubbs catalyst reacted when the membranes were swollen in organic solvents, they were swollen in CH₂Cl₂ with ethyl vinyl ether to terminate the Grubbs catalyst. If the Grubbs catalyst was inactive when the membranes were swollen in CH₂Cl₂, membranes treated with ethyl vinyl ether would have similar properties for the permeation of Co(salen) as those not exposed to ethyl vinyl ether. If the Grubbs catalyst was dormant in the solid PDCPD and further cross-linked PDCPD when swollen in CH₂Cl₂, the addition of ethyl vinyl ether would stop any further cross-linking and affect the permeation of Co(salen). When these membranes were studied for their ability to resist the permeation of Co(salen), all of them allowed Co(salen) to permeate (entries 6-8 in Table A.2). In a control experiment to study whether the addition of ethyl vinyl ether resulted in different permeation rates due to a change in solvent polarity, THF was added to CH₂Cl₂ rather than ethyl vinyl ether (entry 9 in Table A.2). In this experiment Co(salen) did not permeate the membrane which demonstrated that the effect of ethyl vinyl ether could not be explained by a change in solvent polarity.

These experiments provided evidence that the cross-linking of the PDCPD matrix is incomplete when a solid polymer matrix is formed and the membranes must be swollen in organic solvents to have the desired properties to retain Co(salen). In the next section of this report, the density of cross-links in PDCPD before and after swelling in CH_2Cl_2 will be reported that provide further evidence that the Grubbs catalyst is dormant in PDCPD and reacts to form more cross-links when the polymer is swollen in organic solvents.

Measurement of density of cross-links in PDCPD

The density of cross-links in PDCPD was measured using IR spectroscopy. It is important to understand that when dicyclopentadiene is polymerized it yields a hard, solid material that lacks well-defined, empty pores such as those found for zeolites or other nanoporous membranes. PDCPD was studied by scanning electron microscopy to reveal a flat, featureless surface. The surface of PDCPD was investigated by x-ray photoelectron spectroscopy and grazing angle total reflection-infrared (GATR-IR) spectroscopy in prior work.²⁰⁸ The surface of PDCPD had little surface oxidation and its GATR-IR spectrum did not possess any unexplained peaks. Typical methods to characterize the distribution of empty pores were not attempted because of the lack of empty pores within PDCPD.

The most important characteristic of PDCPD is the density of cross-links within the matrix that occur when the five membered ring in the monomer reacts with another polymer chain. The degree of cross-linking of PDCPD was measured using IR spectroscopy by investigating the peak at 704 cm^{-1} that was assigned to the cis oops bending of the unreacted olefin in PDCPD (Figure A.3). Opening of this ring by the Grubbs catalyst led to cross-links in PDCPD; thus, measurement of the concentration of the unreacted cyclic olefin in a PDCPD matrix gave an approximate concentration of cross-links. The peak at 704 cm^{-1} was assigned to the cis oops of the unreacted olefin

based on literature precedent for peaks in this area. Olefins that reacted with the Grubbs catalyst were no longer part of medium sized rings and their values for the oops peak appeared at higher wavenumbers based on analogy to linear molecules. For instance, the oops peak for cis-3 heptene was at 714 cm^{-1} and for cyclopentene it was at 697 cm^{-1} . Trans oops peak typically have values above 720 cm^{-1} . Thus, the peak at 704 cm^{-1} was used to find the concentration of uncross-linked monomer in PDCPD.

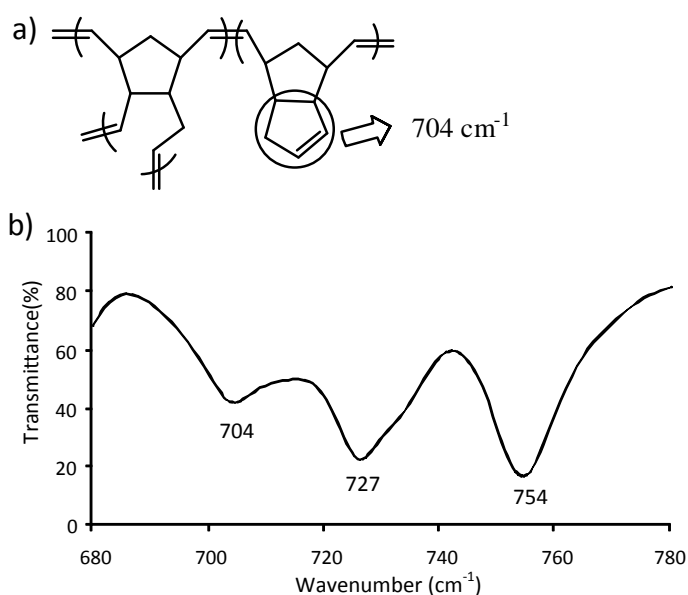


Figure A.3 Cross-linking density in PDCPD. a) The unreacted five membered ring that is responsible for the peak at 704 cm^{-1} . b) The IR spectrum of PDCPD in the region of interest.

A calibration curve for the cis oops peak was obtained by measuring the intensity of the peak for dicyclopentadiene dissolved in dioxane. Dioxane was chosen due to its low dielectric constant and absence of peaks in the area of interest. Briefly, an IR flow cell with 100 micron spacings between the plates was filled with solutions of dicyclopentadiene in dioxane. The IR spectra were obtained for different concentrations and a calibration curve was measured.

Eleven PDCPD membranes were fabricated with molar ratios of dicyclopentadiene to Grubbs catalyst of 5,000:1 and their IR spectra were measured. Next, the membranes were swelled in CH_2Cl_2 for an hour, dried under N_2 , and the solvent was completely removed by placing the membranes under vacuum for 12 h. The IR spectra were again measured for the membranes. The average density of unreacted cyclic olefin as shown by the peak at 704 cm^{-1} was only 47% ($\pm 19\%$) before swelling in CH_2Cl_2 . Thus, approximately 53% ($\pm 19\%$) of the cyclic olefins had reacted to form cross-links. From the prior experiments with $\text{Co}(\text{salen})$ and PDCPD membranes that had been exposed to ethyl vinyl ether (Table A.2), it was known that the Grubbs catalyst was reactive and would further cross-link the membranes when swollen in organic solvent. This conclusion was supported by the IR spectrum of the membranes after swelling in CH_2Cl_2 which showed that approximately 84% ($\pm 12\%$) of the cyclic olefins had reacted. Clearly, the Grubbs catalyst was able to react further when the hard, solid PDCPD membranes were swollen in CH_2Cl_2 for an hour. This result is understandable because of the stability of the Grubbs catalyst in air (particularly when it is embedded in a solid matrix), and the extent that the PDCPD membranes swell in CH_2Cl_2 .

Flux of organic molecules through PDCPD membranes

PDCPD is significantly swollen by organic solvents (Table A.3).²⁰⁹⁻²¹¹ To quantify the ability of solvents to swell PDCPD a series of dry slabs of PDCPD were weighed, immersed in a solvent for 24 h, removed from the solvent, briefly dried of any solvent on the exterior of the slab, and weighed. The data in Table A.3 demonstrated that apolar solvents swelled PDCPD the best which was reasonable considering apolar structure of PDCPD. In addition, PDCPD adsorbed more than its weight in selected solvents.

Table A.3 How solvents swell PDCPD.

Solvent	Weight of swollen PDCPD/weight of PDCPD (g/g)
chloroform	3.38
dichloromethane	2.46
toluene	2.23
tetrahydrofuran	2.06
ethyl acetate	1.35
diethyl ether	1.34
hexanes	1.32
petroleum ether	1.27
dioxane	1.26
acetone	1.14
methanol	1.12

The flux of hexadecane through PDCPD membranes was quantified with CH_2Cl_2 and toluene as the solvents. The membranes were fabricated as before with a molar ratio of 5,000:1 dicyclopentadiene to Grubbs catalyst. The membranes were placed into the apparatus to measure flux and were equilibrated for 30 min with solvent on both sides. After this time period, 1 mmol of hexadecane was added to solvent on one side of the membrane (the upstream side) and aliquots upstream and downstream of the membranes were periodically removed to quantify the concentration of hexadecane. In Figure A.4 the amount of hexadecane – measured in mmoles – downstream of the membranes as a function of time is shown. The values for the flux of hexadecane were calculated to be $1.02 \times 10^{-5} \text{ mol cm}^{-2} \text{ h}^{-1}$ with CH_2Cl_2 as solvent and $6.53 \times 10^{-6} \text{ mol cm}^{-2} \text{ h}^{-1}$ with toluene as solvent. Although these values are lower than those reported for other membranes, such as the OSN membranes used in the chemical industry, the PDCPD membranes were not optimized for their flux. The flux can be increased by using thinner membranes and by applying external pressure.

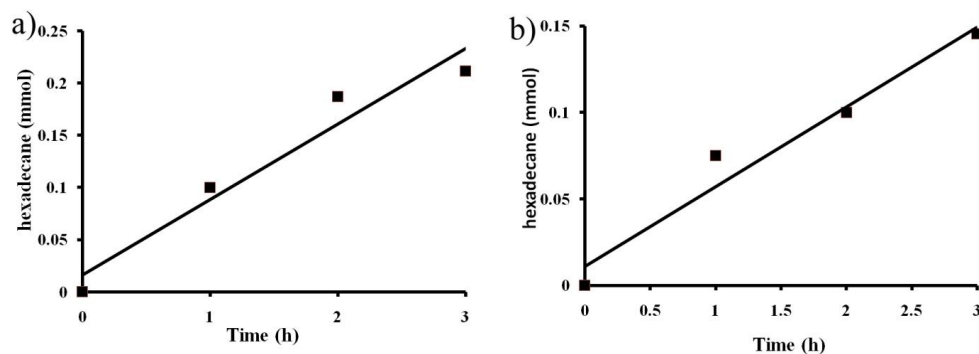


Figure A.4 The amount of hexadecane in mmol that was downstream of a membrane as a function of time. The solvent was a) CH₂Cl₂ and b) toluene.

For comparison, the upper limit for the flux of Co(salen) in entry 4 of Table A.2 with CH₂Cl₂ as the solvent was approximately $4 \times 10^{-10} \text{ mol cm}^{-2} \text{ h}^{-1}$. Thus, the difference for flux of hexadecane and Co(salen) was at least four to five orders of magnitude.

The ability of hexadecane, nitrobenzaldehyde, cholesterol, hexanoic acid, and 1,6-diaminohexane to permeate PDCPD membranes with CH₂Cl₂, toluene, and THF as solvents was studied. In these experiments, each of the molecules and hexadecane were added to solvent on one side of the membrane and the concentrations upstream and downstream were found after 24 and 48 h (Table A.4). Hexadecane was added as an internal control to ensure that each membrane had similar properties and that permeation was measured consistently. Each of these molecules had reasonable rates of permeation through the membranes and, except for cholesterol, the concentrations on either side of the membrane had mostly equilibrated at 48 h.

Table A.4 Flux of five organic molecules through PDCPD membranes

Molecule	Solvent	^a Thickness (μm)	^b S_d/S_u at 24 h	^b S_d/S_u at 48 h
hexadecane	CH_2Cl_2	100	0.68	0.95
hexadecane	Toluene	110	0.82	0.86
hexadecane	THF	100	0.66	0.98
nitrobenzaldehyde	CH_2Cl_2	100	0.82	1.0
nitrobenzaldehyde	Toluene	110	0.96	0.98
nitrobenzaldehyde	THF	100	0.66	1.0
cholesterol	CH_2Cl_2	100	0.44	0.69
cholesterol	Toluene	110	0.54	0.58
cholesterol	THF	100	0.54	0.82
hexanoic acid	CH_2Cl_2	99	0.88	0.94
hexanoic acid	Toluene	110	0.55	0.82
hexanoic acid	THF	89	0.69	1.0
1,6-diaminohexane	CH_2Cl_2	80	0.81	0.93
1,6-diaminohexane	Toluene	98	0.95	0.97
1,6-diaminohexane	THF	120	1.0	1.0

^aThe thickness of the PDCPD membrane that was prepared at a molar ratio of dicyclopentadiene:Grubbs catalyst of 5,000:1. ^bThe ratio of the concentration downstream to the concentration upstream for each molecule.

The permeation of a molecule through a membrane is dependent on the rate of diffusion of that molecule within a membrane multiplied by its solubility in the membrane according to the well known equation $P = DS$.¹³⁵ Each of the five molecules shown in Table 4 permeated the membranes at appreciable rates which demonstrated that they were soluble and possessed reasonable rates of diffusion within the PDCPD matrix. What is notable is that both polar and apolar molecules permeated at similar rates through the hydrophobic, but swollen, PDCPD membranes.

The ability of 14 additional molecules to permeate PDCPD membranes fabricated from a dicyclopentadiene to Grubbs catalyst ratio of 5,000:1 were measured with CH_2Cl_2 as the solvent (Figure A.5 and Table A.5). Similar to other experiments, the molecule of interest and hexadecane were added to solvent upstream of the membranes. The internal

control of adding hexadecane to each experiment ensured that the flux was similar for each membrane and that a lack of flux of a molecule through the membrane was not due to a faulty membrane, but rather it was due to an intrinsic property of the membrane.

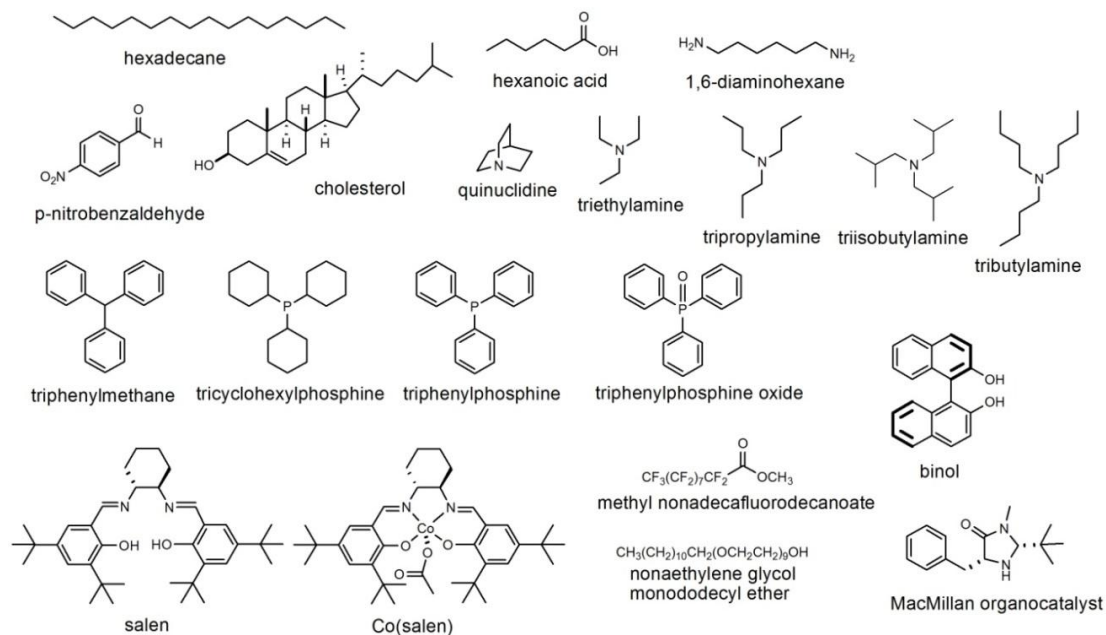


Figure A.5 The molecules that were studied for their permeation through PDCPD membranes.

Table A.5 Permeation of organic molecules using PDCPD membranes and CH₂Cl₂ as the solvent.

Molecule	Molecular Weight (g mol ⁻¹)	^a Thickness (μm)	^b S _d /S _u at 24 h	^b S _d /S _u at 48 h
Quinuclidine	111	100	0.81	0.93
triethylamine	101	97	1.0	0.98
tripropylamine	143	100	0.67	0.87
tributylamine	185	96	≤0.02 ^c	≤0.03 ^c
triisobutylamine	185	100	0.88	1.0
triphenylmethane	244	90	≤0.01 ^c	≤0.01 ^c
MacMillan organocatalyst	246	120	0.32	0.7
triphenylphosphine	262	100	≤0.02 ^c	≤0.03 ^c
triphenylphosphine oxide	278	84	≤0.02 ^c	≤0.03 ^c
^d tricyclohexylphosphine	280	100	≤0.01 ^c	≤0.02 ^c
binol	286	96	≤0.01 ^c	≤0.02 ^c
salen	492	100	≤0.01 ^c	≤0.01 ^c
methyl nonadecafluorodecanoate	528	98	0.85	0.94
nonaethylene glycol monododecyl ether	583	130	0.04	0.33

^aThe thickness of the membrane. ^bThe ratio of the concentration of a molecule downstream to its concentration upstream. ^cThe molecule was not observed downstream of the membrane. ^dLess than 10% of the tricyclohexylphosphine oxidized during these experiments.

Several conclusions can be drawn from the experiments in Table A.5 and those presented earlier in this article. Whether a molecule will permeate PDCPD is clearly not dependent on molecular weight because the two molecules (MW: 528 and 583 g mol⁻¹) with highest molecular weights permeated the membranes but tributylamine (MW: 185 g mol⁻¹) and triphenylphosphine (MW: 262 g mol⁻¹) did not permeate it. Both hydrophobic and hydrophilic molecules permeated the membranes and failed to permeate them. For instance, apolar molecules such as hexadecane, cholesterol, and tripropylamine permeated the membranes but tributylamine, triphenylphosphine, and tricyclohexylphosphine did not permeate them. Triphenylphosphine oxide was chosen

because it is more polar than triphenylphosphine due to the presence of a polar P=O bond but possessed a similar shape. Triphenylphosphine oxide did not permeate the membranes at any detectable amount. The presence of amines or phosphines was not a distinguishing factor for whether a molecule would not permeate a membrane because triphenylmethane did not permeate it also.

Reason for the retention of selected molecules by PDCPD membranes

The flux of molecules through cross-linked polymeric membranes has been described theoretically by others through competing models.¹³⁵ A general description that is agreed upon is that the diffusion, D , of a molecule to move from point to point in a polymer matrix depends exponentially on energy of activation, E_a , according to the equation $D = D_0 \exp(-E_a/RT)$. In a highly cross-linked polymer matrix, small molecules can diffuse with little or no rearrangement of the polymer and the value for E_a is small. Molecules with cross-sectional areas that are comparable or larger than the pores in a cross-linked polymer require substantial rearrangement of the polymer matrix that lead to high values for E_a and low values for diffusion. Thus, the theoretical descriptions of flux and rates of diffusion make extensive use of cross-sectional areas to make predictions or to rationalize observed results. For instance, in a classic paper in 1982 by Berens and Hopfenberg the log of diffusion versus diameter and the square of diameter was plotted for 18 molecules that permeated polystyrene, polymethylmethacrylate, and polyvinyl chloride. Neither plot was superior to the other due to scatter in the data, but it was clear that flux strongly depended on molecular diameter. In fact, the difference in flux for He (diameter = 0.258 nm) and neopentane (diameter 0.580 nm) was approximately ten orders of magnitude. Unfortunately, this difference in flux was not studied for molecules larger than hexanes because of the vanishingly slow values for diffusion. At the other end of the molecular weight spectrum, the separation of polymers from small molecules using

porous polymeric membranes is well known and used in applications such as to dialyze proteins from small molecules.

Most prior membranes to separate organic molecules used molecular weight or hydrophobic/hydrophilic effects to distinguish between molecules. For instance, ionic liquids will not partition into PDMS (a hydrophobic polymer) so they have no measurable flux through membranes composed of PDMS.²¹² Membranes that separate organic molecules possessing molecular weights from 100 to 600 g mol⁻¹ use molecular weight as the criterion for separation rather than cross-sectional area for two reasons. First, molecular weight is straightforward and easy to define but cross-sectional area is a more challenging concept to quantify. Second, separations based on molecular weight are successful and no allowances must be made for molecular size. Molecules below a MWCO permeate the membranes but molecules above the MWCO do not permeate and no exceptions are needed for effects based on cross-sectional area. The use of molecular weight as the criterion for separation does not imply any underlying importance to molecular weight in the mechanisms by which molecules are separated.

In Table A.6 the molecular sizes of molecules that permeated or did not permeate PDPCD membranes are described. The surface area, molecular volume, critical dimension, and critical area were calculated by first minimizing the energy for each molecule using Spartan '08 V1.2.0. Next, the surface area and molecular volume were calculated from space filling models as described in the experimental section. The critical area was defined as the smallest rectangular cross-sectional area of a molecule that must be met for it to pass through a pore. For instance, a penny would be viewed on its side such that its cross-sectional area is a thin rectangle and distinctly smaller than the cross-sectional area for a sphere with the same radius as a penny. This rectangular cross-sectional area was determined using Spartan '08 V1.2.0 for each molecule as described in the experimental section. The critical dimension was the larger of the two distances used to find the critical area.

It is clear from Table A.6 that the critical dimension and area both correlate to whether a molecule will permeate PDCPD. Molecules that permeated through PDCPD membranes had critical dimensions and areas of less than 0.80 nm and 0.38 nm², but molecules that did not flux through the membranes had critical dimensions and areas of at least 0.92 nm and 0.50 nm². Surprisingly, a difference in critical dimension or area significantly less than a factor of two had a substantial impact on the flux of molecules through PDCPD.

Table A.6 The chemical and physical sizes of molecules that did or did not permeate PDCPD membranes

Molecule	Measurable flux	Molecular weight (g mol ⁻¹)	Surface Area (nm ²)	Molecular volume (nm ³)	Critical dimension (nm)	Critical area (nm ²)
triethylamine	Yes	101	1.64	0.138	0.67	0.18
quinuclidine	Yes	111	1.46	0.131	0.42	0.21
hexanoic acid	Yes	116	1.65	0.135	0.28	0.067
1,6-diaminohexane	Yes	116	1.80	0.146	0.28	0.067
tripropylamine	Yes	143	2.20	0.193	0.79	0.32
nitrobenzaldehyde	Yes	151	1.64	0.142	0.43	0.06
tributylamine	No	185	2.86	0.249	0.92	0.5
triisobutylamine	Yes	185	2.82	0.248	0.80	0.38
hexadecane	Yes	226	3.52	0.307	0.28	0.067
triphenylmethane	No	244	2.92	0.285	0.95	0.51
MacMillan organocatalyst	Yes	246	2.96	0.279	0.62	0.36
triphenylphosphine	No	262	2.92	0.286	0.95	0.61
triphenylphosphine oxide	No	278	3.11	0.299	0.95	0.61
tricyclohexylphosphine	No	280	3.24	0.323	0.92	0.57
binol	No	286	2.99	0.298	0.72	0.51
cholesterol	Yes	387	2.29	0.454	0.55	0.28
salen	No	492	6.36	0.630	1.22	0.79
methyl nonadecafluorodecanoate	Yes	528	3.39	0.312	0.43	0.14
nonaethylene monododecyl ether	Yes	583	7.37	0.640	0.28	0.067
Co(salen)	No	662	7.06	0.699	1.22	1.15

The difference in permeation of tripropylamine, triisobutylamine, and tributylamine illustrates the importance of cross-sectional area (Table A.6). Triisobutylamine and tributylamine are constitutional isomers that possess the same molecular weight and similar surface areas and volumes. The major difference between triisobutylamine and tributylamine are their cross-sectional areas, triisobutylamine (0.38 nm^2) has a similar cross-sectional area to tripropylamine (0.32 nm^2), but the cross-sectional area of tributylamine (0.50 nm^2) is larger. In flux experiments tripropylamine and triisobutylamine permeated the membranes but tributylamine did not permeate. These experiments demonstrate the selectivity of the membranes and the need to consider cross-sectional area as the important parameter for the flux of molecules.

Extraction of nitrobenzaldehyde from binol

The ability to efficiently extract a molecule through a PDCCPD membrane while retaining a second molecule was studied using nitrobenzaldehyde and binol. It is important that a high yield of a molecule be obtained after permeation through a membrane, and it is also important that molecules that are retained by a membrane do not remain embedded with the PDCCPD matrix. In some applications it will also be important that molecules that are retained be recycled and accessible after separations. These issues were initially addressed by studying the extraction of nitrobenzaldehyde from binol.

In these experiments, a mixture of nitrobenzaldehyde (484 mg) and binol (264 mg) were added upstream of a membrane in CH_2Cl_2 and extracted downstream using CH_2Cl_2 . After 24 h, the solvent downstream was removed from the apparatus and fresh CH_2Cl_2 was added downstream. After an additional 24 h, the solvent downstream was removed and the extracted yield of nitrobenzaldehyde through two cycles calculated to be 90% with no detectable level of binol contamination. The solvent upstream was also removed from the apparatus and the amount of binol in solution was only 17% of the original amount of binol added to the apparatus. The remainder of the binol was in the

PDCPD matrix and had to be extracted. A fresh aliquot of CH_2Cl_2 was added on the upstream side of the membrane and allowed to sit for 24 h. The CH_2Cl_2 was removed from the apparatus to yield an additional 39% of the original amount of binol. The membrane was cut into pieces and immersed in CH_2Cl_2 to further extract binol. After 24 h an additional 13% of the original amount of binol was isolated which yielded a total isolation of 69% of the original amount of binol. When this experiment was repeated the amount of nitrobenzaldehyde that was isolated downstream of the membrane was 87% and the amount of binol that was isolated was 72%.

These experiments demonstrated that high yields of clean nitrobenzaldehyde could be isolated from significant quantities of binol. Furthermore, most of the binol partitioned into the PDCPD membranes during these experiments, but it was readily extracted into fresh solvent where it was isolated and characterized. The partitioning of binol from solvent into the membranes was a reversible process that allowed much of the binol to be isolated at the end of these experiments.

Extraction of cholesterol from triphenylphosphine,
tricyclohexylphosphine, and tributylamine using a PDCPD
membrane

To demonstrate the selective permeation of a high molecular weight compound from low molecular weight compounds based on their different cross-sectional areas, the extraction of cholesterol (3 mmol) from a mixture of triphenylphosphine (2 mmol), tricyclohexylphosphine (2 mmol), and tributylamine (3 mmol) was investigated. These four molecules were dissolved in 25 mL of CH_2Cl_2 and added to one side of a membrane and 23 mL of CH_2Cl_2 was added downstream of the membrane. A 2 mL aliquot was immediately removed from the upstream side and characterized by ^1H NMR spectroscopy to show the initial mixture of molecules. After 48 h aliquots were removed from both sides of the membrane and characterized by ^1H NMR spectroscopy.

The ^1H NMR spectra in Figure A.6 clearly demonstrate that cholesterol was selectively extracted from the solvent mixture. The ^1H NMR spectra of the initial mixture of the four molecules, the organic molecules upstream of the membrane after 48 h, the organic molecules downstream of the membrane after 48 h, and a sample of pure cholesterol are all shown. Some oxidation of the PCy_3 occurred during the extraction, but the OPCy_3 was also retained by the membrane. The ^1H NMR spectrum of the organic product downstream of the membrane after 48 h matched the ^1H NMR spectrum of cholesterol and no evidence of PCy_3 , OPCy_3 , PPh_3 , or NBu_3 were seen downstream of the membrane. This result was remarkable considering that the molecular weight of cholesterol ($\text{MW}: 387 \text{ g mol}^{-1}$) was much higher than the other molecules ($185\text{-}296 \text{ g mol}^{-1}$).

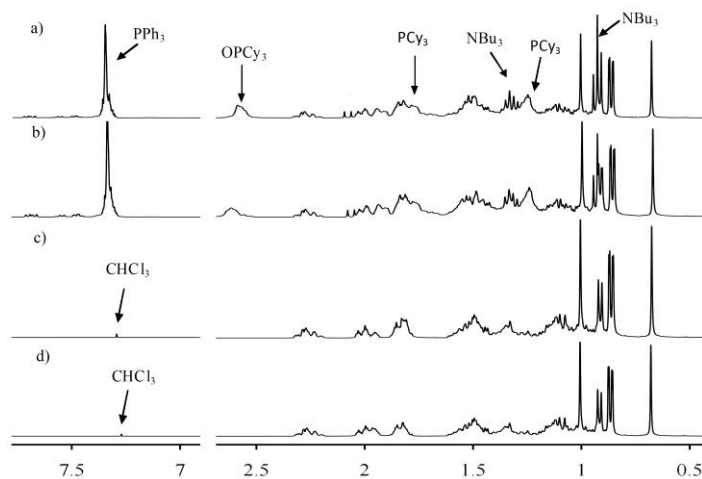


Figure A.6 Extraction of cholesterol from a mixture of molecules. a) The ^1H NMR spectra of the initial mixture of cholesterol, OPCy_3 , PCy_3 , PPh_3 , and NBu_3 ; b) the mixture of molecules upstream of the membrane after 48 h; c) the mixture of molecules downstream of the membrane after 48 h; and d) cholesterol. The peaks for cholesterol at 3.52 and 5.35 ppm were observed in all four spectra but were omitted from this figure to emphasize the region from 0.5 to 2.7 ppm.

Recycling of PDCCPD membranes

The ability to recycle PDCCPD membranes was studied using nitrobenzaldehyde and binol. In this experiment both nitrobenzaldehyde and binol were added upstream of a membrane and nitrobenzaldehyde was isolated downstream of the membrane.

Nitrobenzaldehyde was extracted three times with fresh solvent over 72 h. After 72 h the binol that had permeated into the PDCCPD matrix was extracted by the addition of fresh solvent upstream of the membrane. After the first cycle was complete, fresh nitrobenzaldehyde and binol were added upstream of the membrane and the process was repeated with the same membrane.

A total of three cycles were completed and the extraction of nitrobenzaldehyde was high for each cycle. In the three cycles nitrobenzaldehyde was isolated in 99%, 79%, and 72% yield and the binol was isolated in 40%, 4%, and 82% yield. The fourth cycle was not finished because binol began to permeate the membrane. Notably, nitrobenzaldehyde was isolated as a clean product without any impurities from binol. The binol contained some nitrobenzaldehyde as an impurity and had to be extracted from the PDCCPD membrane. This experiment demonstrates that the membranes can be recycled over several cycles, and future work will study how to optimize this process.

Conclusions

New technologies originate from new materials. Most past examples of membranes that separate organic molecules with molecular weights from 100-600 g mol⁻¹ use the concept of a molecular weight cutoff that hinder the use of these membranes to separate catalysts from products of a reaction. Many catalysts and ligands for metals have modest molecular weights that place a real limitation on what molecules they can be separated from. The problem that PDCCPD membranes solve is that they are the first membranes that separate molecules with molecular weights between 100 and 600 g mol⁻¹ based on the concept of a cross-sectional area cutoff rather than a molecular weight

cutoff. These membranes are significant because of the large number and importance of molecules within this range of molecular weights and the need to separate them in the chemical industry. For instance, many reactions require metal catalysts with ligands such as phosphines. It is important that the final product be clean of all but ppm levels of impurities of metal and phosphines so several purification steps are often required to clean the product. PDCCPD membranes offer a new solution to cleaning the products and recycling the catalysts.

The surprising aspect of PDCCPD membranes is not that they separate molecules based on cross-sectional area because cross-sectional area is well known as a critical parameter that affects flux. Rather, it was surprising that these membranes were the first to have a critical importance of cross-sectional area for the flux of molecules within this range of molecular weights. In addition, the difference in permeation was very large; molecules that did not permeate the membranes were undetected in the solvent downstream of the membrane and possessed values for flux that were 10^4 to 10^5 times slower than molecules that permeated the membranes. The origins of the selectivity of these membranes lies in the size and distribution of pore sizes that result when the polymer is cross-linked, and these materials properties will be studied in more detail in future work. An understanding of what makes PDCCPD so unique may allow the design of more membranes with similar separations but faster flux.

BIBLIOGRAPHY

- (1) Cornils, B.; Hermann, A. *Applied Homogeneous Catalysis with Organometallic Compounds*; Wiley -VCH: Weinheim, Germany, 1999.
- (2) Nicolau, K. C.; Bulger, P. G.; Sarlah, D. *Angew. Chem. Int. Ed.* **2005**, *44*, 4442.
- (3) Guram, A. S.; Rennels, R. A.; Buchwald, S. L. *Angew. Chem. Int. Ed. Eng.* **1995**, *34*, 1348.
- (4) Muci, A. R.; Buchwald, S. L. *Top. Curr. Chem.* **2002**, *219*, 131.
- (5) Wiskur, S. L.; Korte, A.; Fu, G. C. *J. Am. Chem. Soc.* **2004**, *126*, 82.
- (6) Tao, X.; Zhao, Y.; Shen, D. *Synlett* **2004**, *2*, 359.
- (7) Yang, B. H.; Buchwald, S. L. *J. Organomet. Chem.* **1999**, *576*, 125.
- (8) Hartwig, J. F. *Acc. Chem. Res.* **1998**, *31*, 853.
- (9) Hartwig, J. F. *Angew. Chem. Int. Ed.* **1998**, *37*, 2047.
- (10) Kosugi, M.; Kameyama, M.; Sano, H.; Migita, T. *Chem. Lett.* **1983**, 927.
- (11) Nishiyama, M.; Yamamoto, T.; Koie, Y. *Tetrahedron Lett* **1998**, *39*, 617.
- (12) Old, D. W.; Wolfe, J. P.; Buchwald, S. L. *J. Am. Chem. Soc.* **1998**, *120*, 9722.
- (13) Wolfe, J. P.; Tomori, H.; Sadighi, J. P.; Yin, J.; Buchwald, S. L. *J. Org. Chem.* **2000**, *65*, 1158.
- (14) Huang, X.; Anderson, K. W.; D, D. Z.; Jiang, L.; Klapars, A.; Buchwald, S. L. *J. Am. Chem. Soc.* **2003**, *125*, 6653.
- (15) Yin, J.; Buchwald, S. L. **2000**, *2*, 1101.
- (16) Yin, J.; Buchwald, S. L. *J. Am. Chem. Soc.* **2002**, *124*, 6043.
- (17) Yang, B. H.; Buchwald, S. L. *Org. Lett.* **1999**, *1*, 35.
- (18) Clemente, T. E.; Cahoon, E. B. *Plant Physiology* **2009**, *151*, 1030.
- (19) Baer, D. *J. Am. J. Clin. Nutr.* **2012**, *95*, 267.
- (20) Cascio, G.; Schiera, G.; Di, L. I. *Curr. Diabetes. Rev.* **2012**, *8*, 2.
- (21) Dhaka, V.; Gulia, N.; Ahlawat, K. S.; Khatkar, B. S. *J. Food. Sci. Technol.* **2011**, *48*, 534.
- (22) Flock, M. R.; Kris-Etherton, P. M. *Curr. Atheroscler. Rep.* **2011**, *13*, 499.
- (23) Gebauer, S. K.; Chardigny, J. M.; Jakobsen, M. U.; Lamarche, B.; Lock, A. L.; Proctor, S. D.; Baer, D. J. *J. Adv. Nutr.* **2011**, *2*, 232.

- (24) Bhupathiraju, S. N.; Tucker, K. L. *Clin. Chim. Acta* **2011**, *412*, 1493.
- (25) Filip, S.; Fink, R.; Hribar, J.; Vidrih, R. *Food Technol. Biotechnol.* **2010**, *48*, 135.
- (26) Kapoor, R.; Huang, Y.-S. *Curr. Pharm. Biotechnol.* **2006**, *7*, 531.
- (27) Katan, M. B. *Am. J. Clin. Nutr.* **1997**, *66*, 974S.
- (28) List, B. *Chem. Rev.* **2007**, *107*, 5413.
- (29) Dalko, P. I.; Moisan, L. *Angew. Chem. Int. Ed.* **2004**, *43*, 5138.
- (30) Enders, D.; Grondal, C.; Huttl, M. R. M. *Angew. Chem. Int. Ed.* **2007**, *46*, 1570.
- (31) Hajos, Z. G.; Parrish, D. R. *J. Org. Chem.* **1974**, *39*, 1615.
- (32) Cordova, A.; Notz, W.; Barbas, C. F. *Chem. Commun.* **2002**, 3024.
- (33) Ahrendt, K. A.; Borths, C. J.; Macmillan, D. W. C. *J. Am. Chem. Soc.* **2000**, *122*, 4243.
- (34) Paras, N. A.; Macmillan, D. W. C. *J. Am. Chem. Soc.* **2001**, *123*, 4370.
- (35) Bon, S. A. F.; Chen, T. *Langmuir* **2007**, *23*, 9527.
- (36) Astruc, D.; Lu, F.; Aranzaes, J. R. *Angew. Chem. Int. Ed.* **2005**, *44*, 7852.
- (37) Bouchy, C.; Schmidt, I.; Anderson, J. R.; Jacobsen, C. J. H.; Derouane, E. G.; Hamid, S. B. *Journal of Molecular Catalysis A: Chemical* **2000**, *163*, 283.
- (38) Derouane, E. G.; Crehan, G.; Dillon, C. J.; Bethell, D.; He, H.; Hamid, S. B. *Journal of Catalysis* **2000**, *194*, 410.
- (39) Derouane, E. G.; Chang, C. D. *Microporous and Mesoporous Materials* **2000**, *35*, 425.
- (40) Hetterley, R. D.; Kozhevnikova, E. F.; Kozhevnikov, I. V. *Chem. Commun. (Cambridge, United Kingdom)* **2006**, 782.
- (41) Reger, T. S.; Janda, K. D. *J. Am. Chem. Soc.* **2000**, *122*, 6929.
- (42) Kobaslija, M.; Bogdan, A. R.; Poe, S. L.; Escobedo, F.; Mcquade, D. T. *Journal of Polymer Science, Part A: Polymer Chemistry* **2008**, *46*, 2309.
- (43) Kobaslija, M.; Mcquade, D. T. *Macromolecules* **2006**, *39*, 6371.
- (44) Broadwater, S. J.; Mcquade, D. T. *J. Org. Chem.* **2005**, *71*, 2131.
- (45) Poe, S. L.; Kobaslija, M.; Mcquade, D. T. *J. Am. Chem. Soc.* **2007**, *129*, 9216.
- (46) Price, K. E.; Mason, B. P.; Bogdan, A. R.; Broadwater, S. J.; Steinbacher, J. L.; Mcquade, D. T. *J. Am. Chem. Soc.* **2006**, *128*, 10376.
- (47) Price, K. E.; Mcquade, D. T. *Chem. Commun.* **2005**, *13*, 1714.

- (48) Drioli, E.; Giorno, L. *Comprehensive Membrane Science and Engineering: Basic Aspects in Membrane Preparation and their Transport Phenomena*; Elsevier Science, 2010.
- (49) Bhore, N. A.; Gould, R. M.; Jacob, S. M.; Staffeld, P. O.; Menally, D.; Smiley, P. H.; Wildemuth, C. R. *Oil Gas J.* **1999**, 97, 67.
- (50) White, L. S.; Nitsch, A. R. *J. Membr. Sci.* **2000**, 179, 267.
- (51) White, L. S. *J. Membr. Sci.* **2006**, 286, 26.
- (52) Vankelecom, I. F. J.; Smet, K. D.; Gevers, L. E. M.; Livingston, A.; Nair, D.; Aerts, S.; Kuypers, S.; Jacobs, P. A. *J. Membr. Sci.* **2004**, 231, 99.
- (53) Robinson, J. P.; Tarleton, E. S.; Ebert, K.; Millington, C. R.; Nijmeijer, A. *Ind. Eng. Chem. Res.* **2005**, 44, 3238.
- (54) Volkov, A. V.; Paraschuk, V. V.; Kuznetsov, Y. P.; Volkov, V. V. *Krit. Technol. Membrany* **2006**, 31, 14.
- (55) Volkov, A. V.; Stamatialis, D. F.; Khotimsky, V. S.; Volkov, V. V.; Wessling, M.; Plate, N. A. *J. Membr. Sci.* **2006**, 281, 351.
- (56) Volkov, A. V.; Stamatialis, D. F.; Volkov, V. V.; Wessling, M.; Plate, N. A. *Desalination* **2006**, 199, 251.
- (57) Tsuru, T.; Sudou, T.; Kawahara, S.; Yoshioka, T.; Asaeda, M. *J. Colloid. Interface Sci.* **2000**, 228, 292.
- (58) Tsuru, T.; Miyawaki, M.; Yoshioka, T.; Asaeda, M. *Sep. Purif. Technol.* **2003**, 32, 105.
- (59) White, L. S.; Wang, I. F.; Minhas, B. S.; W. R. Grace & Co.: 1993.
- (60) Beller, M.; Cornils, B.; Frohning, C.; Kohlpaier, C. *J. Mol. Catal. A* **1995**, 104, 17.
- (61) Binning, R. C.; Kelly, J. T.; The American Oil Company, Texas City: 1959.
- (62) Scarpello, J. T.; Nair, D.; Santos, L. M. F.; White, L. S.; Livingston, A. G. *J. Membr. Sci.* **2002**, 203, 71.
- (63) Luthra, S. S.; Yang, X.; Santos, L. M. F.; White, L. S.; Livingston, A. G. *J. Membr. Sci.* **2002**, 201, 65.
- (64) GKSS Germany, 1996.
- (65) Bhanushali, D.; Kloos, S.; Bhattacharya, D. *J. Membr. Sci.* **2002**, 208, 343.
- (66) Raman, L. P.; Cheryan, M.; Rajagopalan, N. *Lipid/fett* **1996**, 98, 10.
- (67) Zwijnenberg, H. J.; Krosse, A. M.; Ebert, K.; Peinemann, K.-V.; Cuperas, F. P. *J. Am. Oil. Chem. Soc.* **1999**, 76, 83.

- (68) Bhosle, B. M.; Subramanian, R.; Ebert, K. *Eur. J. Lipid. Sci. Technol.* **2005**, *107*, 746.
- (69) Helms, B.; Guillaudeu, S. J.; Xie, Y.; McMurdo, M.; Hawker, C. J.; Fréchet, J. M. *J. Angew. Chem. Int. Ed.* **2005**, *44*, 6384.
- (70) Mason, B. P.; Price, K. E.; Steinbacher, J. L.; Bogdan, A. R.; McQuade, D. T. *Chem. Rev.* **2007**, *107*, 2300.
- (71) Pollino, J. M.; Stubbs, L. P.; Weck, M. *Macromolecules* **2003**, *36*, 2230.
- (72) Engel, G. D.; Gade, L. H. *Chem. Eur. J.* **2002**, *8*, 4319.
- (73) Astruc, D. *Inorg. Chem.* **2007**, *46*, 1884.
- (74) Voit, B. *Angew. Chem. Int. Ed.* **2006**, *45*, 4238.
- (75) Miller, A. L.; Bowden, N. B. *J. Org. Chem.* **2009**, *74*, 4834.
- (76) Miller, A. L.; Bowden, N. B. *Adv. Mater.* **2008** *20*, 4195.
- (77) Runge, M. B.; Mwangi, M. T.; Miller, A. L.; Perring, M.; Bowden, N. B. *Angew. Chem. Int. Ed.* **2008**, *47*, 935.
- (78) Kofoed, J.; Reymond, J.-L. *Cur. Opin. Chem. Bio.* **2005**, *9*, 656.
- (79) Sabater, M. J.; Corma, A.; Domenech, A.; Fornes, V.; Garcia, H. *Chem. Commun.* **1997**, 1285.
- (80) Nair, D.; Wong, H.-T.; Han, S.; Vankelecom, I. F. J.; White, L. S.; Livingston, A. G.; Boam, A. T. *Org. Proc. Res. Dev.* **2009**, *13*, 863.
- (81) Twyman, L. J.; King, A. S. H.; Martin, I. K. *Chem. Soc. Rev.* **2002**, *31*, 69.
- (82) Hagio, H.; Sugiura, M.; Kobayashi, S. *Org. Lett.* **2006**, *8*, 375.
- (83) Pink, C. J.; Wong, H.-t.; Ferreira, F. C.; Livingston, A. G. *Org. Proc. Res. Dev.* **2008**, *12*, 589.
- (84) Garrett, C. E.; Prasad, K. *Adv. Synth. Catal.* **2004**, *346*, 889.
- (85) Barbaras, D.; Brozio, J.; Johannse, I.; Allmendinger, T. *Org. Proc. Res. Dev.* **2009**, *13*, 1068.
- (86) Buchwald, S. L.; Mauger, C.; Mignani, G.; Scholz, U. *Adv. Synth. Catal.* **2006**, *348*, 23.
- (87) Burgos, C. H.; Barder, T. E.; Huang, X.; Buchwald, S. L. *Angew. Chem. Int. Ed.* **2006**, *45*, 4321.
- (88) Surry, D. S.; Buchwald, S. L. *Angew. Chem. Int. Ed.* **2008**, *47*, 6338.
- (89) Sigma-Aldrich, F., From Sigma-Aldrich.

- (90) Long, T. R.; Gupta, A.; Miller II, A. L.; Rethwisch, D. G.; Bowden, N. B. *J. Mater. Chem.* **2011**, *21*, 14265.
- (91) Thathagar, M. B.; Ten Elshof, J. E.; Rothenberg, G. *Angew. Chem. Int. Ed.* **2006**, *45*, 2886.
- (92) Patterson, D. A.; Lau, L. Y.; Roegnpithya, C.; Gibbins, E. J.; Livingston, A. G. *Desalination* **2008**, *218*, 248.
- (93) Ronde, N. J.; Totev, D.; Muller, C.; Lutz, M.; Spek, A. L.; Vogt, D. *ChemSusChem* **2009**, *2*, 558.
- (94) Aizawa, S.-I.; Majumder, A.; Yokoyama, Y.; Tamai, M.; Maeda, D.; Kitamura, A. *Organometallics* **2009**, *28*, 6067.
- (95) Shin, J.; Bertoia, J.; Czerwinski, K. R.; Bae, C. *Green Chemistry* **2009**, *11*, 1576.
- (96) Velauthamurty, K.; Higgins, S. J.; Rajapakse, R. M. G.; Bacsa, J.; van Zalinge, H.; Nichols, R. J.; Haiss, W. *J. Mater. Chem.* **2009**, *19*, 1850.
- (97) Carroll, M. A.; Wood, R. A. *Tetrahedron* **2007**, *63*, 11349.
- (98) Park, S.-E.; Kang, S. B.; Jung, K.-J.; Won, J.-E.; Lee, S.-G.; Yoon, Y.-J. *Synthesis* **2009**, *5*, 815.
- (99) MacNeil, S. L.; Wilson, B. J.; Snieckus, V. *Org. Lett.* **2006**, *8*, 1133.
- (100) Calwey, M. J.; Cloke, F. G. N.; Fitzmaurice, R. J.; Pearson, S. E.; Scott, J. S.; Caddick, S. *Org. & Biomolecular Chem.* **2008**, *6*, 2820.
- (101) Hill, L. L.; Smith, J. M.; Brown, W. S.; Moore, L. R.; Guevera, P.; Pair, E. S.; Porter, J.; Chou, J.; Woltermann, C. J.; Craciun, R.; Dixon, D. A.; Shaughnessy, K. H. *Tetrahedron* **2008**, *64*, 6920.
- (102) Long, T. R.; Gupta, A.; Miller II, A. L.; Rethwisch, D. G.; Bowden, N. B. *J. Mater. Chem.* **2011**, DOI:10.1039/C1JM10970G.
- (103) Harris, W. S. *J. Nutr.* **2012**, *142*, 600S.
- (104) Lecerf, J.-M. *Garant Publishers* **2001**, 93.
- (105) Pryde, E. H. *Am. Soybean Assoc.* **1980**, 13.
- (106) Van, G. J.; Knothe, G. *AOCS Monogr. Ser. Oilseeds* **2008**, *2*, 499.
- (107) Warner, K. A. *AOCS Monogr. Ser. Oilseeds* **2008**, *2*, 483.
- (108) Winkle, M.; Poole, S. *Cereal Foods World* **2002**, *47*, 378.
- (109) Kris-Etherton, P. M. *Crit. Rev. Food Sci. Nutr.* **2010**, *50*, 29.
- (110) Tardy, A.-L.; Morio, B.; Chardigny, J.-M.; Malpuech-Brugere, C. *Nutr. Res. Rev.* **2011**, *24*, 111.

- (111) Thompson, A. K.; Minihane, A. M.; Williams, C. M. *Eur. J. Clin. Nutr.* **2011**, *65*, 553.
- (112) Thompson, A. K.; Minihane, A. M.; Williams, C. M. *Int. J. Obes.* **2011**, *35*, 315.
- (113) Wallace, S. K.; Mozaffarian, D. *Curr. Atheroscler. Rep.* **2009**, *11*, 423.
- (114) Tardy, A.-L.; Morio, B.; Chardigny, J.-M.; Malpuech-Brugere, C. *Nutr. Res. Rev.* **2011**, *24*, 111.
- (115) Lee, K. W.; Lee, H. J.; Cho, H. Y.; Kim, Y. J. *Crit. Rev. Food Sci. Nutr.* **2005**, *45*, 135.
- (116) Nagpal, R.; Yadav, H.; Puniya, A. K.; Singh, K.; Jain, S.; Marotta, F. *Curr. Top. Nutraceutical Res.* **2007**, *5*, 55.
- (117) Uauy, R.; Aro, A.; Clarke, R.; Ghafoorunissa; L'Abbe, M. R.; Mozaffarian, D.; Skeaff, C. M.; Stender, S.; Tavella, M. *Eur. J. Clin. Nutr.* **2009**, *63*, S68.
- (118) Wallin, A.; Di, G. D.; Orsini, N.; Patel, P. S.; Forouhi, N. G.; Wolk, A. *Diabetes Care* **2012**, *35*, 918.
- (119) Bootello, M. A.; Garces, R.; Martinez-Force, E.; Salas, J. J. *J. Am. Oil Chem. Soc.* **2011**, *88*, 1511.
- (120) Brundiek, H. B.; Evitt, A. S.; Kourist, R.; Bornscheuer, U. T. *Ang. Chem. Int. Ed.* **2012**, *51*, 412.
- (121) Davis, J. P.; Geller, D.; Faircloth, W. H.; Sanders, T. H. *J. Am. Oil Chem. Soc.* **2009**, *86*, 353.
- (122) Ramli, M. R.; Siew, W. L.; Cheah, K. Y. *J. Am. Oil Chem. Soc.* **2009**, *86*, 587.
- (123) Ramli, M. R.; Siew, W. L.; Cheah, K. Y. *J. Food Sci.* **2008**, *73*, C140.
- (124) Senanayake, S. P. J. N. *Woodhead Publ. Ser. Food Sci., Technol. Nutr.* **2010**, *202*, 483.
- (125) Vereecken, J.; Foubert, I.; Smith, K. W.; Sassano, G. J.; Dewettinck, K. *Eur. J. Lipid Sci. Technol.* **2010**, *112*, 233.
- (126) Wanasundara, U. N.; Shahidi, F. *Technomic* **1997**, 225.
- (127) Gupta, A.; Rethwisch, D. G.; Bowden, N. B. *Chem. Commun.* **2011**, *46*, 10236.
- (128) Amendt, M. A.; Chen, L.; Hillmyer, M. A. *Macromolecules* **2010**, *43*, 3924.
- (129) Amendt, M. A.; Roerdink, M.; Moench, S.; Phillip, W. A.; Cussler, E. L.; Hillmyer, M. A. *Aust. J. Chem.* **2011**, *64*, 1074.
- (130) Kovacic, S.; Krajnc, P.; Slugovc, C. *Chem. Commun.* **2010**, *46*, 7504.
- (131) Ren, F.; Feldman, A. K.; Carnes, M.; Steigerwald, M.; Nuckolls, C. *Macromolecules* **2007**, *40*, 8151.

- (132) Rule, J. D.; Moore, J. S. *Macromolecules* **2002**, *35*, 7878.
- (133) Balmer, T. E.; Schmid, H.; Stutz, R.; Delamarche, E.; Michel, B.; Spencer, N. D.; Wolf, H. *Langmuir* **2005**, *21*, 622.
- (134) Banerjee, S.; Asrey, R.; Saxena, C.; Vyas, K.; Bhattacharya, A. *J. Appl. Polym. Sci.* **1997**, *65*, 1789.
- (135) Crank, J. *The mathematics of diffusion*; Clarendon Press: Oxford, 1970.
- (136) Du Pleiss, J.; Pugh, W. J.; Judefeind, A.; Hadgraft, J. *Eur. J. Pharm. Sci.* **2002**, *15*, 63.
- (137) Philip, W. A.; Amendt, M.; O'Neill, B.; Chen, L.; Hillmyer, M. A.; Cussler, E. L. *ACS Appl. Mater. Inter.* **2009**, *1*, 472.
- (138) Philip, W. A.; Martono, E.; Chen, L.; Hillmyer, M. A.; Cussler, E. L. *J. Mem. Sci.* **2009**, *337*, 39.
- (139) Sarveiya, V.; Templeton, J. F.; Benson, H. A. E. *Eur. J. Pharm. Sci.* **2005**, *26*, 39.
- (140) Shah, M. R.; Noble, R. D.; Clough, D. E. *J. Mem. Sci.* **2007**, *287*, 111.
- (141) Tamai, Y.; Tanaka, H.; Nakanishi, K. *Macromolecules* **1995**, *28*, 2544.
- (142) Berens, A. R.; Hopfenberg, H. B. *J. Mem. Sci.* **1982**, *13*, 283.
- (143) Fierro, D.; Boschetti-de-Fierro, A.; Abetz, V. *J. Membr. Sci.* **2012**, *413-414*, 91.
- (144) Fritsch, D.; Merten, P.; Heinrich, K.; Lazar, M.; Priske, M. *J. Membr. Sci.* **2012**, *401-402*, 222.
- (145) Rundquist, E. M.; Pink, C. J.; Livingston, A. G. *Green Chem.* **2012**, *14*, 2197.
- (146) Sereewatthanawut, I.; Lim, F. W.; Bhole, Y. S.; Ormerod, D.; Horvath, A.; Boam, A. T.; Livingston, A. G. *Org. Process Res. Dev.* **2010**, *14*, 600.
- (147) So, S.; Peeva, L. G.; Tate, E. W.; Leatherbarrow, R. J.; Livingston, A. G. *Org. Process Res. Dev.* **2010**, *14*, 1313.
- (148) Szekely, G.; Bandarra, J.; Heggie, W.; Sellergren, B.; Ferreira, F. C. *J. Membr. Sci.* **2011**, *381*, 21.
- (149) van, d. G. P.; Barnard, A.; Cronje, J.-P.; de, V. D.; Marx, S.; Vosloo, H. C. M. *J. Membr. Sci.* **2010**, *353*, 70.
- (150) Dalko, P. I.; Moisan, L. *Angew. Chem. Int. Ed.* **2001**, *40*, 3726.
- (151) Ma, J.; Cahard, D. *Angew. Chem. Int. Ed.* **2004**, *43*, 4566.
- (152) List, B.; Lerner, R. A.; Barbas, C. F. *J. Am. Chem. Soc.* **2000**, *122*, 2395.
- (153) Sakhtivel, K.; Notz, W.; bui, T.; Barbas, C. F. *J. Am. Chem. Soc.* **2001**, *123*, 5260.

- (154) List, B. *Acc. Chem. Res.* **2004**, *37*, 548.
- (155) Mukherjee, S.; Yang, J. W.; Hoffmann, S.; List, B. *Chem. Rev.* **2007**, *107*, 5471.
- (156) Bahmanyar, S.; Houk, K. N. *Org. Lett.* **2003**, *5*, 1249.
- (157) Borgevig, A.; kumaragurubaran, N.; Jorgensen, K. A. *Chem. Commun.* **2002**, 620.
- (158) Thierry, B.; Plaquevent, J. C.; Cahard, D. *Mol. Diversity* **2005**, *9*, 277.
- (159) Arakawa, Y.; Haraguchi, N.; Itsuno, S. *Angew. Chem. Int. Ed.* **2008**, *47*, 8232.
- (160) Luo, S.; Li, J.; Zhang, L.; Xu, H.; Cheng, J. P. *Chem- Eur. J.* **2008**, *14*, 1273.
- (161) Benaglia, M.; Celentano, G.; Cinquini, M.; Puglisi, A.; Cozzi, F. *Adv. Synth. Catal.* **2002**, *344*, 149.
- (162) Guizzetti, S.; Benaglia, M.; Siegel, J. S. *Chem. Commun.* **2012**, *48*, 3188.
- (163) Riente, P.; Yadav, J.; Pericas, M. A. *Org. Lett.* **2012**, *14*, 3668.
- (164) Corma, A.; Boronat, M.; Climent, M. J.; Iborra, S.; Monton, R.; Sabater, M. J. *Phys. Chem. Chem. Phys.* **2011**, *13*, 17255.
- (165) Schmidt, B.; Patel, J.; Ricard, F. X.; Brechtelsbauer, C. M.; Lewis, N. *Org. Process Res. Dev.* **2004**, *8*, 998.
- (166) Muller, S.; Afraz, M. C.; de Gelder, R.; Ariaans, G. J. A.; Kaptein, B.; Broxterman, Z. B.; Bruggink, A. *Eur. J. Org. Chem.* **2005**, 1082.
- (167) Cesur, S.; Gokbel, S. *Cryst. Res. Technol.* **2008**, *43*, 720.
- (168) Murnane, D.; Marriott, C.; Martin, G. P. *Int. J. Pharm.* **2008**, *361*, 141.
- (169) Otsuka, M.; Nishizawa, J.-i.; Shibata, J.; Ito, M. *J. Pharma. Sci.* **2010**, *99*, 4048.
- (170) Pranzo, M. B.; Cruickshank, D.; Coruzzi, M.; Caira, M. R.; Bettini, R. *J. Pharm. Sci.* **2010**, *99*, 3731.
- (171) Qi, S.; Weuts, I.; De Cort, S.; Stokbroekx, S.; Leemans, R.; Reading, M.; Belton, P.; Craig, D. Q. M. *J. Pharma. Sci.* **2009**, *99*, 196.
- (172) Sheth, A. R.; Bates, S.; Muller, F. X.; Grant, D. J. W. *Cryst. Growth Des.* **2004**, *4*, 1091.
- (173) Dijkstra, H. P.; Van Klink, G. P. M.; Van Koten, G. *Acc. Chem. Res.* **2002**, *35*, 798.
- (174) Dijkstra, M. F. J.; Bach, S.; Ebert, K. *J. Mem. Sci.* **2006**, *286*, 60.
- (175) Geens, J.; De Witte, B.; Van der Bruggen, B. *Sep. Sci. Technol.* **2007**, *42*, 2435.
- (176) Silva, P.; Peeva, L. G.; Livingston, A. G. *Adv. Membr. Technol. Appl.* **2008**, 451.

- (177) Gould, R. M.; White, L. S.; Wildemuth, C. R. *Environ. Prog.* **2001**, *20*, 12.
- (178) See-Toh, Y. H.; Silva, M.; Livingston, A. G. *J. Mem. Sci.* **2008**, *324*, 220.
- (179) Toh, Y. H. S.; Loh, X. X.; Li, K.; Bismarck, A.; Livingston, A. G. *J. Mem. Sci.* **2007**, *291*, 120.
- (180) Peeva, L. G.; Sairam, M.; Livingston, A. G. In *Comprehensive membrane science and engineering*; Drioli, E., Giorno, L., Eds.; Elsevier: Boston, 2010; Vol. 2, p 91.
- (181) Anraku, Y.; Kishimura, A.; Oba, M.; Yamasaki, Y.; Kataoka, K. *J. Am. Chem. Soc.* **2010**, *132*, 1631.
- (182) See-Toh, Y. H.; Ferreira, F. C.; Livingston, A. G. *J. Mem. Sci.* **2007**, *299*, 236.
- (183) Asatekin, A.; Gleason, K. K. *Nano Lett.* **2011**, *11*, 677.
- (184) Jirage, K. B.; Hulteen, J. C.; Martin, C. R. *Science* **1997**, *278*, 655.
- (185) Martin, C. R.; Nishizawa, M.; Jirage, K. B.; Kang, M. *J. Phys. Chem. B* **2005**, *105*, 1925.
- (186) Wirtz, M.; Parker, M.; Kobayashi, Y.; Martin, C. R. *Chem. Rec.* **2002**, *2*, 112.
- (187) Hupp, J. T.; O'Donnell, J. L.; Thaitrong, N.; Nelson, A. P. *Langmuir* **2006**, *22*, 1804.
- (188) Snurr, R. Q.; Hupp, J. T.; Nguyen, S. T. *AIChE Journal* **2004**, *50*, 1090.
- (189) Chen, B.; Xiang, S.; Qian, G. *Acc. Chem. Res.* **2010**, *43*, 1115.
- (190) Liu, D.-H.; Zhong, C.-L. *J. Mater. Chem.* **2010**, *20*, 10308.
- (191) Mueller, T. J. J. *Top. Organomet. Chem.* **2006**, *19*, 149.
- (192) Thomas, K. M. *Dalton Trans.* **2009**, 1487.
- (193) Zhao, D.; Timmons, D. J.; Yuan, D.; Zhou, H.-C. *Acc. Chem. Res.* **2011**, *44*, 123.
- (194) Zou, R.; Abdel-Fattah, A. I.; Xu, H.; Zhao, Y.; Hickmott, D. D. *CrystEngComm* **2010**, *12*, 1337.
- (195) Perring, M.; Bowden, N. B. *Langmuir* **2008**, *24*, 10480.
- (196) Martina, A. D.; Graf, R.; Hilborn, J. G. *J. Appl. Polym. Sci.* **2005**, *96*, 407.
- (197) Lee, J. K.; Liu, X.; Yoon, S. H.; Kessler, M. R. *J. Polym. Sci., Part B: Polym. Phys* **2007**, *45*, 1771.
- (198) Bellan, L. M.; Coates, G. W.; Craighead, H. G. *Macromol. Rap. Comm.* **2006**, *27*, 511.
- (199) Cowen, J. A.; Liu, H.; Xiao, P.; Imhof, R. E. *Rev. Sci. Instr.* **2003**, *74*, 764.

- (200) Watson, J. M.; Zhang, G. S.; Payne, P. A. *J. Mem. Sci.* **1992**, *73*, 55.
- (201) Tamai, Y.; Tanaka, H.; Nakanishi, K. *Macromolecules* **1994**, *27*, 4498.
- (202) Mwangi, M. T.; Schulz, M. D.; Bowden, N. B. *Org. Lett.* **2009**, *11*, 33.
- (203) Mwangi, M. T.; Runge, M. B.; Hoak, K. M.; Schulz, M. D.; Bowden, N. B. *Chem. Eur. J.* **2008**, *14*, 6780.
- (204) Miller, A. L.; Bowden, N. B. *Chem. Commun.* **2007**, 2051.
- (205) Jeong, W.; Kessler, M. R. *Chem. Mater.* **2008**, *20*, 7060.
- (206) Lee, J. K.; Gould, G. L. *J. Sol-Gel Sci. Technol.* **2007**, *44*, 29.
- (207) Kessler, M. R.; White, S. R. *J. Poly. Sci. A: Poly. Chem.* **2002**, *40*, 2373.
- (208) Perring, M. L., T. R.; Bowden, N. B. *J. Mater. Chem.* **2010**, *20*, 8679.
- (209) Mwangi, M. T.; Runge, M. B.; Bowden, N. B. *J. Am. Chem. Soc.* **2006**, *128*, 14434.
- (210) Vankelecom, I.; Vercruyssen, K.; Moens, N.; Parton, R.; Reddy, J. S.; Jacobs, P. *Chem. Commun.* **1997**, 137.
- (211) Lee, J. N.; Park, C.; Whitesides, G. M. *Anal. Chem.* **2003**, *75*, 6544.
- (212) Schafer, T.; Di Paolo, R. E.; Franco, R.; Crespo, J. G. *Chem. Commun.* **2005**, 2594.